

Topoisomerase 1 (Top1)-associated genome instability in yeast: effects of persistent
cleavage complexes or increased Top1 levels

by

Roketa Shanell Sloan

University Program in Genetics and Genomics
Duke University

Date: _____

Approved:

Sue Jinks-Robertson, Supervisor

Thomas Petes, Committee Chair

Kenneth Kreuzer

Beth Sullivan

Dissertation submitted in partial fulfillment of
the requirements for the degree of
Doctor of Philosophy in the University Program in Genetics and Genomics
in the Graduate School
of Duke University

2016

ABSTRACT

Topoisomerase 1 (Top1)-associated genome instability in yeast: effects of persistent
cleavage complexes or increased Top1 levels

by

Roketa Shanell Sloan

University Program in Genetics and Genomics
Duke University

Date: _____

Approved:

Sue Jinks-Robertson, Supervisor

Thomas Petes, Committee Chair

Kenneth Kreuzer

Beth Sullivan

An abstract of a dissertation submitted in partial
fulfillment of the requirements for the degree
of Doctor of Philosophy in the University Program in Genetics and Genomics
in the Graduate School of
Duke University

2016

Copyright by
Roketa Shanell Sloan
2016

Abstract

Topoisomerase 1 (Top1), a Type IB topoisomerase, functions to relieve transcription- and replication-associated torsional stress in DNA. Top1 cleaves one strand of DNA, covalently associates with the 3' end of the nick to form a Top1-cleavage complex (Top1cc), passes the intact strand through the nick and finally re-ligates the broken strand. The chemotherapeutic drug, Camptothecin, intercalates at a Top1cc and prevents the crucial re-ligation reaction that is mediated by Top1, resulting in the conversion of a nick to a toxic double-strand break during DNA replication or the accumulation of Top1cc. This mechanism of action preferentially targets rapidly dividing tumor cells, but can also affect non-tumor cells when patients undergo treatment. Additionally, Top1 is found to be elevated in numerous tumor tissues making it an attractive target for anticancer therapies. We investigated the effects of persistent Top1-cleavage complexes and elevated Top1 levels on genome stability in *Saccharomyces cerevisiae*. We found that increased levels of the Top1cc resulted in an increase in reciprocal crossovers, an increase in mutagenesis and an increase in the instability within the rDNA and *CUPI* tandem arrays. Increased Top1 levels resulted in an increase in mutagenesis and increased instability in rDNA locus but did not affect stability at *CUPI*. These results have important implications for understanding the effects of CPT as a chemotherapeutic agent and the genetic consequences of elevated Top1 levels.

Contents

Abstract.....	iv
List of Tables	x
List of Figures.....	xi
Acknowledgements.....	xiv
1. Introduction.....	17
1.1 Types of topoisomerases.....	17
1.2 Type IB Topoisomerase (Top1).....	18
1.2.a. Top1 functional domains.....	21
1.2.b. Top1 deficiency	22
1.3 Top1-induced DNA damage	23
1.4 Transcription-associated mutagenesis (TAM) and Top1.....	28
1.5 Top1 as an anti-cancer drug target.....	34
1.5.a. CPT and genome instability	38
1.5.b. CPT mechanism of action: replication fork collisions with Top1cc and/or accumulation of positive supercoils.....	40
1.6 Top1 in human health and disease.....	42
1.7 This dissertation.....	45
2. Genome-wide effects of persistent Top1 cleavage complexes in yeast by camptothecin	47
2.1 Introduction.....	47
2.2 Experimental methods	49
2.2.a. Strains and plasmids.....	49

2.2.b. Colony sector analysis	51
2.2.c. Sub-culturing.....	53
2.2.d. Analysis of LOH using microarrays	53
2.2.e. Genome-element association analysis of crossovers (COs) on right arm of chromosome IV.....	54
2.2.f. Analysis of a <i>SpeI</i> polymorphism to detect reciprocal crossovers initiating in the rDNA locus	55
2.2.g. Southern hybridization analysis of <i>CUPI</i> tandem arrays.....	55
2.2.h. Other genetic and physical methods	56
2.2.i. Statistical analysis.....	57
2.3 Results.....	57
2.3.a. Stabilization or accumulation of Top1 cleavage complexes (Top1cc) elevates the rate of mitotic crossovers	57
2.3.b. Characterization of reciprocal crossover (RCO) events on chromosome IV associated with stabilized Top1 cleavage complexes	62
2.3.c. Genome-wide LOH and copy-number changes associated with Top1cc.	73
2.3.d. Copy-number variation (CNV) at the <i>CUPI</i> locus is elevated by CPT treatment or Top1-T722A expression.....	75
2.3.e. Crossovers at the rDNA locus increase with CPT treatment and Top1-T722A expression.	80
2.4 Discussion	82
3. Camptothecin-induced mutagenesis	88
3.1 Introduction.....	88
3.2 Methods.....	90
3.2.a. Strain and plasmids.	90

3.2.b. CPT-sensitivity plate spotting assay.	91
3.2.c. Camptothecin-induced mutation frequency assay and mutation spectra generation.	91
3.2.d. Top1 cleavage assay.	93
3.3 Results.....	93
3.3.a. CPT exposure increases mutagenesis at Top1-dependent hotspots	94
3.3.b. CPT exposure increases mutagenesis at the (TC) ₃ hotspot.	97
3.3.c. CPT does not affect ribonucleotide associated deletions.	100
3.4 Discussion.....	100
4. Topoisomerase I overexpression: Can too much of a good thing be bad?	104
4.1 Introduction.....	104
4.2 Experimental methods	105
4.2.a. Strain and plasmids.	106
4.2.b. Copper-induced mutation frequency assay and mutation spectra generation.	106
4.2.c. Quantitative real time RT-PCR (qRT-PCR).....	109
4.2.d. Sub-culturing of diploids	110
4.2.e. Detection of crossovers initiating at the rDNA locus using a <i>SpeI</i> polymorphism.	110
4.2.f. Analysis of the <i>CUP1</i> tandem array by Southern blots.....	111
4.3 Results.....	112
4.3.a. Overexpression of Top1 is mutagenic and leads to an increase in 2-bp deletions.	114
4.3.b. Top1 overexpression elevates deletions in the (TC) ₃ hotspot and reveals novel hotspots.	115

4.3.c. Effect of Top1 overexpression on a ribo-dependent hotspot.	117
4.3.d. Crossovers (COs) at the rDNA locus increase with increasing levels of Top1.	120
4.4 Discussion.....	123
5. Summary and future directions.....	127
5.1 Summary.....	127
5.1.a. Effects of persistent Top1cc.....	127
5.1.b. Mutagenic consequence of increased Top1 levels.....	129
5.2 Future directions	130
5.2.a. Mechanism of CPT-induced CNV	130
5.2.b. CPT-induced 2-bp deletion formation	131
5.2.c. CPT-induced mechanism of lethality.....	132
5.2.d. Top1 overexpression and camptothecin treatment	134
5.2.e. Top1 and Top2 redundancy	135
Appendix 1: Genome-wide effects of persistent Top1cc Supplemental Tables.	137
Appendix 1A. SGD coordinates for heterozygous and homozygous transitions on chromosome IV in CPT treated red/white sectors	137
Appendix 1B. SGD coordinates for heterozygous and homozygous transitions on chromosome IV in <i>top1-T722A</i> red/white sectors	139
Appendix 1C. SGD coordinates for events detected in sub-cultured clones.	141
Appendix 1D. <i>CUPI</i> Southern data for sub-cultured clones.....	142
Appendix 1E. Reciprocal crossovers at the rDNA locus after 10 sub-cultures.....	146
Appendix 2: CPT-induced mutagenesis supplemental material	147
Appendix 2A. CPT-induced mutation frequency data for all three reporters.....	147

Appendix 2B. CPT treatment causes a significant decrease in cell viability.....	147
Appendix 3. Top1 overexpression supplemental tables and figures.....	148
Appendix 3A. Effect of Top1 overexpression on mutations in the (AT) ₂ and (TC) ₃ reporters.	148
Appendix 3B. (AT) ₂ reporter spectra.....	149
Appendix 3C. (TC) ₃ reporter spectra.	150
Appendix 3D. Effect of Top1 overexpression on mutations in the (AG) ₄ reporter..	151
Appendix 3E. (AG) ₄ reporter spectra.....	152
Appendix 3F. (AG) ₄ <i>rnh201</i> Δ spectra.	153
Appendix 3G. (AG) ₄ <i>rnh201 pol2-M644L</i> spectra.	154
Appendix 3H. Crossovers initiated within the rDNA locus in sub-culture 10 clones.	155
Appendix 3I. <i>CUPI</i> Southern hybridization data for sub-culture 10 clones.	155
References.....	156
Biography.....	171

List of Tables

Table 1. Summary of DNA topoisomerases.	19
Table 2. Conversion tracts associated with reciprocal crossovers in CPT-treated red/white sectors.	69
Table 3. Conversion tracts associated with reciprocal crossovers in Top1-T722A red/white sectors.	70
Table 4. Chromosome depictions for events detected in clones sub-cultured 10 times. ..	74
Table 5. Strains for CPT-mutagenesis studies.	92
Table 6. Strains used in Top1 overexpression studies.	107
Table 7. Plasmids.	109
Table 8. Steady-state <i>TOP1</i> transcript levels in WT and <i>pCUP-TOP1</i> strains.	114

List of Figures

Figure 1. Type IB Topoisomerase (Top1) mechanism of action.....	20
Figure 2. Top1 cleavage of DNA.....	21
Figure 3. DNA repair proteins that repair Top1-induced DNA damage.....	25
Figure 4. Partial <i>pGAL-CAN1</i> mutation spectrum.....	29
Figure 5. Model for Top1cc-initiated deletions.....	31
Figure 6. Top1 cleavage at an rNMP.....	32
Figure 7. Model for Top1-initiated deletions at a misincorporated rNMP.....	33
Figure 8. CPT-ternary complex with the Top1cc.....	37
Figure 9. CPT mechanism of action.....	39
Figure 10. Two models of CPT-induced mechanism of lethality.....	42
Figure 11. Detecting RCOs on chromosome IV in JSC25.....	59
Figure 12. CPT treatment elevates the rate of RCOs.....	60
Figure 13. Detecting RCOs on chromosome V in PG311.....	61
Figure 14. Top1-T722A expression increases the rate of RCOs.....	63
Figure 15. Characterizing RCOs on chromosome IV with microarrays.....	65
Figure 16. Gene conversion pattern associated with G1- or G2-initiated DSBs.....	66
Figure 17. Distribution of LOH breakpoints.....	71
Figure 18. CPT treatment increases RCOs during or after DNA synthesis.....	72
Figure 19. Top1-T722A expression increases RCOs during or after DNA synthesis.....	73

Figure 20. <i>CUPI</i> instability associated with Top1-T722A expression detected by microarrays.....	76
Figure 21. <i>CUPI</i> instability associated with CPT treatment or Top1-T722A expression.....	78
Figure 22. Copy number variation (CNV) at <i>CUPI</i> locus associated with CPT treatment or Top1-T722A expression.....	79
Figure 23. CPT treatment and Top1-T722A expression result in increase RCOs at the rDNA locus.....	81
Figure 24. Mechanisms of CNV at the <i>CUPI</i> locus.....	86
Figure 25. CPT treatment for 6 hours decreases cell viability.....	95
Figure 26. CPT-associated mutations occur at a Top1-dependent hotspot.....	96
Figure 27. CPT causes an increase in 2-bp deletions at the (AT) ₂ hotspot.....	96
Figure 28. CPT treatment causes changes in the mutation spectrum in the (TC) ₃ reporter.....	98
Figure 29. CPT differentially affects hotspots in the (TC) ₃ reporter.....	98
Figure 30. Top1 cleavage sites map within the (TC) ₃ repeat and GT dinucleotide.....	99
Figure 31. CPT causes an increase in 2-bp deletions at the (AG) ₄ hotspot.....	101
Figure 32. Proposed model for the CPT-dependent GT deletions.....	103
Figure 33. Top1 overexpression increases 2-bp deletions at the (AT) ₂ hotspot.....	116
Figure 34. Top1 overexpression increases 2-bp deletions at (TC) ₃ hotspot and additional positions.....	117
Figure 35. Top1 overexpression increases 2-bp deletions at the (TC) ₃ hotspot.....	118

Figure 36. Top1 overexpression increases 2-bp deletions at the (AG) ₄ hotspot.....	119
Figure 37. Top1 overexpression results in increased LOH distal to rDNA locus.....	122
Figure 38. Copy number variation (CNV) at <i>CUPI</i> locus is not significantly elevated with Top1 overexpression.....	124

Acknowledgements

I am extremely grateful for all of the support, mentorship, guidance, and opportunities I have received throughout my graduate career. First and foremost, I would like to acknowledge and thank Sue Jinks-Robertson. I want to thank her for embracing me and teaching me everything she could during my time in her lab. Her support, guidance, advice (academic, professional and life), scientific expertise and wisdom have been invaluable to my growth not only as a scientist, but also as an individual.

In addition to Sue, I was fortunate to have the best group of mentors to guide me through different aspects of graduate school and help me become a well-rounded individual. I would like to acknowledge my committee: Sue, Beth Sullivan, Kenneth Kreuzer and Thomas Petes; they were the best committee a girl could ask for. I loved that they were equally invested in my successful transition through graduate school and supportive of everything I wanted to pursue. One of the most valuable lessons they taught me is that it is possible to love science and enjoy life to its full extent and for that, I will always be grateful. I would next like to acknowledge the Duke Graduate School, in particular Deans Jacqueline Looney, Alan Kendrick and Paula McClain. They have provided me with the upmost support and have given me unique opportunities that changed me in so many ways. My professionalism, leadership skills, and confidence have developed tremendously because of their trust and belief in me. I would also like to thank the Summer Research Opportunity Program (SROP) Directors (Ken, Meta Kuehn and Soman Abraham) for allowing me to work with their summer program for three

enjoyable years; I learned many valuable lessons working with SROP and the experiences I shared with the students allowed me to gain skills I will take with me as my career develops. I also want to acknowledge both Dean Valerie Ashby and Carmichael Roberts for their incredible support, pearls of wisdom, and advice towards the pursuit of my ultimate career goals.

I would also like to acknowledge all members, past and present, of both the SJR and Petes' labs and Kristin Scott. It was a pleasure working with them for the last five years, receiving useful feedback, advice, and the camaraderie. In particular, I would like to acknowledge Nayun Kim & Kevin Lehner for guidance, advice, and their help during my transition into working with yeast. I would especially like to acknowledge Xiaoge "Amy" Guo and Anthony Moore for their friendship, thoughtful scientific discussions, and for being the two individuals I shared every grad school struggle with. I thank them for always making sure I strived to do better and for their never-ending support. I would also like to acknowledge Yee Fang "Eva" Hum and Sabrina Andersen, for their patience in teaching me new techniques I had hesitation in performing and for answering all of my questions.

Lastly, I would like to acknowledge the supportive group of family and friends that have been there through the ups and downs of my graduate school career. I would like to specifically acknowledge my parents (Craig and Sarah Sloan and Ronita and Tim Daney) for their emotional, spiritual, mental, and financial support over the years. My siblings (Ashanti and Craig Sloan Jr.) were there whenever I needed anything and

provided a good laugh when the times called for one. Many members of my family did not fully understand the scope of my work but blindly supported me; I cannot express how thankful I am for their support. I would like to thank my Day 1 friends (Krystine Kinsel, Keilli Brathwaite, Nashtelka Thompson, Tiffany & Patrick Hand, Joy & Norman Epps, Brittany Bradley, Sean McLeod, Danielle Cook and Lonna Mollison) that I knew before entering Duke, for their love, support and mandatory enforced breaks. Being at Duke for six years allowed me to really expand my friend group and I met amazing individuals that kept me going through the ups and down. Thank you Tamika John-Payne, Brandi Johnson-Weaver, Cavin Ward-Caviness, Zakiya Whatley, Yuvon Mobley, Monica Gutierrez, José Vargas Muñiz, Christine Daniels, Keisha Melodi McSweeney, Myron Evans, Ba'Carri Johnson, Ashley Queener, Emerson Lovell, Henry Washington, Sean & Jhaniqua Palmer, Malcolm Bonner, Lauren Russell, Lee Barnes III, Dillon Isaac, Sherritta Williams, Casey Adams, Reginald Benbow, Denzel Caldwell, Alec Greenwald, Shaun Jones, Terrance White and Uzoma Ayogu for being there whenever I needed encouragement or a fun break.

1. Introduction

DNA is constantly undergoing topological or structural changes, many of which occur during two basic cellular processes: DNA replication and transcription. DNA strand separation during replication and transcription generates positive supercoils, which can affect the progression of the replication and transcription machinery if not resolved (Wang 2002). Negative supercoils are generated behind the transcription machinery (Wang and Lynch 1993). Additionally, chromosomes and sister chromatids become catenated and must be separated for proper transfer of the genetic material.

Topoisomerases are considered the guardians of the genome due to their ability to relieve topological stress by breaking the phosphodiester backbone, which allows DNA strands to rotate and relieve supercoiling, and then religating the DNA (Wang 2002). This dissertation focuses on the genetic consequences of accumulated type IB topoisomerase cleavage complexes (Top1cc) and elevated levels of Top1 protein using *Saccharomyces cerevisiae* (budding yeast) as a model.

1.1 Types of topoisomerases

DNA topoisomerases resolve topological challenges in the genome by catalyzing two transesterification reactions (Wang 2002). These enzymes are designated as type I or type II based on whether they nick one or both strands of DNA, respectively (Wang

2002). Type IA enzymes catalyze the relaxation of negatively supercoiled, underwound DNA by binding to and unpairing a short stretch of double-stranded DNA. Yeast Top3 (a type IA enzyme), as a complex with Sgs1 and Rmi1, has been primarily implicated in homologous recombination (Nitiss 1998). Type IB enzymes relax both positive and negative supercoils by binding double-stranded DNA and nicking one strand. Yeast Top1 is a type IB enzyme that will be discussed below in more detail (Wang 2002). Top2, a type II topoisomerase associates with replication forks, is tightly bound to chromosomes during mitosis, is essential for the survival of proliferating cells and is required for chromosome segregation (Pendleton *et al.* 2014). **Table 1** summarizes the properties of DNA topoisomerases.

1.2 Type IB Topoisomerase (Top1)

Top1 functions to relieve transcription- and replication-associated torsional stress in DNA (see **Figure 1**) (Wang 2002; Pommier 2006; Koster *et al.* 2007). During replication the unwinding of DNA produces positive supercoils ahead of the replication fork which need to be removed to avoid replication fork arrest (Hsiang *et al.* 1989). During transcription positive supercoils are generated ahead and negative supercoils are generated behind the transcription machinery (Zhang *et al.* 1988; Drolet *et al.* 1994).

The Top1 catalytic cycle can be broken up into four distinct steps: binding of enzyme to DNA, DNA cleavage, single-strand passage and religation of DNA. Top1 binds only to double-stranded DNA and may bind more efficiently in regions of

Table 1. Summary of DNA topoisomerases.

		Mechanism	Linkage to DNA	Action
Type I Topoisomerases				
Type IA	Bacterial topoisomerase I and III Yeast topoisomerase 3 Drosophila topoisomerase III α and III β Mammalian topoisomerase III α and III β	Unpairs a short stretch of double-stranded DNA and introduces a transient break in a single-stranded region. Catalyzes DNA passage via an enzyme-bridge mechanism.	5'-phosphotyrosine	Relaxes negatively supercoiled (underwound) DNA
Type IB	Eukaryotic topoisomerase I Mammalian mitochondrial topoisomerase I Pox virus topoisomerase	Binds double-stranded DNA, transiently cleaves one strand and relieves supercoiling by DNA rotation.	3'-phosphotyrosine	Relaxes positively (overwound) and negatively (underwound) supercoiled DNA
Type II Topoisomerases				
Type IIA	Bacterial gyrase; topoisomerase IV Phage T4 topoisomerase Yeast topoisomerase II Drosophila topoisomerase II Mammalian topoisomerases II α and II β	Catalyze the ATP-dependent transport of one intact DNA double helix through another	5'-phosphotyrosine	Relaxes positive and negative supercoils; decatenates chromosomes; removes intertwinings between newly synthesized DNA double helices
Type IIB	<i>Sulfolobus shibatae</i> topoisomerase VI	Heterotetramer with two A subunits dedicated to DNA cleavage and two B subunits dedicated to ATP hydrolysis	5'-phosphotyrosine	Relaxes both positive and negative supercoils

Wang *et al.* 2002

supercoiled DNA (Nitiss 1998; Pommier *et al.* 1998). The cleavage of DNA by the catalytically active tyrosine hydroxyl of Top1 leads to the formation of the covalent Top1 cleavage complex (Top1cc), in which Top1 covalently associates with the 3' phosphate

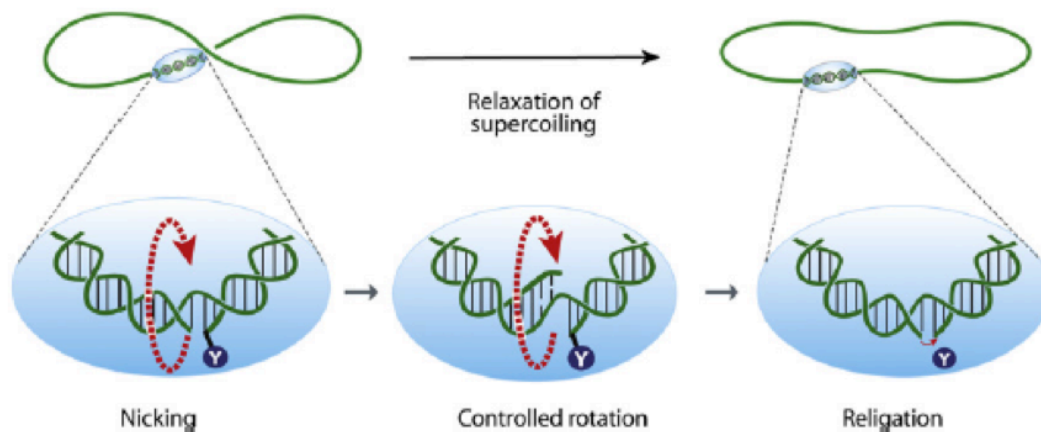


Figure 1. Type IB Topoisomerase (Top1) mechanism of action. Top1 (blue oval) nicks DNA by forming a covalent 3'-phosphotyrosine linkage with the DNA backbone, relaxes supercoiling through a controlled rotation, and religates the DNA. Figure from Pommier *et al.* (2010).

of a broken phosphodiester bond (Pommier *et al.* 1998). This is the first transesterification reaction and is illustrated in **Figure 2**. The cleavage reaction requires that Top1 interacts with both the cleaved and non-cleaved DNA strands (Christiansen *et al.* 1993) and leads to the generation of a single-strand nick. *In vitro*, the eukaryotic Top1 consensus cleavage site was identified as [5'-(A/T)(G/C)(T/A)T-3'] (Been *et al.* 1984). Single-strand passage occurs by a "rotation" where the intact strand is stationary and the nicked strand rotates to remove supercoiling, relieving torsional stress (Stivers *et al.* 1997; Stewart *et al.* 1998). A second transesterification reaction is initiated when the free 5'-hydroxyl group of the scissile strand acts as a nucleophile and attacks the phosphotyrosine linkage. This reaction rejoins the DNA, releases the Top1 and maintains genome integrity (**Figure 2**) (Sekiguchi and Shuman 1997; Reid *et al.* 1998; Vekhoff *et al.* 2012).

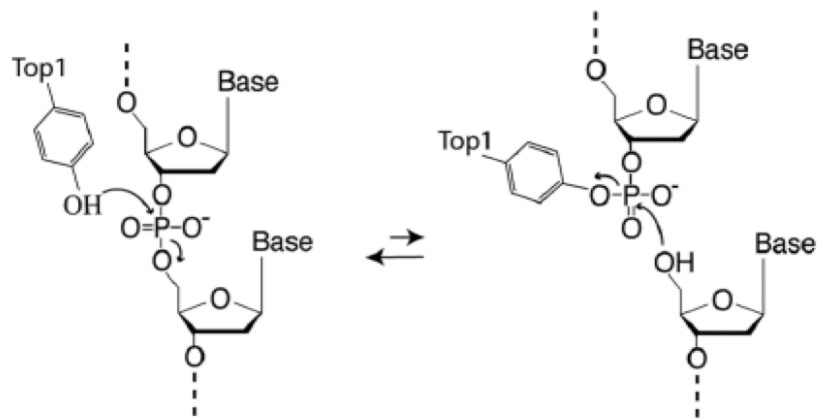


Figure 2. Top1 cleavage of DNA. In the first transesterification reaction, the active site tyrosine of Top1 attacks the DNA backbone generating a covalent 3'-phosphotyrosine bond. In the second transesterification reaction, religation is mediated by the nucleophilic attack of the free 5'-OH on the 3'-phosphotyrosine bond, releasing the Top1 enzyme and religating the DNA backbone. Figure from Kim *et al.* (2011).

1.2.a. Top1 functional domains

Yeast Top1 is a 765 amino acid, 100 kDa protein that is expressed throughout the cell cycle (Heck *et al.* 1988). The Top1 protein is composed of four domains: the N-terminal domain, a conserved core domain, the C-terminal domain and a linker domain. The N-terminal domain contains the nuclear localization sequences and is not conserved among species. The core domain is highly conserved among species, sharing 58% homology between yeast and human Top1. The core domain forms a clamp around the duplex DNA and aids in the rotation of DNA strands (D'Arpa *et al.* 1988; Woo *et al.* 2003). The carboxy-terminal domain is comprised of the last 70 amino acids of the protein and contains the active site tyrosine (Eng *et al.* 1989; Lynn *et al.* 1989); it

displays 68% homology between yeast and human enzymes (D'Arpa *et al.* 1988). The core domain positions the active site tyrosine (yeast amino acid 723, human amino acid 727) of the carboxy-terminal domain within the catalytic pocket of the core domain. The positioning is achieved by the linker domain, which is of variable lengths among species and not essential for Top1 activity (Krogh and Shuman 2000; Woo *et al.* 2003).

Top1 co-immunoprecipitates with the transcription factor IID (TFIID) multiprotein complex and binds directly to the TATA binding protein, suggesting a role in transcriptional initiation. This role is independent of the catalytic activity of Top1, however, with expression of the Top1-Y727F catalytic dead protein in yeast causing no alteration of transcriptional activation (Merino *et al.* 1993). The Top1 domain required for transcriptional regulation is still unknown.

1.2.b. Top1 deficiency

Loss of Top1 in mice and *Drosophila melanogaster* is embryonic lethal suggesting in both model organisms that Top1 is essential for embryonic development (Nitiss 1998). Analysis of *Top-1* homozygous null mouse embryos showed that they are able to develop to the 8-cell stage, but failed to reach the 16-cell stage, indicating Top1 is essential for early cell division and required after fertilization (Morham *et al.* 1996). Using *P*-element mutagenesis to inactivate Top1 in *Drosophila melanogaster* it was demonstrated that Top1 is required during the 6-12hr post-fertilization stage when rapid DNA synthesis occurs (Lee *et al.* 1993).

In the absence of Top1, haploid yeast cells are viable and elevated recombination within the ribosomal DNA (rDNA) gene cluster has been reported (Christman *et al.* 1988; Trigueros and Roca 2002). In addition to elevated mitotic recombination within the rDNA *top1* Δ mutants have disrupted rDNA transcription, the chromosome containing the rDNA locus migrates aberrantly in gels and extrachromosomal rDNA-containing circles are produced (Christman *et al.* 1988; Kim and Wang 1989; El Hage *et al.* 2010).

A study we published in collaboration with the Petes' lab, investigating the genome destabilizing effects associated with Top1 loss in diploid yeast cells, revealed interesting phenotypic consequences. The rate of reciprocal crossovers leading to loss of heterozygosity in a *top1* Δ /*top1* Δ diploid background was not significantly different from that in wild-type (WT) cells. The median recombination-associated repair tracts, however, were longer and more complex than in WT (Andersen *et al.* 2015). In agreement with previous results, *top1* Δ mutants had greatly elevated levels of instability within the tandemly-repeated rDNA genes (Christman *et al.* 1988; Andersen *et al.* 2015).

1.3 Top1-induced DNA damage

Generally, Top1 cleaves the DNA, removes topological stress and religates the DNA. However, base mismatches, abasic lesions and Top1-stabilizing drugs (such as camptothecin [CPT]; described in more detail below) can prevent or significantly delay the religation, leading to a stabilized or persistent cleavage complex (Pourquier and Pommier 2001; Vance and Wilson 2002; Deng *et al.* 2005). Collision of the replication

fork with the Top1cc results in a covalently bound Top1 enzyme at the 3' end of a double-strand break (DSB) that must be removed in order to initiate replication restart or repair.

The major pathway that processes a persistent Top1cc is the Tdp1-mediated pathway (**Figure 3**). Following the proteolytic degradation of the DNA-bound Top1 enzyme, Tdp1 (tyrosyl-DNA phosphodiesterase 1) removes the remaining Top1 peptide by cleaving the covalent Top1-DNA phosphotyrosyl bond, creating a 3'-phosphate terminus (Pouliot *et al.* 1999). In mammals, PNKP (polynucleotide kinase 3'-phosphatase) removes the 3'-phosphate terminus generated by Tdp1 and has a kinase activity that phosphorylates the 5'-terminus, creating 3'-hydroxyl and 5'-phosphate ligatable ends (Iyama and Wilson 2013). In yeast, which lacks PNKP, Tpp1 (DNA 3'-phosphatase) removes the 3'-phosphate generated by Tdp1 (Vance and Wilson 2001); the yeast protein that generates the 5'-phosphate end is unknown. Structural studies of Tpp1 have revealed it has homology with the PNKP 3'-phosphatase domain but lacks the kinase domain. In yeast, Apn1 (AP endonuclease 1) also can remove the 3'-phosphate generated by Tdp1. Not only does Apn1 remove the 3'-phosphate, it additionally removes the 3'-terminal nucleotide (Pouliot *et al.* 2001; Vance and Wilson 2001). A recently characterized protein that functions redundantly with Tdp1 is the metalloprotease Wss1. Loss of both Tdp1 and Wss1 results in yeast cells that are hypersensitive to CPT and accumulate Top1cc in the presence of CPT. *In vitro* analysis indicates that Wss1 is able to cleave Top1 directly when stabilized in a Top1cc (Stingele *et al.* 2014).

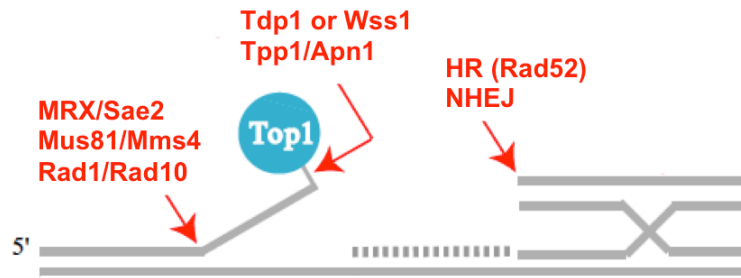


Figure 3. DNA repair proteins that repair Top1-induced DNA damage.

The major pathway that processes a persistent Top1cc is the Tdp1-mediated pathway which cleaves the Top1-DNA phosphotyrosyl bond generating a 3'-phosphate. In the absence of Tdp1, Wss1 is able to act on the Top1-DNA phosphotyrosyl bond. Tpp1 or Apn1 acts on the 3'-phosphate to generate a ligatable end. Alternatively, Rad1/Rad10, Mus81/Mms4 or MRX/Sae2 endonucleases can process 3'-tails to remove the persistent cleavage complex. If a DSB is generated, homologous recombination (HR) or non-homologous end joining (NHEJ) can repair the DSB. Adapted from Pommier *et al.* (2003).

The Rad1/Rad10 complex has been identified as an alternative pathway to remove a stabilized Top1cc. CPT sensitivity assays performed in *tdp1Δ* and *rad1Δ* single mutants showed comparable sensitivity to CPT as wild-type yeast cells. The *tdp1 rad1* double mutant, however, was hypersensitive to CPT suggesting that both pathways are involved in Top1cc processing to remove Top1 (Vance and Wilson 2002). Rad1/Rad10 is required for nucleotide excision repair (NER) and removes nonhomologous tails during recombination and single-strand annealing (Prakash and Prakash 2000). In all these processes the complex removes an unpaired 3' tail. Loss of Rad2 and Rad14 (two NER proteins) does not increase sensitivity to CPT in either a Tdp1- or Rad1-deficient background, demonstrating that the role of Rad1/Rad10 in Top1 repair is independent of

NER (Vance and Wilson 2002). Another 3'-processing activity identified to play a role in Top1 repair is the Mus81/Mms4 complex, which cleaves 3' flaps and branched DNA structures (for example: replication fork-like structures, nicked/partial Holliday junctions and D-loops) *in vitro* (Symington *et al.* 2014). Loss of Mus81 in a *tdp1 rad1* double mutant further increases hypersensitivity to CPT, suggesting that all three proteins/complexes participate in Top1 removal and processing (Vance and Wilson 2002).

A CPT-sensitivity screen of the yeast deletion collection identified three additional endonucleases involved in Top1cc repair: Slx1, Slx4 and Sae2 (Deng *et al.* 2005). Slx1 and Slx4 form a heterodimeric complex that has strong endonuclease activity on branched DNA substrates such as simple Y structures, 5' and 3' flaps, replication forks and Holliday junctions (Fricke and Brill 2003). The *tdp1 slx4* double mutant was sensitive to CPT while the *tdp1 slx1* double was not, suggesting that while Slx1/Slx4 is a heterodimeric complex, the proteins have different functions when it comes to processing a stabilized Top1cc (Deng *et al.* 2005). Loss of the Sae2 endonuclease alone renders yeast cells sensitive to CPT. CPT sensitivity in *sae2 tdp1 rad1* and *sae2 tdp1 mus81* triple mutants is enhanced relative to double mutants, showing that Sae2 plays a functionally redundant role in the repair of Top1cc (Deng *et al.* 2005). The presence of Sae2 has been suggested to be required for the endonuclease role of Mre11-Rad50-Xrs2 (MRX) complex (Mimitou and Symington 2009). By analyzing the nuclease dead version of Mre11, the Mre11-H125N mutant protein, a role of MRX in the repair of Top1cc was demonstrated. While the *mre11-H125N* single mutant is slightly sensitive to CPT the

tdp1 rad1 mre11-H125N triple mutant is hypersensitive, providing evidence that the MRX complex directly removes Top1 from a DNA end. Whether or not Sae2 and MRX act together to repair Top1cc was addressed by comparing a *sae2* single mutant to the *sae2 mre11-H125N* double mutant. No difference in CPT sensitivity was detected. Comparing an *mre11* single mutant to a *sae2 mre11* double mutant also revealed no difference in CPT sensitivity. This suggests that Sae2 and MRX work together. A *sae2 top1* double mutant is not sensitive to CPT, indicating that Sae2/MRX directly act on Top1-generated lesions (Deng *et al.* 2005).

In *Schizosaccharomyces pombe*, the role of the MRX complex and Ctp1 (Sae2 homolog) in the removal of Top1 from a stabilized Top1cc in mitotic cells has been investigated. Analyzing CPT-sensitivity in *S. pombe* cells revealed that *rad50S* (a Rad50 mutant defective in Spo11 removal), *rad32^{mre11}-D65N* (nuclease-dead Mre11 mutant) and *ctp1* single mutants were sensitive to CPT treatment (Hartsuiker *et al.* 2009), similar to results found in budding yeast (Deng *et al.* 2005). A DNA-linked protein detection assay, designed to detect the presence of Top1 covalently bound to DNA, was performed and revealed that bound Top1 levels were significantly higher in the *rad50S* mutant than in WT cells. Covalently bound Top1 levels were higher in the *rad32^{mre11}-D65N* mutant than in WT as well, suggesting that the MRX complex is involved in the removal of Top1. Loss of Ctp1 resulted in a significant decrease in covalently bound Top1 compared to wild-type, suggesting Ctp1 is not directly involved in the removal of Top1 in fission yeast (Hartsuiker *et al.* 2009). The decrease in Top1cc suggests *ctp1Δ* cells are over-proficient in the removal of Top1 and that Ctp1 may have a role in protection of 3'-ends.

1.4 Transcription-associated mutagenesis (TAM) and Top1

High levels of transcription are directly correlated with an increase in mutagenesis, a phenomenon termed transcription-associated mutagenesis (TAM) (Datta and Jinks-Robertson 1995; Kim *et al.* 2007). Most TAM in an unbiased forward mutation assay depends on Top1. In a *CAN1* forward mutation assay performed under high transcription conditions (**Figure 4**), small deletions (2-5 bp) accumulated at distinct hotspots. The distinct hotspots where the deletions occurred were at tandem repeats such as ATAT [(AT)₂], TCTCTC [(TC)₃], or GTTGTT [(GTT)₂], and the size of the deletion equaled the size of the repeat (Lippert *et al.* 2011; Takahashi *et al.* 2011).

In order to investigate the molecular contributors to the 2-5 bp deletion signature, the (AT)₂, (TC)₃ and (AG)₄ hotspots were individually transplanted (about 30 nucleotides surrounding the hotspot) into a *LYS2* frameshift reversion assay that detects 2-bp deletions. Since the system can only detect frameshift mutations, the (GTT)₂ hotspot could not be further investigated (Lippert *et al.* 2011). The 2-bp deletions were elevated under high-transcription conditions, accounting for the majority of mutations detected. The 2-bp deletions were also detected under endogenous (low) levels of transcription, showing that this phenomenon can occur under various transcription conditions and is not limited to high transcription (Lippert *et al.* 2011). Elimination of the *TOP1* gene resulted in loss of the 2-bp deletion signature, indicating the dependence of the deletions on Top1

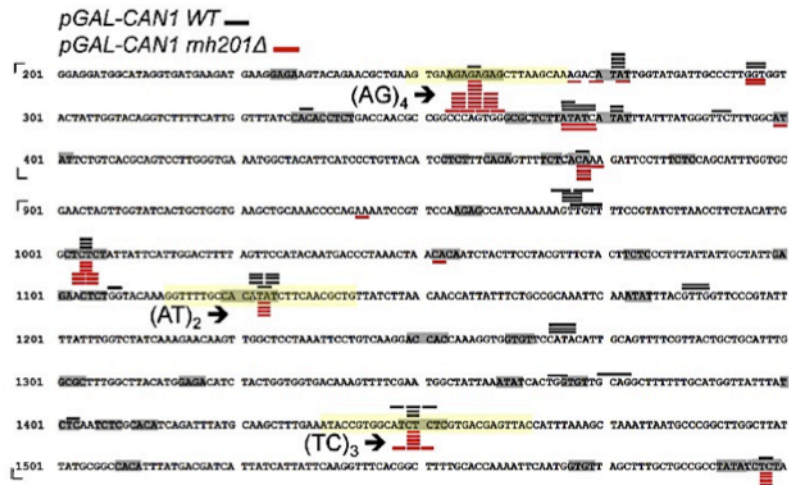


Figure 4. Partial *pGAL-CAN1* mutation spectrum. Deletion events are represented by the bars above or below the sequence. The deletion size equals the size of the repeat. Figure from Cho *et al.* (2013).

(Lippert *et al.* 2011; Takahashi *et al.* 2011). Loss of Tdp1, an enzyme that is reported to aid in the efficient removal of the Top1cc from DNA (Pouliot *et al.* 2001; Liu *et al.* 2004; Deng *et al.* 2005) had no significant effect on 2-bp deletions (Lippert *et al.* 2011; Takahashi *et al.* 2011). Loss of both the Rad1 and Mus81 endonucleases reduced the rate of 2-3 bp deletions 2.7-fold, however, suggesting a role for 3'-flap endonucleases in the removal of trapped Top1 under high-transcription conditions (Takahashi *et al.* 2011).

The transcription-associated increase in deletions is likely due to increased recruitment of Top1 to sites of high transcription and possibly the enhanced trapping of Top1. This was confirmed by chromatin immunoprecipitation (ChIP) analysis with Top1-GFP, which revealed a significant enrichment of Top1-DNA complexes along the *CAN1* ORF under high-transcription conditions. The ChIP signal was 5-fold above that

observed under low-transcription conditions and was weaker around the promoter and downstream of the *CAN1* open reading frame (ORF). However, the enrichment did not correlate well with the 2-3 bp deletion sites (Takahashi *et al.* 2011). **Figure 5** represents the proposed model for the Top1-initiated deletion pathway in which a trapped Top1cc is unable to initiate the Top1-mediated religation reaction (Kim *et al.* 2011; Lippert *et al.* 2011). Following the enzymatic processing of the Top1cc to generate a 2-nt gap, realignment between complementary strands is facilitated by the tandem repeat. Ligation and replication of the scissile strand results in a 2-bp deletion.

Replicative DNA polymerases insert ribonucleotides (rNMPs) into genomic DNA at a low level. Rnh201 is the catalytic subunit of the RNase H2 complex that specializes in the removal of single rNMPs from duplex DNA (Sparks *et al.* 2012). A similar 2-5 bp deletion signature was seen in an Rnh201-deficient background that allows for the persistence of rNMPs in genomic DNA (Nick McElhinny *et al.* 2010). The 2-bp deletion signature associated with rNMP incorporation is also Top1-dependent (Kim *et al.* 2011; Cho *et al.* 2013). Top1 has an endoribonuclease function rendering it capable of nicking 3' of a ribonucleotide incorporated into DNA, a phenomenon originally described with vaccinia virus Top1 (**Figure 6**) (Sekiguchi and Shuman 1997). This activity has more recently been confirmed with biochemical studies using *S. cerevisiae* and human Top1 (Huang *et al.* 2015; Sparks and Burgers 2015). When Top1 nicks 3' of a ribonucleotide the 2'-hydroxyl group of the ribose sugar attacks the phosphotyrosyl linkage, releasing the Top1 from the DNA and generating a 2',3'-cyclic phosphate, as shown in **Figure 6** (Sekiguchi and Shuman 1997).

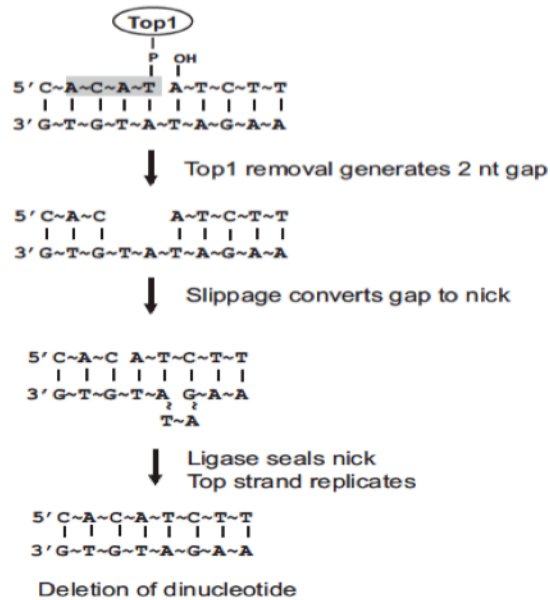


Figure 5. Model for Top1cc-initiated deletions. Top1 cleaves duplex DNA to generate a single-strand break and covalently associates with DNA. Top1cc trapping and enzymatic end processing of the Top1cc results in a 2-nucleotide gap. Repeat-mediated misalignment between strands, followed by ligation and subsequent replication of the Top1-nicked strand will result in a 2-bp deletion. Figure from Lippert *et al.* (2011).

Several studies have led to the identification of two classes of Top1-dependent mutation signatures: ribonucleotide-independent and ribonucleotide-dependent (Kim *et al.* 2011; Lippert *et al.* 2011; Cho *et al.* 2013). In the absence of RNase H2, the Top1 signature was elevated in the (TC)₃ and (AG)₄ hotspots shown in **Figure 4**, but not in the (AT)₂ hotspot. This suggests that 2-bp deletion events at the (TC)₃ and (AG)₄ hotspots are ribonucleotide-dependent, but that those at (AT)₂ are not and presumably reflect processing of a Top1cc (Kim *et al.* 2011; Cho *et al.* 2013). Expression of the Top1-

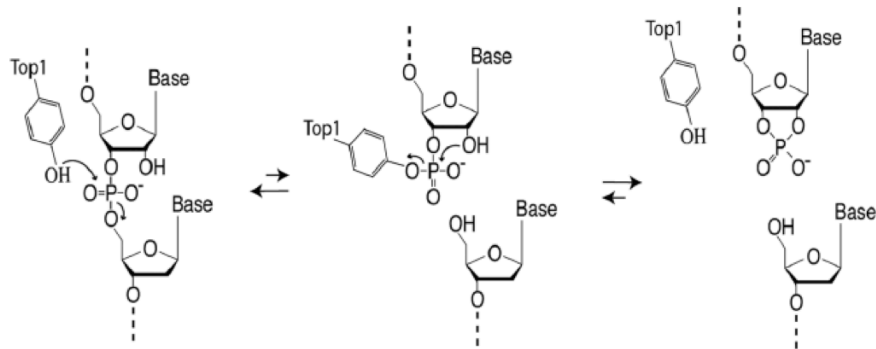


Figure 6. Top1 cleavage at an rNMP. The active site tyrosine of Top1 attacks the DNA backbone generating a covalent 3'-phosphotyrosine bond. If the free 5'-OH attacks the Top1cc then the DNA will religate to release Top1. A ribose sugar contains a 2'-OH that acts as a nucleophile and attacks the 3'-phosphotyrosine. This generates a 2',3'-cyclic phosphate and releases the Top1 enzyme, creating a single-strand break. Figure from Kim *et al.* (2011).

T722A mutant protein, which has reduced Top1-mediated religation activity (Megenigal *et al.* 1997) in strains containing the (TC)₃ and (AG)₄ Top1-dependent hotspots resulted in an unexpected decrease in the 2-bp deletion signature (Cho *et al.* 2013). This suggested a role for Top1-mediated ligation in ribonucleotide-dependent deletions. **Figure 7** illustrates the proposed model for ribonucleotide-dependent deletions. Top1 cleavage occurs 3' of the rNMP, the 2'-hydroxyl attacks the phosphotyrosyl bond releasing Top1 and generating the free 2'-3' cyclic phosphate end. Top1 then cleaves upstream of the single-strand break and becomes trapped. Upon spontaneous release of the short oligonucleotide between the first and second Top1 cleavage sites, realignment is

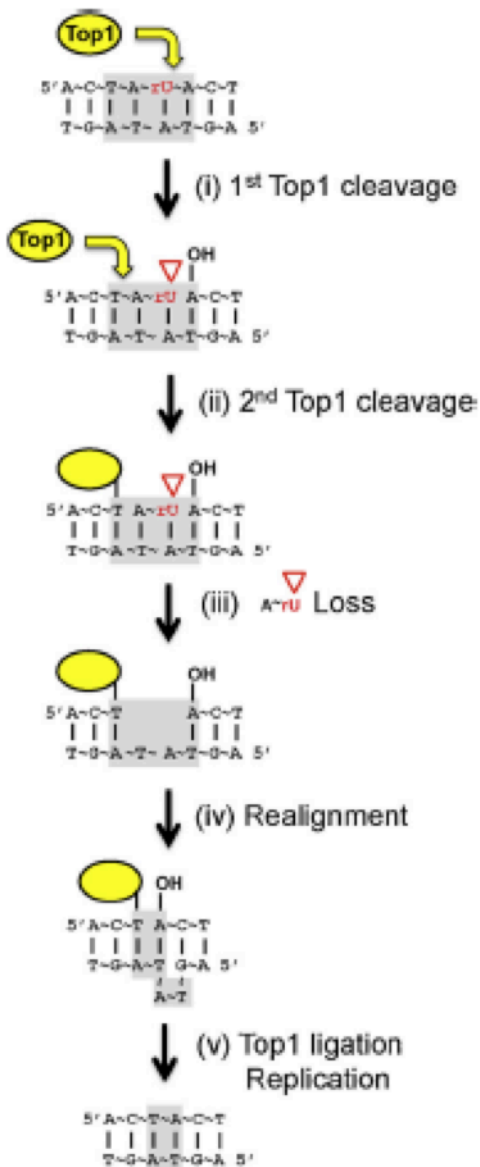


Figure 7. Model for Top1-initiated deletions at a misincorporated rNMP. Top1 cleaves 3' of the inserted rNMP, resulting in a non-canonical break. Top1 cleaves upstream of the single strand break and the short oligonucleotide is lost. Misalignment or a slippage event followed by ligation and replication of the strand where the rNMP was inserted results in a 2-bp deletion. Figure from Cho *et al.* (2013).

facilitated by the tandem repeat and the 5'-hydroxyl mediates the religation and Top1 release (Kim *et al.* 2011; Cho *et al.* 2013).

Biochemical studies have shown that Top1 can cleave DNA substrates containing a pre-existing nick, supporting the ability of Top1 to perform a sequential cleavage reaction (Christiansen and Westergaard 1999). Recent work indicates that reversal of the 2',3'-cyclic phosphate formed by the first Top1-cleavage occurs and is favored over the second Top1 cleavage (Sparks and Burgers 2015). The second Top1 cleavage reaction to remove the 2',3'-cyclic phosphate predominantly occurs 2 nucleotides upstream of nick; cleavage 3, 4 and 5 nucleotides upstream occurs at a low frequency and cleavage 1 nucleotide upstream of a nick was not detected. Biochemically, there is a requirement for repeat sequences at the nick for slippage realignment to occur during Top1-mediated deletion formation. At least *in vitro*, realignment can occur at an imperfect repeat with one-base pair homology during Top1-mediated deletion formation (Sparks and Burgers 2015).

1.5 Top1 as an anti-cancer drug target.

In the 1960s, the CPT molecule was isolated from the Chinese tree *Camptotheca acuminata*. Early research studies showed that CPT had anti-tumor activity in leukemia cells, both inhibiting the growth and decreasing the size of tumor cells (Oberlies and Kroll 2004). However, the toxicity of CPT was too high in patients, resulting in severe

cystitis, myelosuppression, vomiting and diarrhea and its use was discontinued (Oberlies and Kroll 2004; Legarza and Yang 2006). About 20 years later, CPT once again became a chemotherapeutic of interest when it was discovered that the drug solely targets Top1 (Dancey and Eisenhauer 1996; Oberlies and Kroll 2004). Elevated levels of Top1 have been detected in colon adenocarcinoma, ovarian, esophageal, stomach, breast, lung carcinomas, leukemia cells and malignant melanomas (Giovanella *et al.* 1989; Dancey and Eisenhauer 1996).

Elevation of Top1 levels in tumors makes Top1 a relevant molecular target for chemotherapeutic treatment. This finding led to the synthesis of CPT derivatives that have the same mechanism of action, retain or improve efficacy, and have less toxic side effects than CPT (Dancey and Eisenhauer 1996; Ulukan and Swaan 2002; Oberlies and Kroll 2004; Koster *et al.* 2007). CPT derivatives topotecan (or Hycamtin) and irinotecan (or Camptostar) are currently the only two FDA approved derivatives in clinical use. Topotecan is used to treat ovarian and small cell lung cancer, while irinotecan is used for colorectal and gastroesophageal malignancies. Both drugs have recently been used to treat primary brain malignancies, sarcomas, and cervical cancers (Pommier 2013).

To date, Top1 is the only known target of CPT and Top1 deficient cells are resistant to CPT (Pommier *et al.* 1999). Additionally, phenotypes associated with CPT treatment are absent in Top1 null cells, providing further evidence that Top1 is the only cellular target of CPT (Nitiss and Wang 1988). Eukaryotic cells that are resistant to CPT have acquired mutations in the *TOP1* gene that typically affect normal protein function (Pommier *et al.* 1998). Human cancer cells that are resistant to CPT are depleted of Top1

(Miao *et al.* 2007). Finally, biochemical evidence for the requirement of Top1 for the cytotoxicity of CPT is supported by the formation of Top1cc in cells treated with CPT (Covey *et al.* 1989; Subramanian *et al.* 1995; Padget *et al.* 2000; Miao *et al.* 2007).

CPT is a planar molecular that interacts stereospecifically with Top1. CPT forms a ternary complex with the Top1cc (**Figure 8**), where CPT stacks against the Top1-mediated DNA cleavage site at the +1 nucleotide (Pommier *et al.* 1998; Redinbo *et al.* 1998). Studies from multiple labs revealed that CPT preferentially stabilizes a subset of Top1cc that have a guanine in the +1 position and a thymine at -1 (Thomsen *et al.* 1987; Jaxel *et al.* 1988; Porter and Champoux 1989; Jaxel *et al.* 1991; Tanizawa *et al.* 1993). Intercalation of CPT with the Top1cc after DNA cleavage prevents the Top1-mediated religation of DNA and results in an accumulation of stabilized (trapped) Top1cc, which promotes toxic DSB formation (Jaxel *et al.* 1991; Dancy and Eisenhauer 1996; Pommier *et al.* 2003; Koster *et al.* 2007).

The CPT mechanism of action preferentially targets rapidly dividing tumor cells, but also affects non-tumor cells (Pommier *et al.* 1999; Ulukan and Swaan 2002; Pommier *et al.* 2010). Single molecule nanomanipulation studies showed that both CPT and topotecan (TPT) interaction with the Top1cc slows down uncoiling significantly. Religation does not occur until after the completion of the uncoiling phase, which is 20-fold slower than with just Top1 alone (Koster *et al.* 2007). The religation reaction is 400 times slower in the presence of TPT and significantly increasing the lifetime of the normal transient Top1cc (Koster *et al.* 2007). Top1 relieves both positive and negative

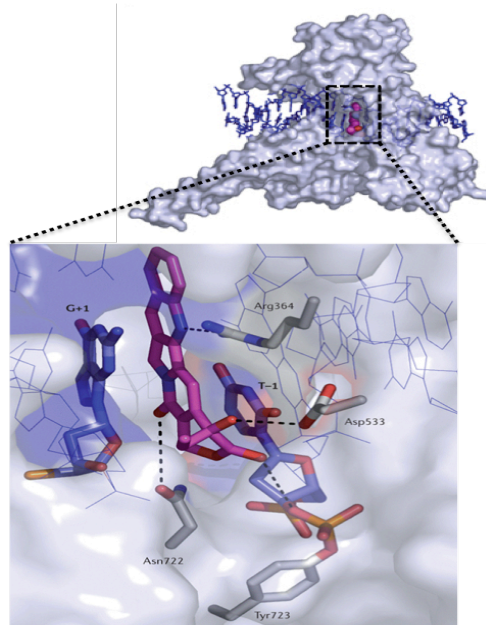


Figure 8. CPT-ternary complex with the Top1cc. The tyrosine (Tyr723) of Top1 (gray) is covalently bound to the DNA (T -1 positions on the scissile strand, blue). CPT (purple structure) hydrogen bonds with the Top1 and DNA. The positioning of CPT inhibits the G+1 nucleotide (blue) from religating the DNA. Figure from Pommier and Marchand (2012).

supercoils at the same rate, but in the presence of CPT the uncoiling of positive supercoils is much slower than the uncoiling of negative supercoils (Koster *et al.* 2007).

CPT significantly delays the religation of nicked DNA and the drug-mediated stabilization of the Top1cc is the direct cause of cell death. Collision of the trapped Top1cc with a replication fork converts the unresolved single-strand break to a toxic DSB (Nitiss and Wang 1988; Pommier *et al.* 2003; Koster *et al.* 2007). Collision of the transcriptional machinery with a trapped Top1cc also results in an irreversible single-

strand break (**Figure 9**) (Hsiang *et al.* 1989; Ulukan and Swaan 2002; Pommier *et al.* 2003). In a normal environment a DSB can be repaired by error-free homologous recombination (HR), which uses a homologous chromosome or a sister chromatid as a repair template. BRCA2 (a major homologous recombination protein in mammals) has been shown to be mutated in breast cancers (Engel and Fischer 2015), enabling the persistence of unrepaired toxic DSB. Yeast cells deficient for Rad52 (major HR protein) are hypersensitive to CPT treatment, providing direct evidence that CPT-induced DNA damage is repaired primarily through recombination (Nitiss and Wang 1988; Hsiang *et al.* 1989; Pommier *et al.* 1999; Pommier *et al.* 2003). Another process called non-homologous end joining (NHEJ) is considered error prone as it does not use homology to repair DSBs. The sensitivity of cells to CPT is substantially enhanced in a background deficient in both HR and NHEJ, suggesting roles for each in the repair of Top1 associated damage (Shao *et al.* 1999; Pouliot *et al.* 2001; Pommier *et al.* 2003). Finally, multiple repair proteins have been identified that aid in the repair of a CPT-stabilized Top1cc, including Tdp1, Rad1/10, Mus81/Mms4, MRX/Sae2 and others (**Figure 3**).

1.5.a. CPT and genome instability

Over 15 years ago CPT was reported to be highly mutagenic, with CPT treatment resulting in a significant increase in mutation frequency in Chinese hamster fibroblast cell lines (Hashimoto *et al.* 1995). This study along with another study reporting an increase

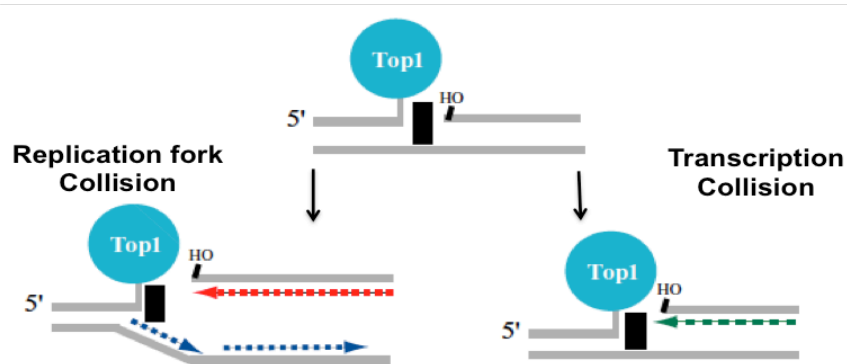


Figure 9. CPT mechanism of action. Top1 (blue circle) cleaves and covalently associates with DNA. CPT (black rectangle) intercalates with the Top1cc, trapping it and preventing the religation of the nicked strand. The replication fork (red arrow) collides with the CPT-Top1cc, causing the formation of a toxic double-strand break. Collision of the transcription machinery with the CPT-Top1cc results in the formation of an irreversible single-strand break. Figure from Pommier *et al.* (2003).

in mutagenesis in Chinese hamster ovary cells after CPT treatment suggested that the mutagenic potential of CPT could lead to secondary malignancies (Hashimoto *et al.* 1995; Balestrieri *et al.* 2001). These studies also provided genetic evidence that CPT stabilizes the Top1cc and that CPT-stabilized Top1cc blocks replication fork progression, leading to DSBs. Attempts to repair the DSBs can lead to elevated sister chromatid exchange or nonhomologous recombination, resulting in deletions or other types of rearrangements (Hashimoto *et al.* 1995; Balestrieri *et al.* 2001).

In a red/white colony assay that measures the ability for heterozygous yeast strains to become homozygous at the *ADE1* or *ADE2* locus, CPT treatment led to increased loss of the WT allele. The level of recombination increased over time (up to 24

hours), with a significant increase in as little as 4 hours or roughly two divisions (Nitiss and Wang 1988). The ability of CPT to induce gene conversions at the *HIS7* locus to generate His⁺ mutants was also examined and a 50-fold elevation in heteroallelic gene conversion was reported (Nitiss and Wang 1988). Another study showed that CPT treatment stimulates sister chromatid exchange 4-fold between tandem truncated *his3* alleles. When the truncated *his3* alleles were placed on chromosomes II and IV, recombination was elevated and non-reciprocal and reciprocal translocations were detected (Fasullo *et al.* 2004). Haploid strains with the *top1-103* allele (proposed CPT mimetic) had significantly elevated recombination within the naturally occurring rDNA locus, with loss of an *ADE2* marker inserted in the rDNA locus occurring approximately 250-fold more often than in wild-type. The *top1-103* allele also caused an elevation in recombination at the *CUPI* locus, where loss of the *CUPI:URA3* marker was 11-fold higher than in wild-type. Finally, loss of *URA3* between tandemly duplicated *HIS4* genes was elevated 24-fold in the *top1-103* mutant as well (Levin *et al.* 1993).

1.5.b. CPT mechanism of action: replication fork collisions with Top1cc and/or accumulation of positive supercoils.

Topoisomerase inhibitors are effective and commonly used anticancer drugs (Pommier 2013). CPT, along with other topoisomerase inhibitors, is classified as a reversible enzyme poison rather than a catalytic inhibitor. Many studies have shown that Top1 is required for the cytotoxicity of CPT and direct evidence comes from the demonstration that Top1-deficient cells are resistant to CPT (Pommier *et al.* 1999), as

previously mentioned. In determining the molecular mechanism of action for CPT, the interfacial inhibition concept was conceived and provides justification for CPT-sequence specificity.

Cytotoxic lesions that are generated are generally assumed to occur when the advancing replication fork collides with the CPT-stabilized Top1cc. Evidence supporting the S-phase dependent generation of CPT-induced cytotoxic lesions comes from experiments performed in the presence of both CPT and aphidicolin, a DNA replication inhibitor, where CPT-sensitivity is no longer detected (Nitiss and Wang 1988; Hsiang *et al.* 1989). A recent study has revealed a new consequence of CPT treatment using single molecule nanomanipulation studies and analyzing global supercoiling in yeast cells (Koster *et al.* 2007). The single molecule nanomanipulation studies showed that CPT slows down the uncoiling and religation of supercoiled DNA and that positive supercoils uncoil much slower than negative supercoils. In global supercoiling analysis, human Top1 was expressed in *top1Δ* yeast cells in the presence or absence of CPT and two-dimensional gel electrophoresis was performed to resolve the distributions of 2μM plasmid DNA topoisomers. An accumulation of positive supercoils was detected in the presence of CPT but not in its absence. To confirm that this was the result of CPT, a catalytically active but CPT-resistant Top1 mutant (Top1-G365C) was expressed in *top1Δ* yeast cells and the mutant failed to accumulate positive supercoils in the presence of CPT (Koster *et al.* 2007). This result suggests positive supercoil accumulation as a possible mechanism for inducing cell death in the presence of CPT (**Figure 10**). The CPT-associated accumulation of positive supercoils could act as a direct barrier for

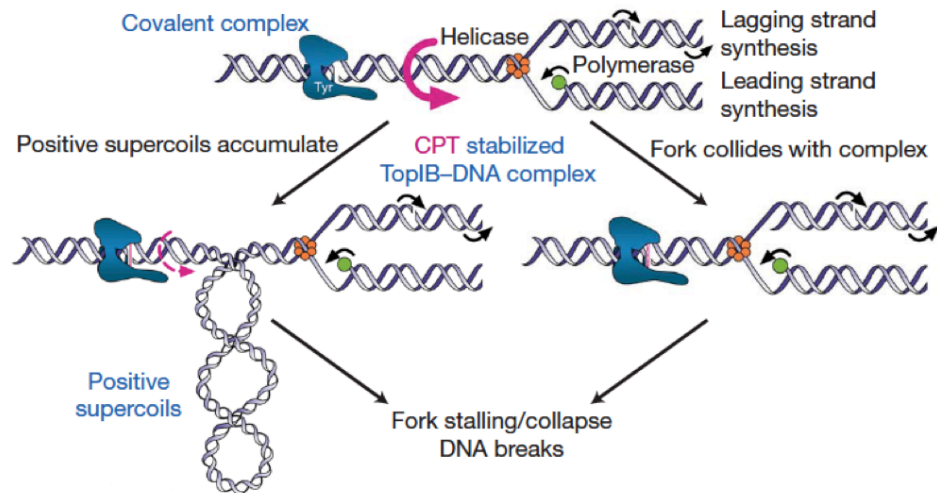


Figure 10. Two models of CPT-induced mechanism of lethality. CPT stabilizes or prolongs the life of the Top1cc (blue). Either a stabilized Top1cc or unresolved positive supercoils can lead to fork stalling and/or collapse, which leads to cell death. Figure from Koster *et al.* (2007).

replication fork progression, leading to fork stalling/collapse or even fork reversal and processing into a DSB (Koster *et al.* 2007; Ray Chaudhuri *et al.* 2012).

1.6 Top1 in human health and disease.

Top1 has been implicated in various human diseases and viruses, such as: cancer, autism, HIV-1, Epstein Barr Virus and herpes simplex, which will be discussed below.

When comparing tumor tissues to matched normal tissues, Top1 levels have been reported to be higher in some tumor types (Giovanello *et al.* 1989). A significant increase

in Top1 levels have been detected in surgical specimens or cultures for the following cancers: colon adenocarcinoma, ovarian, esophageal carcinoma, non-Hodgkin's lymphoma, leukemia, stomach carcinoma, breast carcinoma, lung carcinoma and malignant melanomas (Potmesil 1994). Importantly, cells expressing high levels of Top1 have been shown to be hypersensitive to CPT (Bjornsti *et al.* 1989; Madden and Champoux 1992). Several studies have shown that Top1 transcription level increases during cell proliferation (Sobczak *et al.* 1989; Romig and Richter 1990), which correlates with higher levels of Top1 in cancerous cells. In baby hamster kidney cells overexpressing Top1, there was no affect on cell growth or change in cell morphology compared to cells expressing wild-type Top1 levels. Although these cells were hypersensitive to CPT, results suggest that higher levels of Top1 alone are not cytotoxic to the cell and, therefore, not sufficient to cause cell transformation (Madden and Champoux 1992).

A study using fluorescence *in situ* hybridization (FISH) to measure *TOP1* gene levels in 154 colorectal cancer (CRC) tumors revealed 80% of samples had elevated *TOP1* gene copy numbers compared to normal mucosa. In addition to extra copies of the *TOP1* gene, 64% had additional copies of chromosome 20 indicating that high *TOP1* gene copy number was often the result of aneuploidy. The increased proliferation of CRC tumors was not correlated with high *TOP1* gene copy number or aneuploidy of chromosome 20 (Romer *et al.* 2012; Romer *et al.* 2013). To determine if Top1 inhibitors would be effective in the presence of high *TOP1* gene levels, 10 CRC cell lines (7 of the cell lines with increased *TOP1* gene copies) were treated with the active metabolite of

irinotecan (SN-38) and cell lines with high *TOP1* gene copies had increased sensitivity (Romer *et al.* 2012). *FISH* has additionally been used to measure *TOP1* gene copy number in metastatic breast, bile duct and pancreatic cancers. All three cancers had elevated *TOP1* gene copy numbers in 30%, 58% and 65% of tumor tissues analyzed, respectively (Grunnet *et al.* 2015; Kumler *et al.* 2015). These results provide strong evidence that measuring Top1 gene copy number can serve as a tool for determining the effectiveness of Top1 inhibitors, which increases with increased *TOP1* levels.

Top1 has been implicated in playing a regulatory role in the neurodevelopmental disorder autism. Some studies have indicated that individuals with autism spectrum disorder are likely to have mutant Top1 (Iossifov *et al.* 2012; Neale *et al.* 2012), suggesting that Top1 plays a regulatory role in the prevention of autism. A recent study revealed that Top1 is important for facilitating the transcription of long genes, particularly those over 200kb in length. Top1 inhibition led to reduced expression of long genes in mouse and human neurons, including ASD candidate genes involved in neuronal development and synaptic function (King *et al.* 2013). These results suggest the regulatory role for Top1 in preventing autism.

Top1 plays an important role in viral DNA replication and transcription (Champoux 1988). Numerous studies have examined the role of Top1 in viral DNA replication by utilizing the Top1 inhibitor CPT or one of its clinically approved derivatives. Such Top1-targeting drugs are potent inhibitors of type 1 human immunodeficiency virus (HIV-1) replication and transcription (Li *et al.* 1993). These results suggest that Top1 could potentially be an effective drug target for treatments

inhibiting the transcription of HIV-1. HeLa cells infected with HIV-1 showed elevated reverse transcriptase activity, which was reduced in the presence of CPT (Takahashi *et al.* 1995). The ability of Top1 to enhance reverse transcriptase activity suggest that Top1 inhibitors could potentially act as effective antiretroviral therapies (Warren *et al.* 2009).

Studies with Raji B cells infected with Epstein-Barr virus (EBV) showed that when treated with CPT, both viral and total protein synthesis was inhibited. CPT inhibited the amplification of EBV DNA in a dose-dependent manner, reduced the amounts of amplified viral DNA and specifically affected replicating DNA versus the amount of endogenous EBV DNA, suggesting a role for Top1 in the lytic phase of the EBV life cycle (Kawanishi 1993).

Finally, a role of Top1 in herpes simplex virus 2 (HSV2) growth was shown by examining the effect of CPT on human embryonic fibroblasts infected with HSV2. The growth of HSV2-infected cells was inhibited and was hypersensitive to CPT. CPT treatment suppressed the synthesis of early viral proteins and of proteins of large molecular weights and reduced the level of early viral mRNA. These findings suggested a vital role for Top1 in both the replication and transcription of HSV2 (Yamada *et al.* 1990).

1.7 This dissertation

This dissertation examines Top1-associated genome instability in yeast and has two major areas of focus. The majority of my work focused on investigating the effects of persistent Top1cc on recombination and mutagenesis. Chapter 2 examines recombinogenic effects of persistent Top1cc, where Top1cc were stabilized by CPT or by expression of the mutant *top1-T722A* (CPT mimetic) allele. Chapter 3 examines the mutagenic effects of persistent Top1cc, specifically looking at the potential for CPT to induce mutagenesis at Top1-dependent deletion hotspots. Finally, Chapter 4 investigates the mutagenic potential of elevated Top1 protein levels.

2. Genome-wide effects of persistent Top1 cleavage complexes in yeast by camptothecin

2.1 Introduction

Camptothecin (CPT) and its derivatives (topotecan and irinotecan) are drugs widely used in the treatment of a variety of malignancies that include colorectal, non-small cell lung, cervical, small cell lung, breast, head & neck and ovarian cancers (Dancey and Eisenhauer 1996; Ulukan and Swaan 2002; Oberlies and Kroll 2004; Pommier 2013). To date, Top1 is the only known target of CPT and Top1-deficient cells are resistant to CPT (Dancey and Eisenhauer 1996; Pommier *et al.* 1999; Oberlies and Kroll 2004). Elevated levels of Top1 have been detected in numerous carcinomas (Giovannella *et al.* 1989; Dancey and Eisenhauer 1996), making Top1 a relevant molecular target for chemotherapeutic treatment.

The intercalation of CPT with a DNA-bound Top1 cleavage complex (Top1cc) prevents the religation of DNA, which both aids in toxic double-strand break (DSB) formation and causes an accumulation of stabilized (trapped) Top1cc (Jaxel *et al.* 1991; Dancey and Eisenhauer 1996; Pommier *et al.* 2003; Koster *et al.* 2007). This mechanism of action preferentially targets rapidly dividing tumor cells, but also affects non-tumor cells (Pommier *et al.* 1999; Ulukan and Swaan 2002; Pommier *et al.* 2010). Although CPT prevents religation of nicked DNA, the drug-mediated stabilization of the Top1cc does not directly cause cell death. Rather, collision of the trapped Top1cc with a

replication fork converts the unresolved single-strand break to a toxic DSB (Nitiss and Wang 1988; Pommier *et al.* 2003; Koster *et al.* 2007). Collision of transcriptional machinery with a trapped Top1cc results in an irreversible single-strand break, which also can be converted to a DSB during replication (Hsiang *et al.* 1989; Ulukan and Swaan 2002; Pommier *et al.* 2003). The genome changes produced in cells that survive chemotherapeutic treatment with CPT analogs are of clinical interest because of their potential role in driving secondary neoplasms.

In this chapter I present our examination of global genomic consequences of conditions that elevate the levels of Top1cc in diploid strains. An elevated frequency of cleavage complexes was produced by treatment of WT cells with CPT or by expression of a CPT-mimetic *top1* mutant allele (*top1-T722A* (Megenigal *et al.* 1997). Single-nucleotide polymorphism (SNP)-detecting microarrays were used to map positions of mitotic crossovers on the right arm of chromosome IV, and to monitor loss of heterozygosity (LOH) genome wide (St. Charles *et al.* 2012; St. Charles and Petes 2013). Top1-T722A expression or CPT treatment of WT cells substantially increased LOH throughout the genome, including that associated with rDNA tandem repeats. CPT treatment of WT or Top1-T772A expression also greatly stimulated copy-number variation (CNV) within the repetitive *CUP1* locus, suggesting that CNV is a frequent consequence of stabilized Top1 cleavage complexes. The data presented here is my contribution to a manuscript entitled, “Genome-destabilizing effects associated with Top1 loss or accumulation of Top1 cleavage complexes in yeast” published in PLoS Genetics (Andersen *et al.* 2015).

2.2 Experimental methods

2.2.a. Strains and plasmids

All experiments were done using diploids formed by crossing derivatives of the haploid strains W303-1A (Thomas and Rothstein 1989) and YJM789 (Wei *et al.* 2007). The resulting diploids were heterozygous for about 55,000 SNPs. The wild-type *TOP1/TOP1* diploids used in the study were JSC25 (*MATa/MAT α Δ ::HYG leu2-3,112/LEU2 his3-11,15/HIS3 ura3-1/ura3 GAL2/gal2 ade2-1/ade2-1 trp1-1/TRP1 can1-100 Δ ::NAT/CAN1 Δ ::NAT RAD5/RAD5 IV1510386::KANMX-can1-100/IV1510386::SUP4-o*) and PG311 (*MATa/MAT α Δ ::NAT ade2-1/ade2-1 trp1-1/TRP1 ura3-1/URA3 can1-100/can1- Δ ::SUP4-o gal2/GAL2 ho/ho::hisG*); the constructions of the wild-type diploids have been described previously (Lee *et al.* 2009; St. Charles and Petes 2013). These diploids are isogenic except for changes introduced by transformation; JSC25 has the *SUP4-o* gene located near the right end of chromosome IV, and PG311 has *SUP4-o* located near the left end of chromosome V. The *top1/top1* diploid SLA46.D4 (which has the *TOP1*-containing plasmid pWJ1491) is a derivative of SLA43D generated by replacing the *MAT α* gene with the *HYG* marker. This replacement was done using a PCR fragment amplified from a *MAT α Δ ::HYG* strain (SLA46.19) using the primers Malpha::URA3F(big) (5'-AATCGTCCTGTCCCATTACG-3') and Malpha::URA3R(big) (5'-TTGGAAACACCAAGGGAGAG-3'). SLA43D was constructed by mating the haploids SLA36.A and SLA42.5. SLA36.A was constructed in

several steps. First, W1588-4C, a *RAD5* derivative of W303-1A (Zhao *et al.* 1998), was transformed with a *top1* Δ -containing PCR fragment generated by amplifying the *NAT*-containing plasmid pAG25 (Goldstein and McCusker 1999) with primers top1-NAT F (5'-

TCTCTGTTACTCTAATTACCTGAGTCCTATTCTTATAGTATTTAAAACAGCCGTA
CGCTGCAGGTCGAC-3') and top1-NAT R (5'-

ACTTGATGCGTGAATGTATTTGCTTCTCCCCTATGCTGCGTTTCTTTGCGATCG
ATGAATTCGAGCTCG-3'). The resulting *top1* Δ strain (SLA24.5) was transformed with a PCR fragment generated by amplifying the plasmid pFA6a (Wach *et al.* 1994) with primers 1510336 KANMX (5'-

CCTATTTTTCATACGTTATGCACTTCATTCTTCTTGTCGGTTTGATAACAACGC
TGCAGGTCGAC-3') and 1510435 KANMX (5'-

GGTATGGCTTCTGCCGGGCTAACGTTCAAATTAAGGAACTAGATTCTGCATC
GATGAATTCGAGCTCG-3'). The resulting strain (SLA30) had an insertion of the *KANMX* cassette near the right end of chromosome IV. The strain SLA30 was transformed with the *TOP1*-containing plasmid pWJ1491 (described below) to generate the haploid SLA36.A.

SLA42.5, the other haploid parent of SLA46.D4, is isogenic with YJM789 (Wei *et al.* 2007) except for changes introduced by transformation. To generate this strain, haploid PSL4 (Lee *et al.* 2009) was transformed with a PCR fragment produced by amplifying genomic DNA of JSC21 (St. Charles and Petes 2013) with primers IV:SUP4-o Wide F (5'-AACCGCCGGAAGAAGTTTGG-3') and IV:SUP4-o Wide R (5'-

AGTTGTAATGGTTCTACCTAGCAAAGG-3’). The resulting strain (SLA35.9) had an insertion of *SUP4-o* near the right end of chromosome IV. SLA42.5, the *top1Δ::NAT* derivative of SLA35.9, was constructed by the same method as described above for SLA24.5.

In different experiments, SLA46.D4 was transformed with pRS416 (*CEN*- and *URA3*-containing control plasmid; (Sikorski and Hieter 1989)), pWJ1490 (pRS416 containing the *pCUP1-top1-T772A* gene), or pWJ1491 (pRS316 containing the *pCUP1-TOPI* gene). The control vector pRS416 was described previously (Sikorski and Hieter 1989). The plasmids pWJ1490 and pWJ1491 were derived from the plasmids pWJ1440 and pWJ1441 (Reid *et al.* 2011), respectively, and were constructed by R. Reid and R. Rothstein (Columbia University). The plasmid pWJ1440 was treated with *EagI*, and the fragment containing the *pCUP1-top1-T772A* fusion gene was inserted into the *EagI* site of pRS416 to make pWJ1490. The same approach was used to insert the *pCUP1-TOPI* gene derived from pWJ1441 into *EagI*-treated pRS416 to construct pWJ1491.

2.2.b. Colony sector analysis

For CPT sectoring assays, cells were grown non-selectively in YPD (1% yeast extract, 2% Bacto-peptone, 2% dextrose; 2% agar for plates) with only 10μg/ml adenine hemisulfate (Lee *et al.* 2009; Lee and Petes 2010; St. Charles *et al.* 2012; St. Charles and Petes 2013) to saturation, diluted to 3×10^5 cells/mL in YPD medium containing either 500μM CPT (Sigma C9911, 20mg/ml stock dissolved in DMSO) or DMSO (untreated

control) and grown at 30°C for 6 hours. After CPT treatment, cells were washed with H₂O and appropriate dilutions were plated on synthetic complete dextrose medium containing a reduced amount of adenine hemisulfate (10µg/ml) and lacking arginine with (SD/low Ade-Arg) to determine total cell number and screen for sectors. In the case of PG311, cells were plated on SD/low Ade-Arg plates that contained 240µg/ml canavanine to screen for sectors; a higher concentration of canavanine was used to reduce background growth.

To measure sectoring in a *top1*Δ background, SLA46.D4 was streaked on YPD plates and then replica plated onto synthetic complete dextrose medium lacking uracil (SD-Ura) to identify colonies that had lost the complementing *TOP1-URA* plasmid (pWJ1491). To examine the effect of the *top1-T722A* allele on sectoring, appropriate plasmids were introduced by lithium acetate transformation and transformants were selected on SD-Ura plates (Cho *et al.* 2013). Individual Ura⁺ colonies were resuspended in water and an appropriate dilution plated on SD/low Ade-Arg-Ura plates to determine total cell number and to screen for sectors. Following purification, presence of the *SUP4-o* marker in the white portion of the sector was confirmed by patching onto SD-Ade medium; presence of the appropriate drug resistant marker in the red sector was confirmed by patching onto YPD plates containing Kanamycin (for JSC25) or Hygromycin (for PG311). Only verified sectors were used to calculate sectoring rates.

2.2.c. Sub-culturing

To measure the effects of CPT on genome stability, we streaked JSC25 or PG311 to yield single colonies on YPD plates, YPD plates containing 500 μ M CPT + DMSO, or YPD plates containing an equivalent amount of DMSO. Plates were incubated at 30°C for two days and a single colony was then streaked again onto the same type of medium. The re-streaking of a single colony was repeated 10 times, with each re-streaking corresponding to one sub-culture. Following transformation of a *TOP1*-containing, *top1-T722A*-containing or control plasmid into SLA46.D4, selected colonies were sub-cultured as described above on SD-Ura plates in order to maintain the plasmids.

2.2.d. Analysis of LOH using microarrays

Oligonucleotide-containing DNA microarrays that contained oligonucleotides were perfectly matched to either W303-1A-specific SNPs or YJM789-specific SNPs; similar arrays were used previously by Gresham *et al.* (Gresham *et al.* 2010). Two types of microarrays were used: one that was specific for SNPs located on the right arm of chromosome IV (St. Charles and Petes 2013) and one that could be used to assay LOH throughout the genome (St. Charles *et al.* 2012).

Using the methods employed previously (St. Charles and Petes 2013; Yin and Petes 2013), we examined correlations between the breakpoints of these events and various chromosome elements such as centromeres, tRNA genes, and retrotransposons.

2.2.e. Genome-element association analysis of crossovers (COs) on right arm of chromosome IV

To determine whether particular genome features were over- or under-represented at CO breakpoints, we first delineated a window for each CO as the region most likely to have contained the recombinogenic DNA break. In the case of the CPT treated sectors analyzed, the windows included from the last heterozygous SNP to the first homozygous SNP. The windows were summed (2.00×10^6 kb total) and then divided by the total amount of the genome that was screened for COs (1.1×10^6 kb of chromosome IV in each of 20 sectors, or 2.2×10^7 kb total). This calculation yielded 2.12×10^{-2} as the fraction of the total kb examined that is contained within the windows. For each genome feature we determined how many total features were detectable within the 2.2×10^7 kb total region screened, then multiplied that by the fraction of the region found within the windows (2.12×10^{-2}) to yield an expected number of features. For example, there are 28 ARS elements within the 1.1×10^6 kb of sequence screened for COs on the right arm of chromosome IV and, therefore, 560 ARS elements total in the 20 sectors. Of the 560 ARS elements, 12 ($560 \times 2.12 \times 10^{-2}$) are predicted to fall within our CO-associated windows. We counted the number of each feature that overlapped with the CO-associated windows to generate the observed number. Chi-square analysis was then used to compare the expected and observed numbers for each genome feature. For Ty elements we used midpoint coordinates rather than the full element, as their large size made them more likely to overlap the windows and be over-represented. The same method was used to delineate genome associations from the 20 *top1-T722A* expressing sectors.

2.2.f. Analysis of a *SpeI* polymorphism to detect reciprocal crossovers initiating in the rDNA locus

A region ~21 kb downstream of the rDNA locus on Chromosome XII was PCR amplified from the genomic DNA or sub-cultured colonies. A PCR product of about 750 bp was generated using primers ChrXIIF490730 (5'-CTGATGAGTTCTGCATCTGTCC-3') and ChrXIIR491473 (5'-TCCGTTACCATTGCATACAGAA-3'). Within this fragment, there is a *SpeI* restriction site specific to the YJM789 allele. Digestion of the PCR product with *SpeI* results in two fragments of about 500 and 250 bp when the YJM789 allele is present, and a single 750 bp fragment when the W303-1A allele is present. *SpeI* digests were analyzed on a 1% agarose gel to determine whether the diploid strain remained heterozygous or became homozygous for relevant SNP during sub-culturing.

2.2.g. Southern hybridization analysis of CUP1 tandem arrays

Genomic DNA was isolated from 5 ml of saturated YPD cultures using a modified standard isolation procedure (http://jinksrobertsonlab.duhs.duke.edu/protocols/yeast_prep.html) or was extracted in agarose plugs as described by Lobachev *et al.* (Lobachev *et al.* 2002). If DNA plugs were used, the plugs were equilibrated in CutSmart Restriction Digestion Buffer before overnight digestion with *EcoR*. Digested samples were examined by electrophoresis on

1% agarose using the BioRad CHEF Mapper XA System. The switching interval was optimized for DNA molecules in the 10-60 kb range. Following transfer of the separated DNA fragments to a nitrocellulose membrane, the membrane was hybridized to a DIG-labeled *CUPI* probe at 42°C for at least 16 hours. To obtain the probe, we PCR-amplified a 1 kb segment of the *CUPI* repeat (including the entire *CUPI* gene) from genomic DNA of an isogenic derivative of the strain SJR282 (Datta and Jinks-Robertson 1995) using primers CUP1-amp3 and CUP1-amp5-2 (Zhao *et al.* 2014). The PCR product was then labeled with digoxigenin-UTP (DIG) using the Roche Diagnostics DIG-High Prime DNA Labeling and Detection Starter Kit II (Roche 11585614910). Hybridization of the probe to the filter was detected with the CSPD chemiluminescent alkaline phosphatase substrate (Roche 11755633001). Alterations in the number of *CUPI* repeats per array was detected by comparing the sizes of *CUPI*-hybridizing fragments to those in the starting strain. When multiple bands were observed, our conclusions were based on the two strongest bands. To estimate the number of *CUPI* repeats lost or gained, we plotted the molecular size in kb versus the distance migrated in millimeters using Bioline Hyperladder VI or BioRad CHEF DNA Size Standard as standards. We then generated a trend line to estimate the size of the *CUPI* fragment based on the distance migrated.

2.2.h. Other genetic and physical methods

Standard methods were used for mating, transformation, and media preparation (Guthrie C 1991).

2.2.i. Statistical analysis

Depending on the experiment, statistical comparisons were done using the chi-square test, the Fisher exact test, or the non-parametric Mann-Whitney test. These tests were done using the VassarStats Website (<http://vassarstats.net>). To determine 95% confidence limits on the proportions of sectored colonies, we used Method 3 described by Newcombe (Newcombe 1998).

2.3 Results

2.3.a. Stabilization or accumulation of Top1 cleavage complexes (Top1cc) elevates the rate of mitotic crossovers

We used diploid strains constructed by mating derivatives of two sequence-diverged haploids, W303-1A and YJM789 that differ by 55,000 single-nucleotide polymorphisms (SNPs) (Wei *et al.* 2007), to detect mitotic recombination events between homologs; specifically we can detect loss of heterozygosity (LOH) events. JSC25 and SLA46.D4 have an insertion of the ochre-suppressing *SUP4-o* gene near the right telomere (SGD coordinate 1510386) of chromosome IV on the YJM789-derived homolog and an insertion of a *KANMX* gene, conferring geneticin resistance, inserted at the exact same position on the W303-1A-derived homolog. This diploid is also homozygous for the *ade2-1* ochre allele; zero, one or two copies of the *SUP4-o* in a

diploid *ade2-1/ade2-1* background result in red, pink or white colonies, respectively. JSC25 and SLA46.D4 thus form pink colonies, but can be screened for red/white sectored colonies that result from a reciprocal crossover (RCO) events between the centromere on chromosome IV (*CEN4*) and the inserted *SUP4-o/KANMX* markers (**Figure 11**). As pictured, the red portion of the sectored colony (**Figure 11**, white arrow) contains no copy of *SUP4-o* and is geneticin-resistant, while the white portion contains two copies of *SUP4-o* and is geneticin-sensitive. The formation of a sectored colony requires that a recombination event occur at the time of plating so the frequency of sectored colonies is equivalent to a rate measurement. The production of a sectored colony also requires that each daughter cell contain one recombinant and one non-recombinant chromosome (**Figure 11**).

In order to examine the effect of stabilized Top1cc, we used two approaches to stabilize Top1cc: (1) camptothecin (CPT), a drug that targets and stabilizes the Top1cc and (2) the *top1-T722A* mutant allele. In CPT experiments, we incubated JSC25 for six hour in rich growth medium that contained 500 μ M CPT dissolved in dimethyl sulfoxide (DMSO) or DMSO only, as a control. As seen in **Figure 12**, CPT treatment elevated the rate of RCOs about 8-fold. We found 79 sectors among 3.1×10^5 total colonies screened from CPT-treated cells (rate= 2.5×10^{-4}) and four sectors in 1.3×10^5 colonies from DMSO treated control cells (rate= 3.1×10^{-5}); this is a statistically significant difference ($p < 0.0001$ by a chi-square test using Yates derivative). Although only four sectored colonies were detected among DMSO-treated cells, the calculated rate is in agreement with that reported previously (St. Charles and Petes 2013).

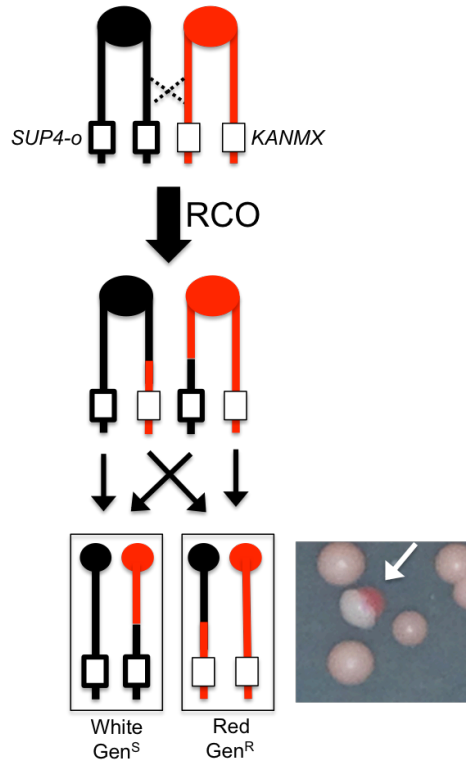


Figure 11. Detecting RCOs on chromosome IV in JSC25. JSC25 chromatids shown in red are derived from W303-1A and contain a *KANMX* cassette on the right arm of chromosome IV. Chromatids in black are derived from YJM789 and contain a *SUP4-o* marker on the right arm of chromosome IV. In addition the diploid strain is homozygous for the *ade2-1* mutation. An RCO that leads to LOH generates a red/white sectorized colony (white arrow) when the daughter cells segregate.

To confirm that the CPT effect on crossovers was not limited to RCOs on chromosome IV, we used a related diploid strain PG311 in which crossovers on the left arm of chromosome V can be more easily detected. In PG311, one homolog has the *can1-100* ochre allele located about 33kb from the left end of chromosome V; on the other homolog, the *CAN1* gene was replaced with the ochre-suppressing *SUP4-o* allele.

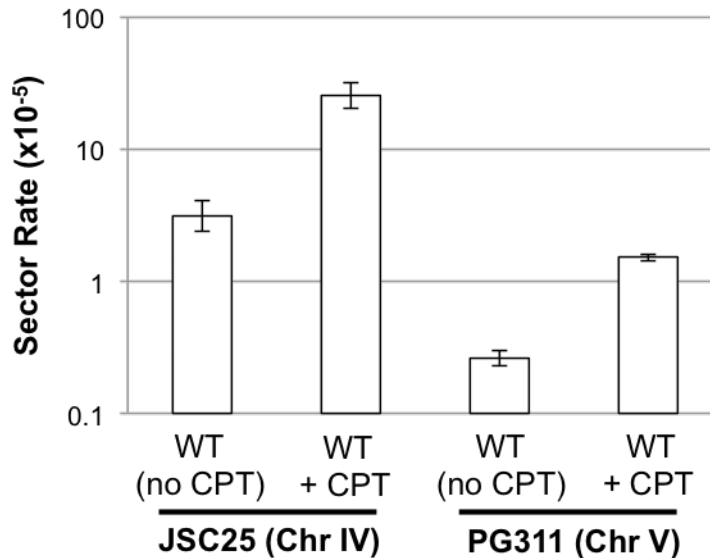


Figure 12. CPT treatment elevates the rate of RCOs. Rates of red/white sectoring associated with CPT treatment.

This diploid is also homozygous for the *ade2-1* ochre mutation. Crossovers between *CEN5* and the *can1-100/SUP4-o* markers result in canavanine-resistant red/white colonies (**Figure 13**). Because only canavanine-resistant colonies of PG311 need to be screened for red/white sectors (as opposed to all JSC25 colonies) we can obtain a more accurate measurement of the rate of RCOs in the control and experimental strains. We found that treatment of PG311 with CPT elevated the rate of RCOs 6-fold relative to the untreated control (**Figure 13**). We observed 190 Can^R red/white sectoring colonies (total of 7.3×10^7 cells plated) in the untreated control compared to 761 sectoring colonies (total of 5×10^7 cells plated) in the CPT treated cells, a difference that is significant ($p=0.001$)

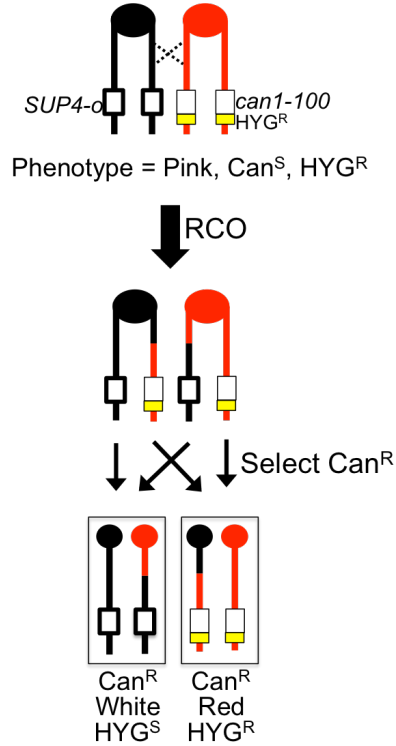


Figure 13. Detecting RCOs on chromosome V in PG311. Chromatids in red are derived from W303-1A and contain a *can1-100* ochre mutation with a closely-linked Hygromycin resistance cassette (HYG^R , yellow box) cassette on the left arm of chromosome V. Chromatids in black are derived from YJM789 and contain a *SUP4-o* marker on the left arm of chromosome V. In addition, the diploid strain is homozygous for the *ade2-1* mutation. In the event a reciprocal crossover occurs that leads to loss of heterozygosity (LOH), a red/white sectorized Can^R colony will form after the daughter cells segregate.

by chi-square test. The difference in RCO rates on chromosomes V and IV is consistent with the difference in the size of the intervals monitored.

Next we looked at the effect of Top1-T722A expression on RCOs on the right arm of chromosome IV. We transformed *top1Δ/top1Δ* strain (SLA46.D4) with the

pWJ1490 plasmid (single copy plasmid that contains the coding sequence of the *top1-T722A* allele fused to the copper-inducible *CUP1* promoter, *pCUP1* (Reid *et al.* 2011)). For controls, SLA46.D4 was transformed with empty vector (pRS416) or with a *pCUP1-TOPI* construct (pWJ1491). Because the addition of copper to the plasmid-selective growth medium was not required for induction of the *pCUP1-top1-T722A* allele (Reid *et al.* 2011), experiments were performed without the addition of exogenous copper. Expression of the *top1-T722A* allele elevated the red/white sector frequency 5-fold ($p < 0.0001$) relative to cells containing either empty vector (*top1Δ/top1Δ*) or the *pCUP1-TOPI* allele (**Figure 14**).

2.3.b. Characterization of reciprocal crossover (RCO) events on chromosome IV associated with stabilized Top1 cleavage complexes

The diploid yeast strains used here were derived by mating haploids that differ by 55,000 SNPs. LOH events involving about 15,000 SNPs distributed throughout the genome can be monitored using SNP microarrays. To molecularly characterize RCO events occurring on the right arm of chromosome IV (a 1 Mb region) microarrays containing SNPs specific for this region were used (St. Charles and Petes 2013). Briefly, genomic DNA was isolated from colonies derived from both the red and white sides of individual sectorized colonies. DNA from the experimental samples was labeled using nucleotides tagged with a fluorescent dye (Cy5-dUTP) and was mixed with DNA from a control heterozygous strain that had been labeled with a different fluorescent tag (Cy3-

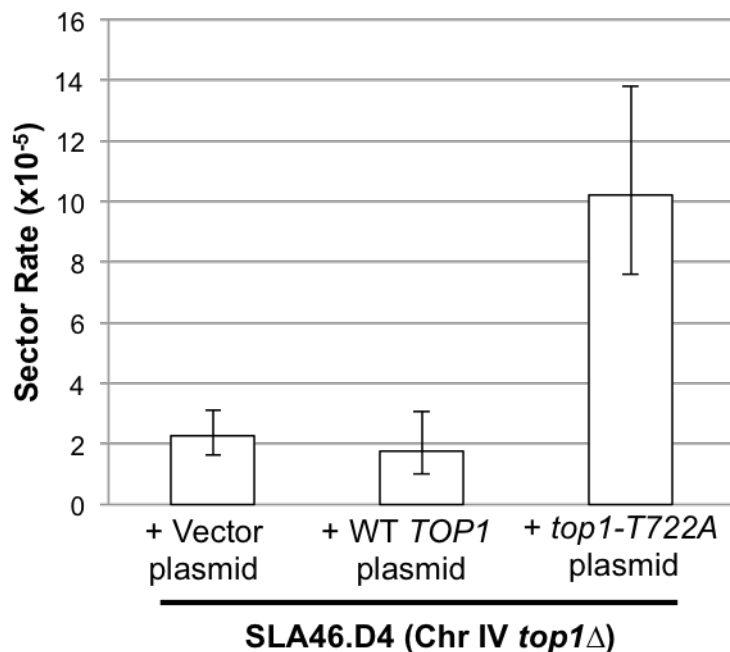


Figure 14. Top1-T722A expression increases the rate of RCOs. Rates of red/white sectoring associated with Top1-T722A expression are shown.

dUTP). The experimental and control samples were then mixed and competitively hybridized to oligonucleotide-containing microarrays. Chromosome IV-specific microarrays monitored about 2300 SNPs located between *CEN4* and the *SUP4-o/KANMX* markers. Each SNP was represented by four 25-base oligonucleotides: two correspond to the Watson and Crick strands of the W303-1A allele and two to the Watson and Crick strands of the YJM789 allele (for SNP-specific oligonucleotide sequences, see (St. Charles and Petes 2013)). Following hybridization to the SNP microarray, the ratio of Cy3 to Cy5 hybridization to each individual oligonucleotide was determined. After appropriate normalization steps, a Cy3: Cy5 hybridization ratio of 1 at a specific SNP

indicated that the experimental strain was heterozygous at that SNP. If the experimental sample had an LOH event that resulted in homozygosity for the YJM789-derived SNP, hybridization to the YJM789-specific oligonucleotides was 1.5 to 2-fold greater than that of the heterozygous control. Concurrently, the same experimental sample had a decreased relative hybridization to the W303-1A-specific oligonucleotides, with a ratio of 0.1-0.5 relative to the heterozygous control. This is illustrated in **Figure 15**, where the relative hybridization levels show some variation because the specificity of a particular oligonucleotide for one allele or the other is a complex function of the melting temperature of perfectly-matched versus imperfectly-matched duplexes. The transition between heterozygous and homozygous SNPs is usually unambiguous (**Figure 15**).

Determining LOH transition points in the red/white sectors provides critical information about the nature of the corresponding recombination event (Lee *et al.* 2009; Lee and Petes 2010; St. Charles *et al.* 2012; St. Charles and Petes 2013; Song *et al.* 2014). Identical LOH transition points in red/white sectors correspond to a simple CO event with no associated gene conversion tract. **Figure 16** illustrates gene conversion patterns predicted to be associated with DSBs that arise in G2 or G1 of the cell cycle. If an LOH transition in the red sector occurs centromere-proximal to the transition in the white sector (**Figure 16**, left panel) there is a region (boxed in green) in which three of the chromatids have red (W303-1A) SNPs and one has black (YJM789) SNPs. This 3:1

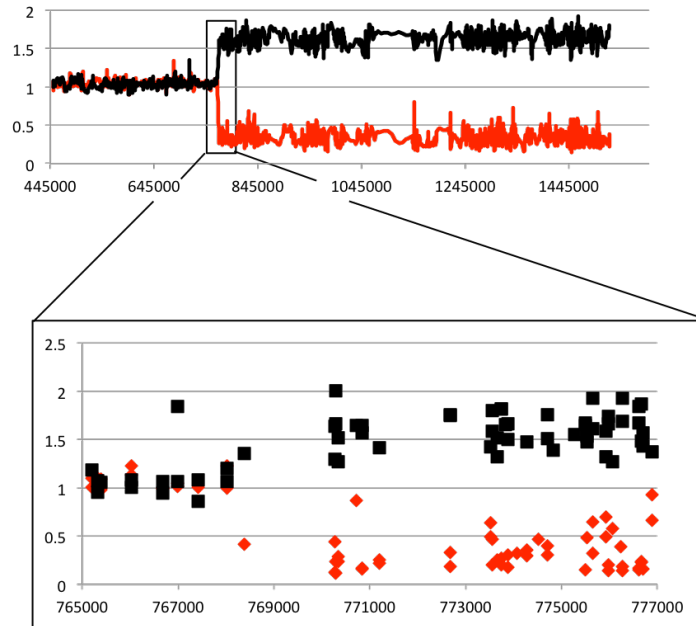


Figure 15. Characterizing RCOs on chromosome IV with microarrays. The W303-1A-related SNP hybridization signal is shown as a red line and that of YJM789 is the black line. A hybridization value of ~ 1 indicates a single copy of a given SNP is present (heterozygous SNP), a value between 1.5 and 2 indicates two copies of the SNP, and a value of 0-0.5 indicates no copy of the SNP is present. Shown is the white side of a sector with a transition from heterozygous to YJM789-homozygous SNPs.

pattern signals a mitotic gene conversion (GC) associated with the selected crossover event (St. Charles *et al.* 2012; St. Charles and Petes 2013). A GC reflects repair of the broken chromosome via a non-reciprocal transfer of DNA sequence from an intact chromosome, and occurs near the site of the initiating lesion (Heyer *et al.* 2010). The transfer of information often involves heteroduplex formation, followed by repair of the resulting mismatches within the heteroduplex (Petes 1991). GC events in yeast are associated with crossovers about 40% of the time (Yim *et al.* 2014) and roughly 90% of

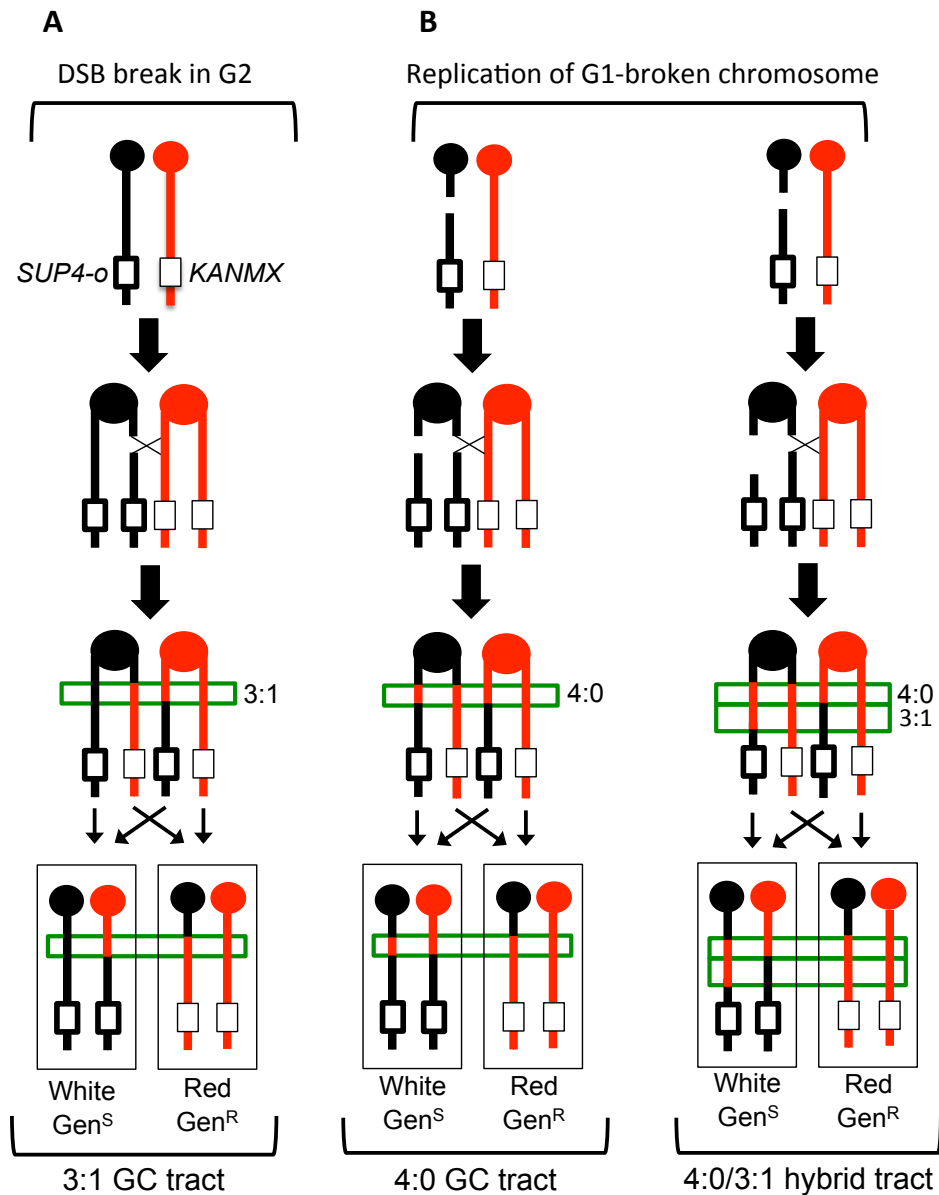


Figure 16. Gene conversion pattern associated with G1- or G2- initiated DSBs. *Left.* A DSB is generated in one sister chromatid after DNA synthesis and repair of the sister chromatid from the homolog results in a 3:1 conversion tract, which is within the green box. *Middle and right.* A DSB occurs in G1 and the chromosome is replicated to form two broken sister chromatids. Repair of the two broken chromatids from the homolog results in a 4:0 conversion tract. Middle panel, the two conversion tracts are the same length. On the right, the lengths of the gene conversion tracts differ, giving rise to a hybrid 3:1/4:0 event. W303-1A and YJM789 chromatids are red and black, respectively.

crossovers are associated with a detectable GC event (St. Charles and Petes 2013).

Mitotic conversion tracts are variable in length, ranging from less than 100bp to more than 50kb (Yim *et al.* 2014), with a median length of 10.6kb for spontaneous conversion events (St. Charles and Petes 2013).

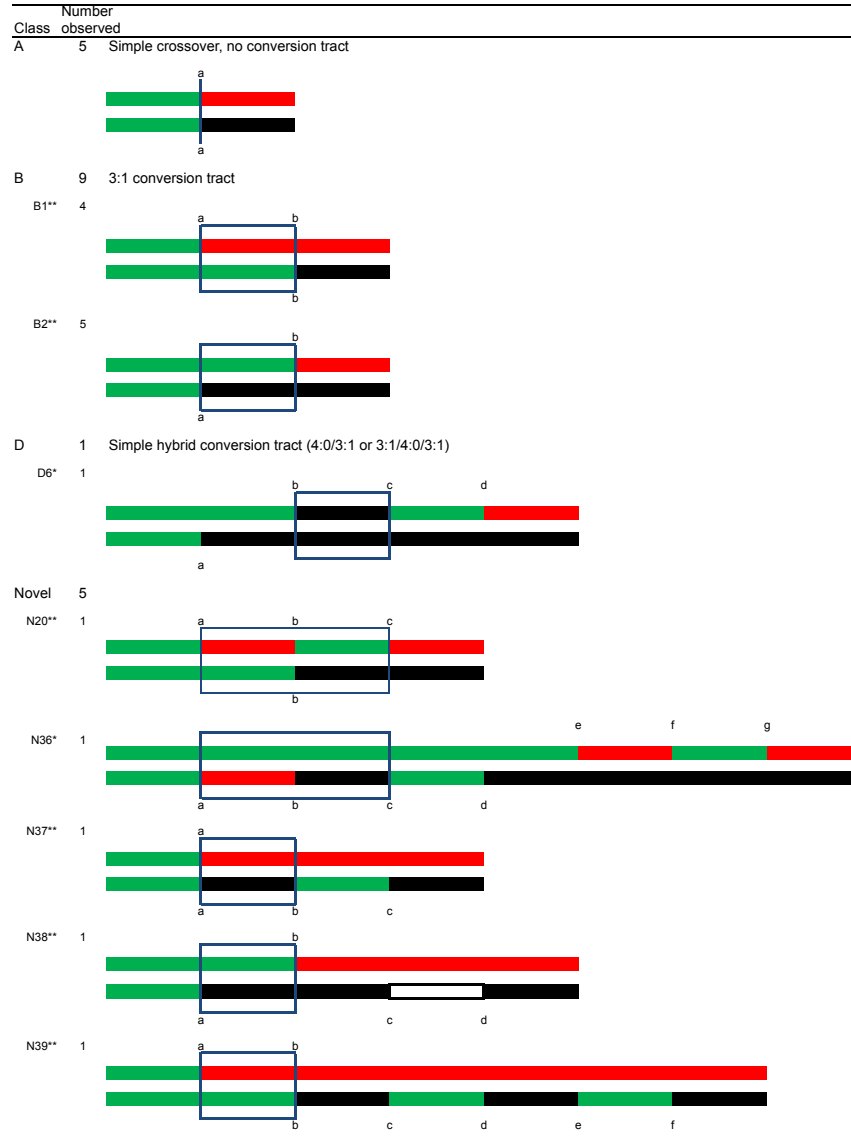
The 3:1 pattern depicted in the left panel of **Figure 16** is consistent with the repair of a single chromatid broken in S or G2 of the cell cycle. The broken chromosome loses information that is replaced by sequences from the donor. We also observed events that were consistent with the repair of two sister chromatids broken at approximately the same position (middle panel of **Figure 16**). In these events, there is a region adjacent to the crossover in which all four chromatids have SNPs derived from one homolog (4:0 GC tract) and this can be interpreted as a DSB in G1 followed by replication of the broken chromatid to yield broken sister chromatids (Lee *et al.* 2009; Lee and Petes 2010; St. Charles and Petes 2013). In addition to 4:0 GC tracts, 4:0/3:1 hybrid conversion tracts were observed (right panel of **Figure 16**). These tracts are likely initiated by a DSB in G1, with the broken chromosome replicating to yield sister chromatids broken at the same position. These two broken chromatids are then repaired to generate different sized conversion tracts. To summarize, analysis of a sectored colony by microarrays allows: mapping the position of the crossover, measurement of GC tract lengths associated with the crossover, determination of which homolog had the initiating DNA lesion and inference about the timing of the initiating DNA lesion.

We mapped the positions and types of crossover-associated gene conversion events on the right arm of chromosome IV in 20 CPT-induced sectors (**Table 2 and**

Appendix 1A) and in 20 sectors isolated during expression of the mutant Top1-T722A protein (**Table 3 and Appendix 1B**); the profiles were compared to those previously reported for WT by St. Charles and Petes (St. Charles and Petes 2013). In the previous analysis of JSC25, they identified seven peaks of recombination termed HS1-HS7 (St. Charles and Petes 2013), **Figure 17** shows the comparison of the previously reported WT profile to CPT-treated and Top1-T722A profiles. HS4 is highlighted because it appears to be completely absent in the CPT-treated profile, but the effect of CPT treatment or Top1-T722A expression was not statistically significant ($p=0.36$ and $p=1$, respectively by Fisher's exact test), most likely because of the small sample size.

Using the logic introduced in **Figure 16**, we examined conversion tracts to determine if CPT treatment and/or Top1-T722A expression produced G1-like (4:0 tracts) or G2-like (3:1 tracts) crossover-associated conversion events. **Figure 18** presents the percentage of each type of conversion event we detected in CPT-treated sectors; two of the 20 (10%) were G1-like, 13 (65%) were G2-like and five (25%) had no detectable conversion tract and were classified as a simple COs. Sectors derived from the mutant expressing Top1-T722A showed the same distribution as CPT-treated cells, with two G1-like, 13 G2-like and five simple CO events, as shown in **Figure 19**. When compared to the cell-cycle distribution of DSBs in WT (untreated) sectors using previously published data (St. Charles and Petes 2013), the differences in number of G1- and G2- events was significant ($p<0.0001$ for both comparisons by Fishers exact test). This data suggest that a

Table 2. Conversion tracts associated with reciprocal crossovers in CPT-treated red/white sectors.

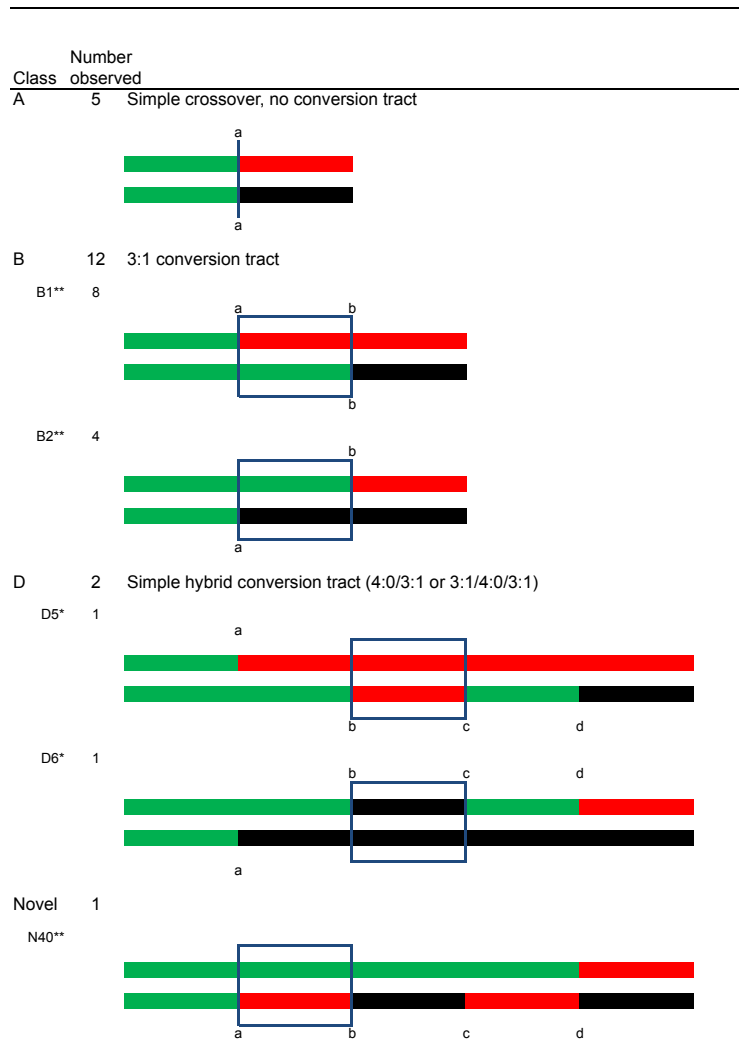


* G1-initiated DSB, ** G2-initiated DSB

Green, red and black represent heterozygosity for SNP, homozygosity for W303-1A SNPs, and homozygosity for YJM789 SNPs, respectively.

The top line represents the red side of the indicated sector and the bottom line represents the white side of the sector. Green, red and black represent heterozygosity for SNPs, homozygosity for W303-1A SNPs, and homozygosity for YJM789 SNPs, respectively. The lowercase letters located above and below the lines mark transitions from heterozygosity to homozygosity and are correlated with transition labels shown in Appendix 1A. Blue boxes enclose the regions that are likely to be associated with DSB formation; for details on the event classification of sectors, please refer to St. Charles *et al.* (2013). Novel class of sectors (N) are sectors that have not been observed in previous studies. The lengths of conversion tracts are not drawn to scale. One asterisk (*) and two asterisks (**) indicate a G1 and G2 DSB, respectively.

Table 3. Conversion tracts associated with reciprocal crossovers in Top1-T722A red/white sectors.



* G1-initiated DSB, ** G2-initiated DSB

Green, red and black represent heterozygosity for SNP, homozygosity for W303-1A SNPs, and homozygosity for YJM789 SNPs, respectively.

The top line represents the red side of the indicated sector and the bottom line represents the white side of the sector. Green, red and black represent heterozygosity for SNPs, homozygosity for W303-1A SNPs, and homozygosity for YJM789 SNPs, respectively. The lowercase letters located above and below the lines mark transitions from heterozygosity to homozygosity and are correlated with transition labels shown in Appendix 1B. Blue boxes enclose the regions that are likely to be associated with DSB formation; for details on the event classification of sectors, please refer to St. Charles *et al.* (2013). Novel class of sectors (N) are sectors that have not been observed in previous studies. The lengths of conversion tracts are not drawn to scale. One asterisk (*) and two asterisks (**) indicate a G1 and G2 DSB, respectively.

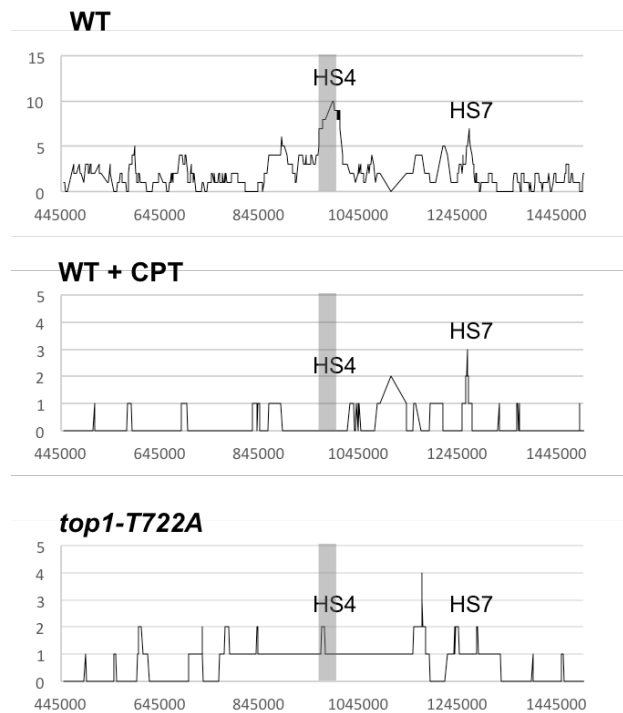


Figure 17. Distributions of LOH breakpoints. Plotted is the number of times each SNP was included in a crossover-associated conversion tract (Y-axis) and the SGD coordinates for chromosome IV (X-axis) in WT, WT + CPT, and *top1-T722A* sectors are shown. Hotspot 4 (HS4: Chr IV SGD coordinates 970-1000kb) was previously noted in a WT background (St. Charles *et al.* 2013) and is indicated by the shaded region.

stabilized Top1cc generates DSBs predominantly during rather than prior to DNA replication.

The median lengths of conversion tracts in the CPT-treated sectors were 24.8kb (G1), 4.7kb (G2) and 7.2kb (all conversions); by Mann-Whitney test, none of these tract lengths were statistically different from published conversion tract lengths in JSC25 (14.8kb, 4.7kb, and 10.6kb, respectively) (St. Charles and Petes 2013). In the Top1-

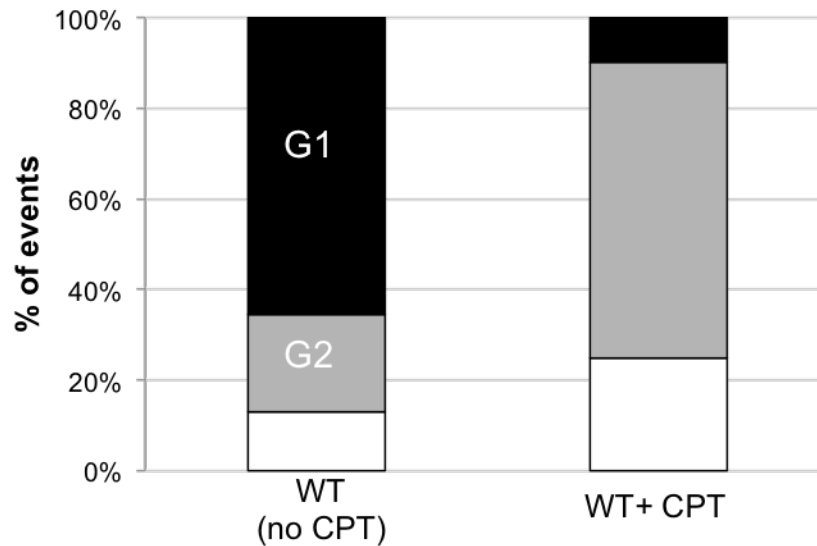


Figure 18. CPT treatment increases RCOs during or after DNA synthesis. The cell cycle phase when an RCO-initiating event occurred was inferred by the associated gene conversion pattern in CPT-treated red/white sectors stimulates initiation primarily in G2. Black, G1-associated; gray, G2-associated; white, simple CO (no GC).

T722A sectors the median conversion tract lengths were 18.8kb (G1), 9.3kb (G2) and 9.3kb (all conversions). The lengths of G2-associated and all conversion tracts were significantly different from WT ($p=0.04$ and $p=0.05$, respectively). The G2-associated events included two very large conversion tracts of ~100kb and 400kb, which are much larger than most tracts seen previously (Lee *et al.* 2009; St. Charles and Petes 2013). If these two events are considered false sectors and removed from the dataset, the G2-like and total conversion tract length differences are no longer significant.

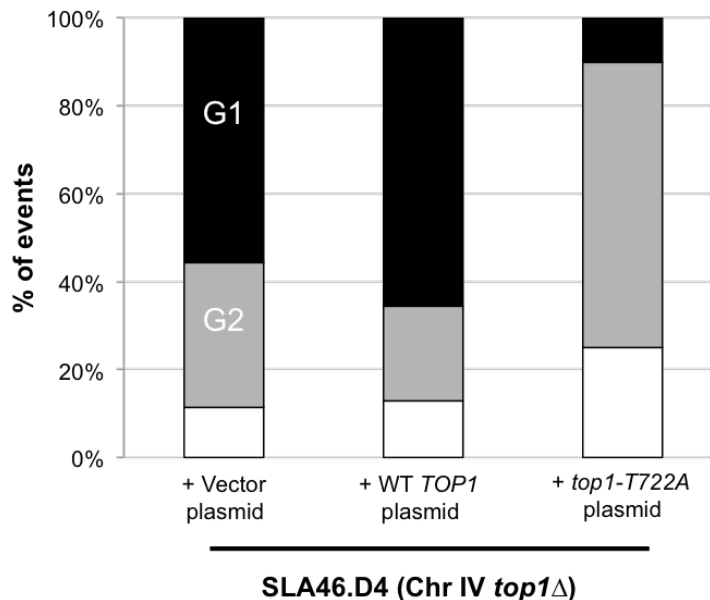


Figure 19. Top1-T722A expression increases RCOs during or after DNA synthesis. The cell cycle phase when an RCO-initiating event occurred was inferred by the associated gene conversion pattern in Top1-T722A expression stimulates initiation primarily in G2. Black, G1-associated; gray, G2-associated; white, simple CO (no GC).

2.3.c. Genome-wide LOH and copy-number changes associated with *Top1cc*.

We analyzed unselected events induced by CPT throughout the genome in cells sub-cultured 10 times, which is equivalent to roughly 250 generations. After DNA was extracted we examined four sub-cultures using whole-genome microarrays. As a control, we looked at two untreated (DMSO) sub-cultures as well. In the untreated sub-cultures, we detected two alterations: one interstitial and one terminal LOH event (**Table 4** and **Appendix 1C**). The interstitial event could be the result of a conversion event while the

Table 4. Chromosome depictions for events detected in clones sub-cultured 10 times.

Strain	Genotype	Condition	Event Class	Number observed	Event description	
JSC25	WT	YPD + DMSO	a	1	Terminal LOH	
			a1	1		
			b	1	Gene Conversions	
		b1	1			
		YPD + CPT	a	4	Terminal LOH	
			a1	1		
	a2		2			
	a3		1			
	b		3	Gene Conversions		
	b2		3			
	SLA46.D4	<i>top1Δ</i>	+ <i>top1-T722A</i> plasmid	a	1	Terminal LOH
				a1	1	
b				5	Gene Conversions	
b2			1			
b3			4			
c			4	Amplifications and Deletions at <i>CUP1</i> locus (Chromosome VIII)		
c1		3				
c2		1				
e		e	2	Amplifications and Deletions		
		e1	2			

Green, red and black represent heterozygosity for SNP, homozygosity for W303-1A SNPs, and homozygosity for YJM789 SNPs, respectively.

The colored line represents a chromosome. Green, red and black represent heterozygosity for SNPs, homozygosity for W303-1A SNPs, and homozygosity for YJM789 SNPs, respectively. The lengths of chromosomes are not drawn to scale.

terminal LOH could be either a crossover or break-induced replication (BIR) event.

When we combine the data from these two sub-cultures with 13 WT isogenic isolates (sub-cultured without CPT or DMSO and only one LOH event was observed), we estimate ~0.5 LOH events per isolate after 250 generations or 10 sub-cultures.

The four JSC25 isolates were sub-cultured on YPD plates containing 500μM CPT dissolved in DMSO. One sub-culture had no detectable LOH events, one had a terminal LOH event on chromosome XII with a breakpoint in the rDNA locus, one had an

interstitial and a terminal LOH event and one had two interstitial and three terminal LOH events (**Table 4** and **Appendix 1C**). The average number of LOH events per isolate in the presence of CPT was ~two, and hence about four times higher than in untreated isolates.

We next looked at the effect of expressing Top1-T722A on the genome after 250 generations in four sub-cultured isolates (**Table 4** and **Appendix 1C**). In four independent isolates of SLA46.D4 expressing the *top1-T722A* mutant allele, we detected five interstitial LOH events, one terminal LOH event, and two deletions, resulting in an average of two LOH events per isolate. Additionally, all four sub-cultured isolates had copy-number variation at the *CUPI* locus.

2.3.d. Copy-number variation (CNV) at the *CUPI* locus is elevated by CPT treatment or Top1-T722A expression

Each of the four sub-cultured *top1-T722A* isolates displayed changes in the number of *CUPI* genes by microarray analysis; three increases and one reduction in the W303-1A specific SNPs were detected (**Figure 20**). The *CUPI* locus is a naturally occurring tandem array of the metallothionein-encoding *CUPI* gene on chromosome VIII. Different yeast strains have variations both in the total number of *CUPI* repeats and in the size of the repeat unit. The W303-1A derived homolog has 14 copies of a 2-kb repeat and the YJM789 derived homolog has seven copies of a 1.2-kb repeat. In the whole genome microarrays used, the *CUPI* locus is represented by oligonucleotides that are specific for W303-1A repeat. We thus only detect changes in the number of repeats

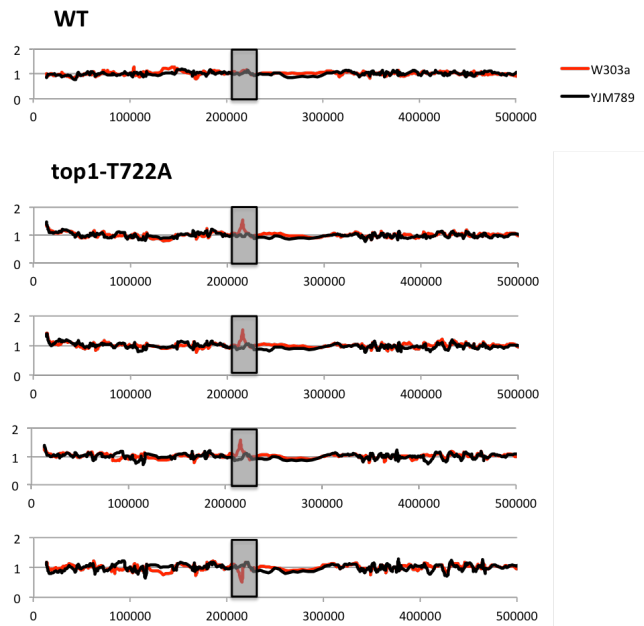


Figure 20. *CUP1* instability associated with Top1-T722A expression detected by microarrays. Illustrates an increase or decrease in the number of *CUP1* repeats on the W303-1A allele (red peak in boxed region) as detected by microarrays when Top1-T722A is expressed.

on the W303-1A homolog and cannot detect alterations on the YJM789 homolog. Also, although microarrays can easily detect changes in copy number that involve five or more repeats, smaller changes are much more difficult to detect. For these reasons, we examined alterations in the number of *CUP1* repeats by Southern hybridization analysis.

The restriction enzyme *EcoRI* has no recognition sites within either the 1.2 or 2.0 kb *CUP1* repeats, but cuts within sequences that closely flank the repeats (Zhao *et al.* 2014). In the parental diploid, treatment of genomic DNA with *EcoRI*, followed by Southern analysis with a *CUP1*-specific probe, produced two fragments of about 30 kb

(the W303-1A array) and 12 kb (the YJM789 array). Southern analysis confirmed the CNV detected by the microarrays in the four *top1-T722A* sub-cultured clones, and additionally revealed CNV in three of the four sub-cultured WT clones treated with CPT (data not shown).

To more accurately quantitate *CUPI* instability resulting from Top1 cleavage complexes, we sub-cultured additional isolates of the WT strain with and without CPT treatment, the *top1-T722A* strain, and the *top1Δ/top1Δ* diploid strain. As shown in **Figure 21**, both deletions and additions of *CUPI* repeats were observed. In some isolates, only one array was altered (**Figure 21**, lane 3) whereas, in others (**Figure 21**, lane 9), both arrays changed in size. In addition, some genomic samples had more than two *CUPI*-hybridizing DNA fragments (**Figure 21**, lane 2). These additional fragments likely represent deletions and additions that occurred in the final sub-culturing. This was confirmed by examining the *CUPI* locus after the first subculture, at which point faint fragments were frequently evident in isolates expressing Top1-T722A or treated with CPT (**Appendix 1D**). Our conclusions about the nature of copy number changes after ten sub-cultures were based on analysis only of the two fragments that hybridized most strongly to the *CUPI* probe. When both arrays were altered in size, we assume that the larger of the new fragments was from the W303-1A-derived homolog and the smaller from the YJM789-derived homolog.

Changes in the number of *CUPI* repeats are summarized in **Figure 22**, where we show the percentage of chromosome VIII homologs with changes in *CUPI* repeat number after ten rounds of sub-culturing; the complete data set is presented in **Appendix**

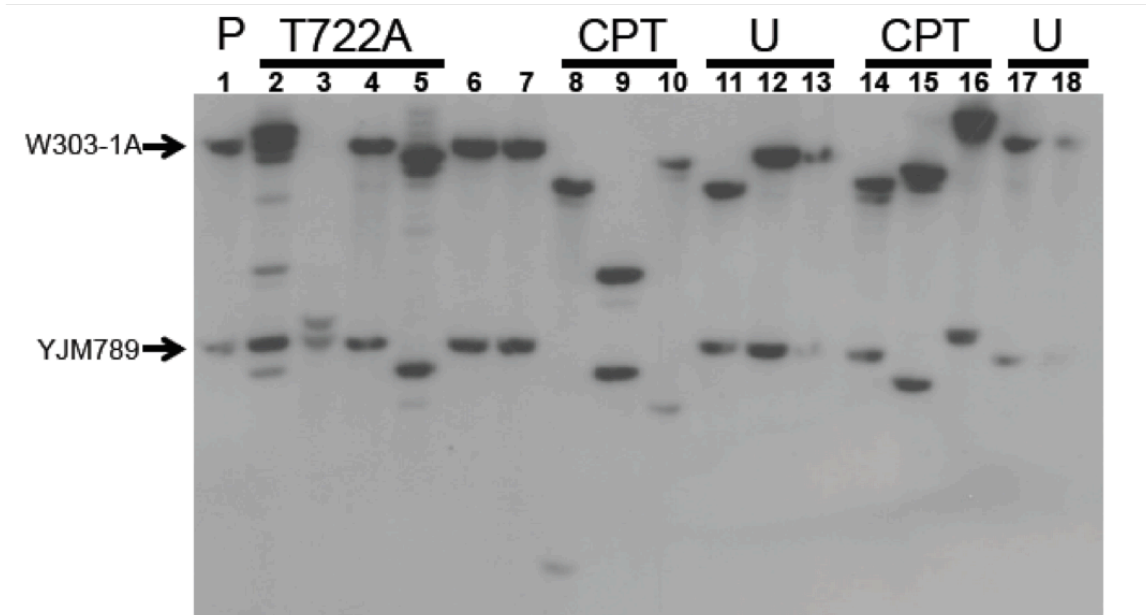


Figure 21. *CUP1* instability associated with CPT treatment or Top1-T722A expression. In a representative *CUP1* Southern blot is shown. DNA isolated from cells sub-cultured 10 times (~250 generations) was digested with *EcoRI* and the size of the array on each homolog was examined by Southern blot using a *CUP1*-specific probe. The arrows indicate the sizes of the *CUP1* arrays in the parent. The most robust band was used as the measure for gain or loss.

1D. Control data were derived from two nearly-isogenic *TOP1/TOP1* strains (JSC25 and PG311) grown either in rich medium or in rich medium containing DMSO. Thirteen of the 152 homologs analyzed (9%) from the control strains had alterations in the number of *CUP1* repeats. In strain JSC25 treated with CPT, 43 of the 58 homologs (74%) had changes in the number of *CUP1* repeats. The *top1-T722A*-expressing strain had similarly high levels of *CUP1* instability, with 17 of 28 (61%) homologs exhibiting CNV. The level of instability for the *top1Δ* strain was no different than in the WT control ($p=0.75$).

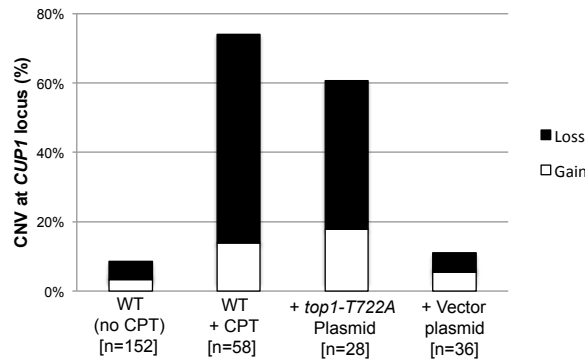


Figure 22. Copy number variation (CNV) at *CUP1* locus associated with CPT treatment or Top1-T722A expression. CPT treatment or Top1-T722A expression lead to a significant increase in CNV after 10 sub-cultures. Also shown is the percentage of alleles that lose (black bars) compared to alleles that gained *CUP1* repeats (white bars).

For the strains examined in our study, the number of deletions generally exceeded the number of additions (**Figure 22**). The WT control strains had eight deletions and five additions ($p=1$); the sums of all alterations for the CPT-treated and the Top1-T722A-expressing strains were 47 deletions and 13 additions ($p=0.002$). As discussed further below, the deletion bias is relevant to the likely mechanism of repeat instability at *CUP1*. Our demonstration that CPT treatment or expression of Top1-T722A leads to elevated rates of deletions and duplications in *CUP1* is consistent with previous results showing that the *top1-103* mutation increases the rate of loss of *URA3* integrated into the *CUP1* array (Levin *et al.* 1993).

2.3.e. Crossovers at the rDNA locus increase with CPT treatment and Top1-T722A expression.

In the *top1Δ/top1Δ* strain SLA46.D4, three of four red/white sector colonies and nine of ten sub-cultured clones had LOH events with breakpoints at the rDNA locus (see above). To better quantitate the effect of Top1 on rDNA stability and to examine possible rDNA instability associated with the Top1cc, we monitored a restriction site polymorphism (a *SpeI* site present in YJM789 but absent in W303-1A) located ~21 kb centromere-distal to the rDNA locus. Using primers that flank the polymorphism, we PCR-amplified genomic DNA and then treated the resulting fragment with *SpeI*. Heterozygous strains have three DNA fragments of ~750, 500 and 250 bp. Strains homozygous for the YJM789 allele produce only the 500 and 250 bp fragments, while those homozygous for the W303-1A allele produce only the 750 bp fragment.

We sub-cultured strains of various genotypes ten times, and then examined them for LOH of the *SpeI* polymorphism (**Figure 23** and **Appendix 1E**). Among the 61 isolates of WT strain JSC25 examined, no LOH events were detected. In contrast, 20 of 44 *top1Δ/top1Δ* diploids had an LOH event. These results confirm our microarray analyses as well as the conclusion of previous studies (Christman *et al.* 1988). CPT treatment of JSC25 greatly stimulated inter-homolog mitotic crossovers on chromosome XII, with 20 of 43 clones exhibiting LOH ($p < 0.0001$ relative to control). In addition, in strains expressing the *top1-T722A* mutant allele, 34 of 44 sub-cultures had LOH for the *SpeI* polymorphism. Unexpectedly, the *top1Δ* strain containing the plasmid-borne *TOP1* gene (SL146.D4/pWJ1491) also exhibited an elevated level of LOH relative to WT

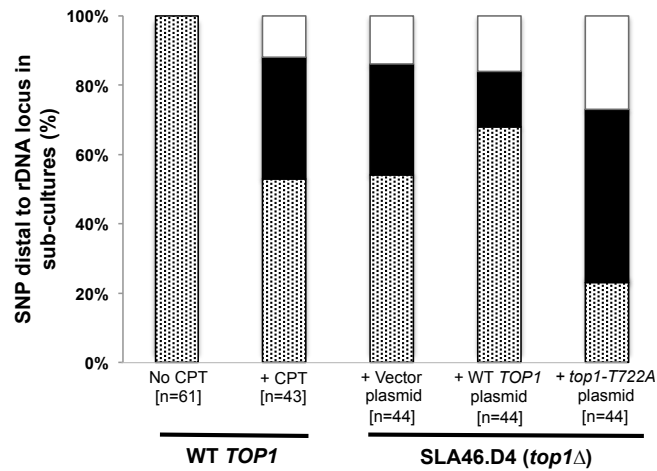


Figure 23. CPT treatment and Top1-T722A expression result in increase RCOs at the rDNA locus. An rDNA-distal PCR product from sub-culture 10 clones was digested with *SpeI* and analyzed by gel electrophoresis. Dotted, heterozygous; black, homozygous for W303-1A; white, homozygous for YJM789.

JSC25, with 14 of 44 isolates exhibiting LOH. This frequency of LOH is significantly lower than that observed in strains expressing Top1-T722A ($p < 0.0001$), and similar to that observed in the *top1*Δ strain with the vector ($p = 0.27$). Although this suggests that the plasmid-borne *TOP1* gene likely fails to fully complement the chromosomal deletion, it also is possible that overexpression of Top1 from the *CUP1* promoter might drive instability.

2.4 Discussion

The main conclusions of this study are: (1) elevated levels of Top1 cleavage complexes, resulting from CPT treatment or expression of the *top1-T722A* allele, stimulate both inter-homolog recombination and inter-sister chromatid recombination, and (2) the recombinogenic DNA lesions caused by the Top1 cleavage complexes likely induce recombination in S or G2. Each of these conclusions will be discussed further below.

The Top1 topoisomerase has a variety of roles in the yeast, including preventing the accumulation of positive supercoils in front of the transcription and replication machineries, and preventing accumulation of negative supercoils behind transcribing RNA polymerase. It is thus difficult to predict the effects of removing Top1 on recombination. Loss of Top1, for example, might induce recombination because accumulation of supercoils leads to stalled replication forks or because R-loops give rise to recombinogenic DNA lesions. Alternatively, some spontaneous mitotic recombination events might be a consequence of Top1-induced nicks that, if unrepaired, lead to recombinogenic double-stranded breaks (DSBs). The latter mechanism is responsible for the hyper-recombination (hyper-rec) phenotypes of strains defective in RNase H2, which initiates removal ribonucleotides embedded in duplex DNA (Potenski and Klein 2014).

Strains with elevated levels of the Top1cc are expected to be hyper-rec. In numerous studies, it has been shown that yeast strains with mutations affecting DSB repair are sensitive to CPT (reviewed by (Fiorani and Bjornsti 2000; Malik and Nitiss

2004), and there are likely several ways of generating a recombinogenic DNA lesion by CPT. Replication of a DNA molecule with a Top1cc could directly produce a DSB through replication-run-off, or nucleolytic cleavage of a fork regressed because of topological stress could generate a DSB (Ray Chaudhuri *et al.* 2012). In addition, some transcription-stimulated mutations have the properties expected from the repair of a Top1cc-associated single-stranded gap (Cho *et al.* 2013), which could be processed into a DSB by a nearby nick on the complementary strand.

In our analyses, six hours of CPT treatment elevated the frequency of inter-homolog crossovers on the right arm of chromosome IV and the left arm of chromosome V by 6-8 fold. The *top1-T722A* mutation had a similar quantitative effect on the right arm of chromosome IV, increasing the frequency of crossovers by 5-fold; its effect on chromosome V was not examined. In addition to elevating the rates of recombination on chromosomes IV and V, we observed an elevation in rDNA-associated terminal LOH events on chromosome XII in the *top1-T722A* strain and in the WT strain treated with CPT.

As described previously, the type of gene conversion (3:1, 4:0, hybrid 3:1/4:0, etc.) associated with the crossover in sectored colonies allows us to infer whether the event involved a single broken chromatid (a G2-break) or a pair of sister chromatids broken at the same position (a G1-break). About 75% of the spontaneous events in a wild-type strain are G1 breaks (St. Charles and Petes 2013). In the *top1-T722A* mutant or CPT-treated WT strain, only 13% of the crossovers were associated with a G1 break.

These results indicate that most Top1cc-associated DNA lesions originate in S or G2, consistent with formation of associated DSBs in the context of DNA replication.

Our recombination assays that involve detection of sectored colonies or microarray-based analysis of genomic DNA primarily detect recombination events between homologs. In particular, recombination between perfectly- or imperfectly aligned sister chromatids does not lead to LOH. Unequal sister-chromatid recombination within a tandem array of genes, however, can lead to a duplication or deletion of repeats that is sometimes detectable by microarrays and this observation provided the initial indication that the tandem array at the *CUPI* locus is destabilized upon accumulation of Top1 cleavage complexes (**Figure 20**). We subsequently used Southern blot analysis to more efficiently detect alterations in the number of repeats in the *CUPI* array. This analysis showed that *top1-T722A* mutant and CPT-treated WT strains had highly elevated rates of CNV at the *CUPI* locus.

CNV at *CUPI* could represent either intra- or inter-homolog interactions, but several arguments suggest that most events reflect either inter-sister-chromatid interactions or intra-chromatid events. First, if the copy-number alterations involved inter-homolog recombination, we would have expected to find many sub-cultured isolates with terminal LOH distal to the *CUPI* cluster. No such events were observed. Additionally, Kadyk and Hartwell (Kadyk and Hartwell 1992) showed that DNA damage resulting from irradiating G2-synchronized yeast cells was primarily repaired by recombination between sister chromatids rather than inter-homolog recombination.

Several different types of inter-sister or intrachromatid interactions can alter the number of repeats within a tandem array, including unequal crossing-over, break-induced replication (BIR), gene conversion, single-strand annealing (SSA) and intrachromatid “pop-out” recombination that produces an extrachromosomal circle and a shorter array (**Figure 24**). Although our current studies cannot distinguish between these mechanisms, the first three are expected to generate both deletions and additions of repeat units, while the latter two produce only deletions. The strong bias we observed for deletions argues that mechanisms producing equal numbers of deletions and additions are likely not the major source of *CUPI* instability. Other studies have indicated that SSA is more common than “pop-out” recombination (Paques and Haber 1999), leading us to speculate that SSA is a primary source of CNV at *CUPI*.

In summary, our analysis shows that elevated levels of the Top1cc elevate genomic instability. Elevated levels of the Top1cc increased the rate of inter-homolog crossover at many sites in the yeast genome, including the rDNA. These complexes also strongly induced CNV formation within the *CUPI* locus. Although there are some differences in the repair of DNA lesions in yeast and mammalian cells (Jasin and Rothstein 2013), it is likely that the recombinogenic effects of Top1 cleavage complexes we have observed in yeast will generate similar types of genome instability in mammalian cells. Indeed, Hashimoto *et al.* (Hashimoto *et al.* 1995) and Balestrieri *et al.* (Balestrieri *et al.* 2001) reported that CPT treatment of mammalian cells resulted in large deletions and/or rearrangements, but the source and nature of these were not explored. Our findings in yeast are likely relevant to potential downstream effects of using CPT-

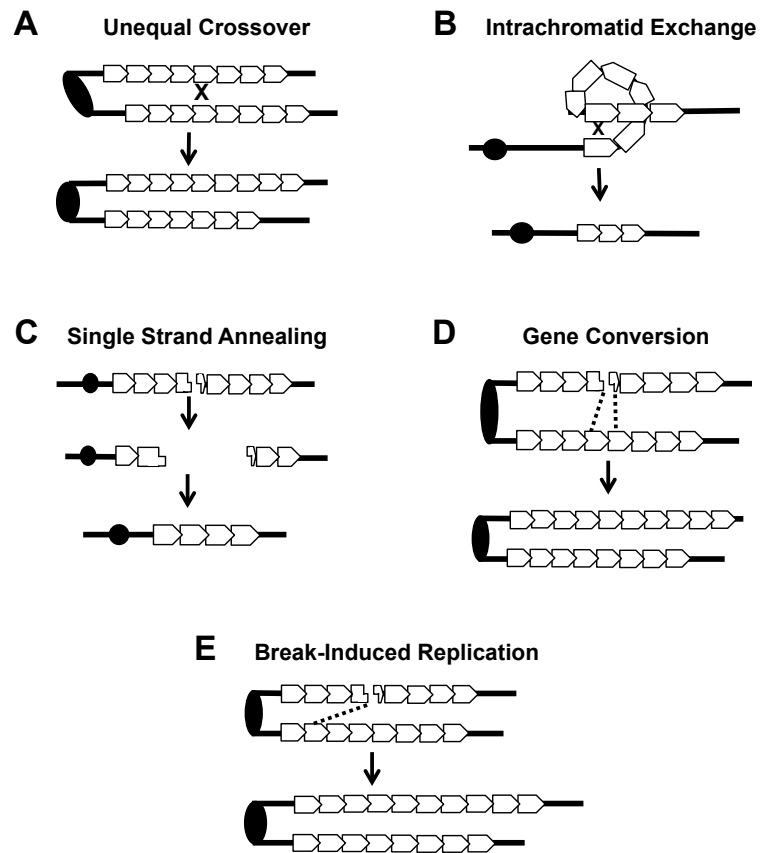


Figure 24. Mechanisms of CNV at the *CUP1* locus. (A) An **unequal crossover** between two misaligned sister chromatids results in one chromatid gaining repeats and the other losing repeats. This event can occur between sister chromatids or homologous chromosomes. (B) **Break-induced replication (BIR)**. A DSB can be repaired using the sister chromatid or homolog as a template. Replication to the end of the template chromosome restores the broken chromosome and the template remains unchanged. (C) **Gene conversion (GC)**. Repair of a DSB with either the sister chromatid or homologous chromosome by GC results in the repaired chromatid gaining (or losing) copies of the *CUP1* repeat while the donor chromatid remains the same. (D) **Single strand annealing (SSA)**. A double strand break (DSB) can be resected to a region of homology and annealing/rejoining of ends leads to a loss of *CUP1* repeats. (E) An **intrachromatid exchange** that involves repeats on the same chromatid results in a loss of multiple *CUP1* repeats.

related compounds in chemotherapy, especially with regard to associated LOH and CNV that could promote tumor progression.

3. Camptothecin-induced mutagenesis

3.1 Introduction

Camptothecin (CPT) and its derivatives (topotecan and irinotecan) are drugs widely used in the treatment of a variety of malignancies (Pommier 2013). To date, the only known target of CPT is Top1, which functions to relieve transcription- and replication-associated torsional stress in DNA. Top1 cleaves one strand of double-stranded DNA, covalently associates with the 3' end of the nicked DNA to form a covalent Top1-cleavage complex (Top1cc), passes the intact strand through the nick and finally re-ligates the broken strand. CPT intercalation with the Top1cc after DNA cleavage prevents the religation of DNA, which both aids in toxic double-strand break (DSB) formation and causes an accumulation of stabilized (trapped) Top1cc (Jaxel *et al.* 1991; Dancey and Eisenhauer 1996; Pommier *et al.* 2003; Koster *et al.* 2007).

Stabilization of the Top1cc generates DSBs and strongly stimulates HR in yeast (Pourquier and Pommier 2001). The gross chromosomal rearrangement assay (GCR) developed by Richard Kolodner's lab, which detects events originating from a DSB, also was used to look at the effect of CPT. A 50-fold elevation in GCR rate above the spontaneous rate was observed (Myung and Kolodner 2003). CPT induced a 4-fold increase in mutagenesis at the *CAN1* locus, suggesting that although CPT has strong

effects on homologous recombination, it is only weakly mutagenic (Nitiss and Wang 1988).

In addition to yeast, CPT has been previously reported to be mutagenic in mammalian cells. In V79 Chinese hamster fibroblast cell lines, for example, CPT treatment resulted in a dose-dependent, 6- to 19-fold increase in 6-thioguanine (6-TG)-resistant clones, which detects mutations in the *hypoxanthine phosphoribosyl-transferase locus (HPRT)* locus (Hashimoto *et al.* 1995). Experiments performed with topotecan (TPT, FDA approved CPT derivative) produced equivalent results in mutagenesis at the *HPRT* locus, confirming the potential for Top1-inhibitors to induce mutagenesis. Restriction fragment length polymorphism (RFLP) analysis of TPT-treated 6-TG-resistant clones revealed that 6 of the 12 analyzed clones had undergone gene deletions or rearrangements at or within the *HPRT* locus, similar to results reported previously with Top2 inhibitors (Hashimoto *et al.* 1995). A second study reported an increase in mutagenesis in Chinese hamster ovary (CHO) cells after CPT treatment (Balestrieri *et al.* 2001). They found CPT treatment increased *hpert* mutation frequency 20- to 50-fold over the spontaneous frequency in a dose-dependent manner. Analysis of CPT-treated 6-TG resistant clones by multiplex PCR revealed that 16 out of 20 (80%) of clones analyzed had undergone a deletion or rearrangement. Four different classes of events were seen in the 16 clones: single exon deletion (5/16), multiple exon deletion (3/16), total *HPRT* gene deletion (6/16), and multiple exon deletion involving non-adjacent exons within the *HPRT* locus (2/16). The first three classes were categorized as deletion events, whereas

the fourth class was considered a rearrangement; all classes are likely the result of a repaired DSB (Balestrieri *et al.* 2001).

Based on previous studies, we speculate that mutagenesis associated with CPT treatment could be a direct cause for secondary tumor formation and could play a significant role in the acquisition of chemotherapeutic drug resistance. Because the molecular target of CPT is Top1 (Pommier *et al.* 1999), this chapter focuses on molecularly characterizing the effect of CPT treatment on novel Top1-dependent deletion hotspots that do not reflect DSB repair.

3.2 Methods

3.2.a. Strain and plasmids.

Haploid yeast strains used in the *lys2* reversion assays were derived from YPH45 (*MATa ura3-52 ade2-101oc trp1Δ1*) (Sikorski and Hieter 1989). The (AT)₂ WT and *top1Δ*; (TC)₃ WT; and (AG)₄ WT and *rnh201Δ* strains were previously described (Lippert *et al.* 2011; Cho *et al.* 2013). All WT strains are Top1- and Rnh201-proficient. The *ERG6* gene was deleted in all strains via one-step gene disruption (Rothstein 1983) using primers ERG6KANF (5'-
AAAAACAAGAATAAAATAATAATATAGTAGGCAGCATAAGATGAGTGAAAC
AGAATTGAGCAGCTGAAGCTTCGTACG-3') and ERG6KANR (5'-
TTATCTGCATATATAGGAAAATAGGTATATATCGTGCGCTTTATTTGAATCTT
ATTGATCAGGCCACTAGTGGATCTG-3') to amplify a *TRP1* or *URA3Kl* cassette

from pUG6 (Guldener *et al.* 1996) or pUG72 (Gueldener *et al.* 2002), respectively. For a complete list of all strains used and their genotypes, see **Table 5**.

3.2.b. CPT-sensitivity plate spotting assay.

Sensitivity in the presence of CPT was determined as previously described (Knab *et al.* 1993). Briefly, 1mL YPD (1% yeast extract, 2% yeast peptone, 2% dextrose and 2% agar for plates) cultures were inoculated with a single colony, diluted 100-fold and the dilution was incubated overnight at 30°C with shaking. These cultures were diluted to 10^7 cells/mL and 2.5 μ L of 10-fold serial dilutions were spotted on YPD plates containing 100 μ M CPT (in DMSO) or an equivalent amount of DMSO.

3.2.c. Camptothecin-induced mutation frequency assay and mutation spectra generation.

YPD cultures were inoculated as above and incubated overnight; at least three independent cultures were started per isolate. From each overnight culture (cell density between 5×10^6 to 5×10^7 cells/mL), two cultures were diluted to 10^5 cells/mL in fresh YPD; one was supplemented with 100 μ M CPT (Sigma, 4mg/mL stock dissolved in DMSO) and the other with an equivalent amount of DMSO (untreated control). Cultures were incubated at 30°C for six hours with shaking. Following the six-hour incubation, appropriate dilutions were plated on YPD to determine total colony-forming units (CFUs) and on synthetic complete dextrose plates lacking lysine (SD-Lys) to determine the number of Lys⁺ revertants. The Lys⁺ revertant frequency was calculated by taking the

Table 5. Strains for CPT-mutagenesis studies.

Name	Strain ID	Genotype
(AT) ₂ <i>erg6</i>	SJR3446	<i>MATa ura3-52 ade2-101_{oc} trp1Δ1 lys2Δ::hyg leu2-K:TetR⁻-Ssn6:LEU2 [pSR857] his4Δ::kan-pTET-lys2FΔA746,NR, (AT)₂ erg6Δ::loxP-TRP1-loxP</i>
(AT) ₂ <i>top1 erg6</i>	SJR3590	<i>MATa ura3-52 ade2-101_{oc} trp1Δ1 lys2Δ::hyg leu2-K:TetR⁻-Ssn6:LEU2 [pSR857] his4Δ::kan-pTET-lys2FΔA746,NR, (AT)₂ top1Δ::loxP-TRP1-loxP erg6Δ::loxP-URA3KI-loxP</i>
(TC) ₃ <i>erg6</i>	SJR3447	<i>MATa ura3-52 ade2-101_{oc} trp1Δ1 lys2Δ::hyg leu2-K:TetR⁻-Ssn6:LEU2 [pSR857] his4Δ::kan-pTET-lys2FΔA746,NR, (TC)₃ erg6Δ::loxP-TRP1-loxP</i>
(AG) ₄ <i>erg6</i>	SJR3888	<i>MATa ura3-52 ade2-101_{oc} trp1Δ1 lys2Δ::hyg leu2-K:TetR⁻-Ssn6:LEU2 [pSR857] his4Δ::kan-pTET-lys2FΔA746,NR, (AG)₄ erg6Δ::loxP-TRP1-loxP</i>
(AG) ₄ <i>rnh201 erg6</i>	SJR3889	<i>MATa ura3-52 ade2-101_{oc} trp1Δ1 lys2Δ::hyg leu2-K:TetR⁻-Ssn6:LEU2[pSR857] his4Δ::pTET-lys2FΔA746,NR,(AG)₄ rnh201Δ::NAT erg6Δ::loxP-TRP1-loxP</i>

number of Lys⁺ revertants and dividing by the total number of viable cells. Cell viability at time of plating was determined by dividing the total number of viable cells by the number of cells as determined using a hemocytometer.

To generate mutation spectra, independent Lys⁺ revertants were sequenced. An 800 bp fragment of the *LYS2* reversion window was PCR-amplified with the following primers: LYSWINF (5'-GCCTCATGATAGTTTTTCTAACAAATACG-3') and LYSWINR (5'-CCCATCACACATACCATCAAATCCAC-3'). The PCR-generated products were sequenced by Eton Bioscience (Research Triangle Park, NC) with the primer MO18 (5'-GTAACCGGTGACGATGAT-3'). The frequency of a specific mutation class was calculated by multiplying the proportion of the class in the spectrum by the corresponding median Lys⁺ frequency. After calculating the median 2-bp deletion frequency, the effect of CPT was assessed using a two-sample t-test (vassarstats.net).

3.2.d. Top1 cleavage assay.

An *in vitro* Top1 cleavage assay was performed as previously described with two modifications (Kim *et al.* 2011). A 45-nucleotide fragment (5'-TTTGAAATACCGTGGCATCTCTCGTGACGACTTACCATTAAAGC-3') was end-labeled at the 3' end prior to annealing to a complementary fragment. 140nM of recombinant human Top1 and 10 μ M CPT were added to the reaction mixture composed of 20-500nM end-labeled DNA substrate, 10mM Tris-HCl, 50mM KCl, 5mM MgCl₂, 0.1mM EDTA, 1mM DTT, 15 μ g/mL BSA and 10% DMSO (Huang *et al.* 2015). Following incubation of reactions at 25°C for 1 hour, the reactions were stopped by the addition of 0.5% SDS. Samples were analyzed on a 20% polyacrylamide gel and labeled fragments were detected using a PhosphoImager. This assay was performed by S-Y Huang in Yves Pommier's lab.

3.3 Results

The *lys2* reversion system is ideal for investigating CPT-induced mutagenesis at a defined locus. Not only does this system allow the examination of whether CPT treatment induces the same mutation signature as a trapped Top1cc, it also allows mutagenesis to be studied in the context of high transcription, where mutations are easily detectable and

are Top1-dependent. Additionally, investigating Top1-dependent mutagenesis under high transcription conditions may have relevance in tumor cells, which are reported to have altered expression levels of genes (Lin *et al.* 2012). The availability of strains that contain Top1-dependent deletion hotspots, as well as optimized assays for calculating mutation frequency and sequencing, made an investigation of the role of CPT mutagenesis feasible.

3.3.a. CPT exposure increases mutagenesis at Top1-dependent hotspots

The Lys⁺ mutation frequency was measured in exponentially growing unsynchronized cells, using *LYS2* frameshift reversion alleles containing the (AT)₂, (TC)₃ or (AG)₄ hotspot (**Table 5**). The frameshift alleles contained a 1-bp deletion that reverts to a lysine prototroph by acquiring a net +1 mutation within a 150 bp reversion window (Harfe and Jinks-Robertson 1999). All strains had the *lys2* gene under the control of the highly inducible *TET* promoter (*pTET*) (Kim *et al.* 2007) and all experiments were done under high transcription conditions. It should be noted that the permeability of CPT in yeast cells is poor and can be increased by disrupting the function of Erg6, a membrane sterol transmethylase (Nitiss and Wang 1988). Therefore, all experiments were performed in an *erg6Δ* background.

Median Lys⁺ revertant frequencies were determined following growth in the presence of 100μM CPT or DMSO (untreated) for six hours. In addition to measuring mutagenesis, CPT-induced cell death following the six-hour treatment was measured. Cell viability decreased 42% in the presence of CPT (see **Figure 25**). In a reporter

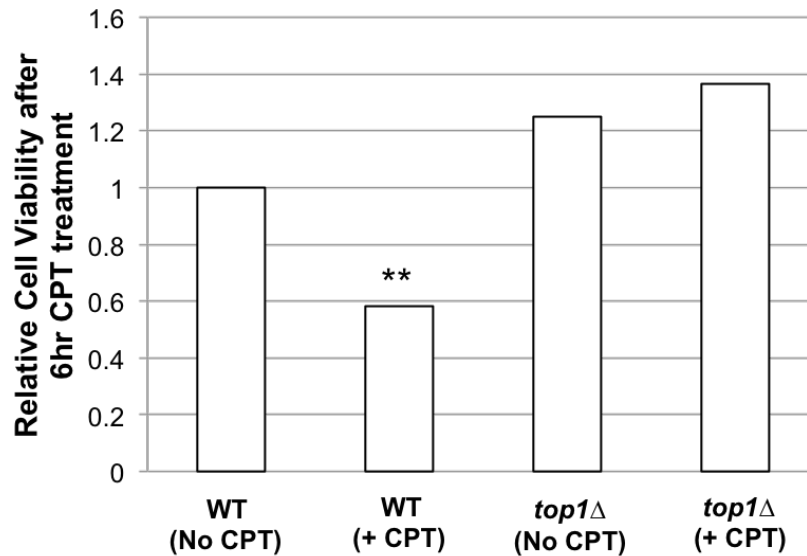


Figure 25. CPT treatment for 6 hours decreases cell viability. Cell viabilities were based on 24 cultures. ******(T-test two-tailed $p=0.002$)

containing the (AT)₂ hotspot, the Lys⁺ median mutation frequency increased 3-fold in the presence of CPT, from 1.5×10^{-5} to 4.2×10^{-5} (**Appendix 2A**). Mutation spectra for the (AT)₂ reporter (**Figure 26**) in the presence and absence of CPT indicate that the 3-fold (t-test two-tailed $p=0.0005$) increase in mutation frequency directly reflects the Top1-dependent 2-bp deletion signature at the (AT)₂ hotspot (**Figure 27 and Appendix 2A**). This result supports earlier conclusions that deletions at the (AT)₂ hotspot are the result of stabilization or trapping of the Top1cc. Analysis in the *top1*Δ background confirmed the Top1-dependence of the 2-bp deletions (**Appendix 2A**). Additionally, I confirmed the CPT-resistant phenotype of our *top1*Δ strain background in a plate spotting assay (**Appendix 2B**).

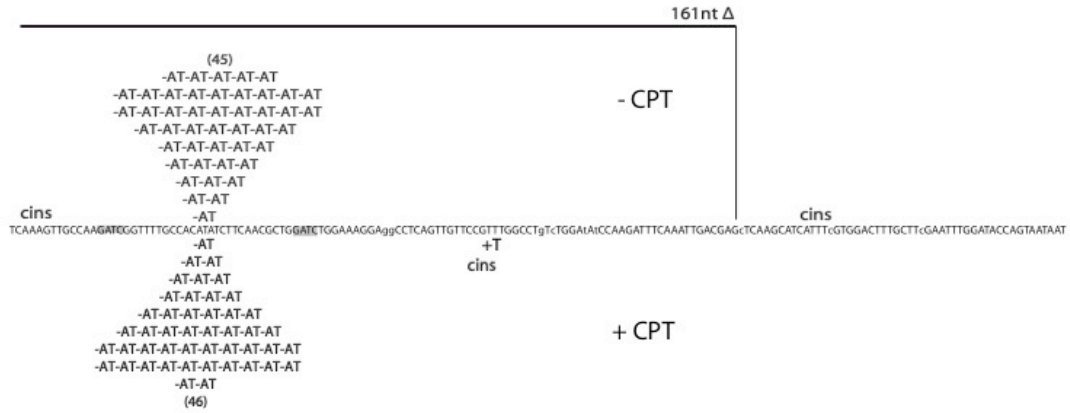


Figure 26. CPT-associated mutations occur at a Top1-dependent hotspot. A majority of mutations accumulate at Top1-dependent hotspot in (AT)₂ reporter. The mutation spectra is presented in the absence (above sequence, N=48) and presence (below sequence, N=48) of 100μM CPT.

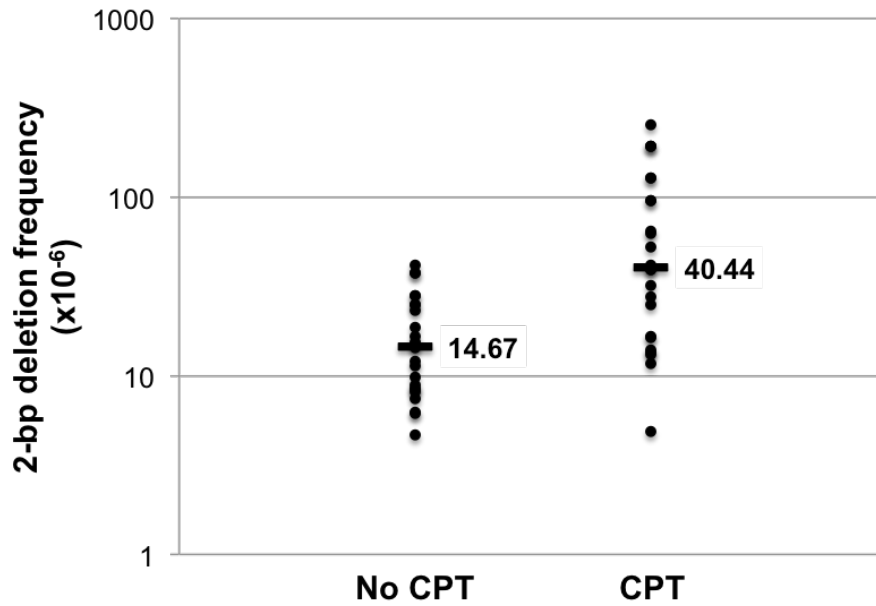


Figure 27. CPT causes an increase in 2-bp deletions at the (AT)₂ hotspot. Shown are the median 2-bp deletion frequencies (black bars) and individual 2-bp deletion frequencies for each culture (black circles) at the (AT)₂ hotspot in the absence and presence of 100μM CPT. Frequencies are based on 24 cultures.

3.3.b. CPT exposure increases mutagenesis at the (TC)₃ hotspot.

Next, I assessed the mutagenic potential of CPT at the (TC)₃ hotspot. This hotspot is unique because it displays both ribo-dependence and ribo-independence (Kim *et al.* 2011). With the (TC)₃ reporter, CPT increased the total Lys⁺ reversion frequency 6-fold, from 3.6×10^{-6} to 2.2×10^{-5} (**Appendix 2A**). **Figure 28 (Appendix 2A)** illustrates the spectrum of mutations obtained which, when combined with the Lys⁺ frequency, revealed that 2-bp deletions at the hotspot (-TC) increased 4-fold in the presence of CPT (t-test two-tailed $p=0.0015$) (**Figure 29**). The spectrum also revealed a new distinct class of 2-bp deletions, which surprisingly do not occur at a perfect tandem repeat (**Figure 28**). We detected a GT deletion in the sequence TCGTGAC at an elevated level in the presence of CPT. The frequency of GT 2-bp deletions increased approximately 40-fold (t-test two-tailed $p<0.0001$) in the presence of CPT (**Figure 29**).

Whether or not the GT deletion was coincident with a Top1-cleavage site was assessed by performing a Top1 cleavage assay. A double-stranded and a nick-containing substrate were used, and each revealed a Top1-cleavage site at the terminal thymine within the (TC)₃ repeat and at the thymine of the deleted GT (**Figure 30**). The cleavage site within the (TC)₃ repeat results in a 22-nt band (**Figure 30, blue arrow**) and is present in both the double-stranded and nick-containing substrates. Neither cleavage site was previously detected, most likely because a shorter, 30-bp duplex was used in cleavage assays (Kim *et al.* 2011). Additionally, half of the concentration of recombinant human Top1 (70nM instead of 140nM) was used previously, which could also explain the higher

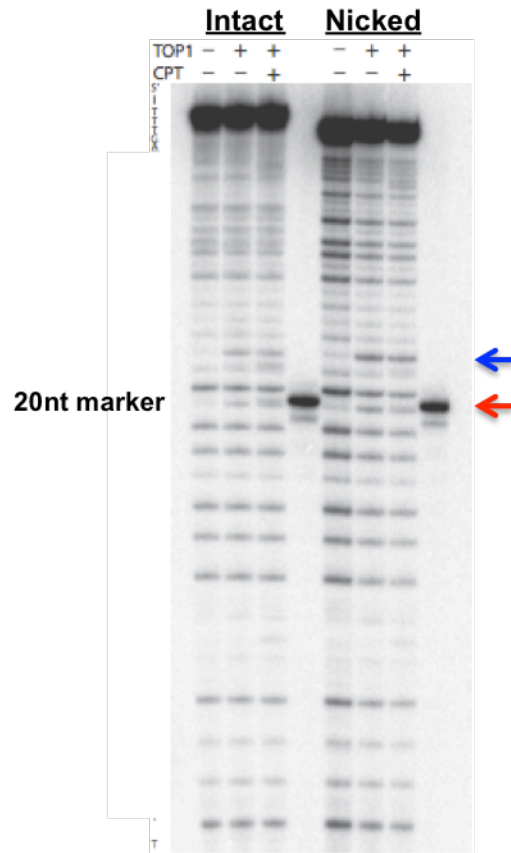
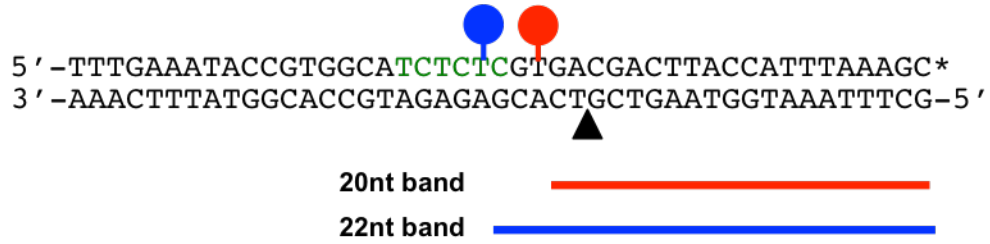


Figure 30. Top1 cleavage sites map within the (TC)₃ repeat and GT dinucleotide. A Top1 cleavage assay performed on a 3'-end labeled 45bp-substrate containing the (TC)₃ repeat revealed a Top1 cleavage site within the (TC)₃ dinucleotide repeat (blue). It also revealed a cleavage site flanking the "GT" sequence (red, 20nt marker). The sequence of the 45bp-substrate is shown with the detected Top1 cleavage sites within (TC)₃ repeat (blue) flanking the "GT" sequence (red). Shown below the 45bp-substrate are the corresponding bands expected for cleavage at sites following same color scheme. The gel displays the Top1 cleavages mapped within the 45bp-substrate, with arrows highlighting the cleavages sites within the (TC)₃ repeat and at the GT sequence (blue and red arrows, respectively). *This assay was performed by Shar-yin Huang in Yves Pommier's lab at NCI (Bethesda, MD).*

sensitivity of the current assay. Finally, the nick-containing substrate generated somewhat stronger cleavage product, which presumably reflects enhanced trapping of the cleavage intermediate. Given the CPT dependence of the GT deletion, we would have expected the corresponding cleavage product to be more abundant in the presence of CPT. However, the intensity of the fragment was similar in both the absence and presence of CPT.

3.3.c. CPT does not affect ribonucleotide associated deletions.

To determine if CPT treatment can affect ribo-associated Top1-dependent deletions, I examined the (AG)₄ reporter in a *RNH201* or *rnh201Δ* background. **Figure 31 (Appendix 2A)** presents the CPT-induced mutation frequency at the (AG)₄ hotspot. In the Rnh201-proficient background there was a 3-fold increase 2-bp deletions at hotspot (t-test two-tailed p=0.03) in the presence of CPT. However, in an Rnh201-deficient background there was no change in Lys⁺ reversion frequency in the presence of CPT (**Appendix 2A**), suggesting that CPT-induced mutagenesis is independent of persistent ribonucleotides.

3.4 Discussion

CPT was previously reported to be weakly mutagenic in yeast (Nitiss and Wang 1988), but no molecular analysis of CPT-dependent mutations was done. Additionally, studies in Chinese hamster cell lines have shown that CPT treatment causes a significant increase in mutation frequency and primarily causes deletions at the *HPRT* locus

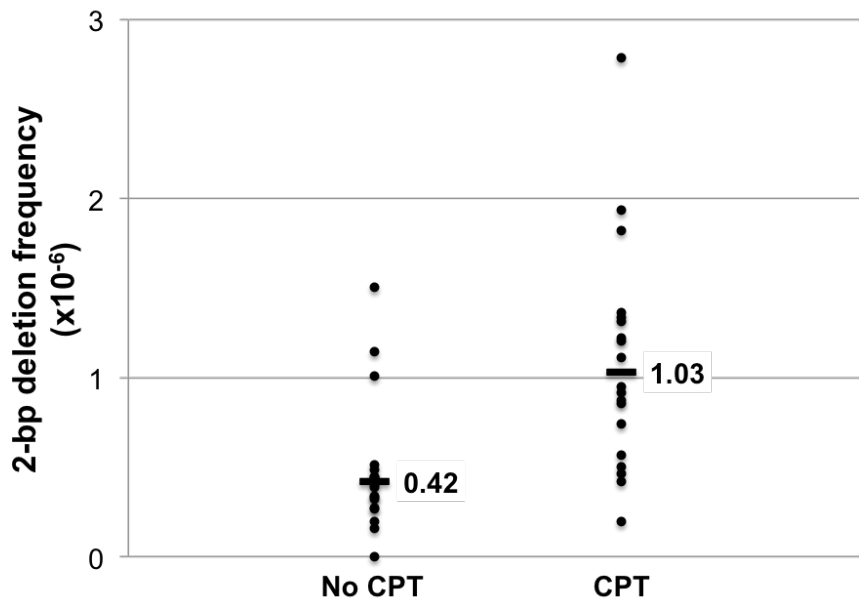


Figure 31. CPT causes an increase in 2-bp deletions at the (AG)₄ hotspot. Shown are the median 2-bp deletion frequencies (black bars) and individual 2-bp deletion frequencies for each culture (black circles) at the (AG)₄ hotspot in the absence and presence of 100 μ M CPT. Frequencies are based on 18 cultures.

(Hashimoto *et al.* 1995; Balestrieri *et al.* 2001). The work presented in this chapter examined the mutagenic effect of CPT on known Top1-dependent hotspots that do not involve a DSB intermediate. The stimulation of 2-bp deletions in all three reporters [(AT)₂, (TC)₃ and (AG)₄] demonstrate that CPT is mutagenic and is consistent with additional, replication-independent effects of Top1 stabilization. CPT stabilization of Top1cc has been reported to be sequence specific (Jaxel *et al.* 1991), and the appearance of a new, CPT-dependent hotspot in the (TC)₃ hotspot is consistent with this. The novel GT deletion occurs at an imperfect repeat (GTGA), whereas most Top1-dependent

deletions have occurred at perfect repeats. A recently published study showed biochemically, however, that Top1-dependent 2-bp deletions can occur at imperfect repeats as long as there was 1-bp homology at the cleavage site to facilitate the realignment (Sparks and Burgers 2015). **Figure 32** illustrates how the mapped cleavage site at the GT deletion hotspot would satisfy this requirement. Currently, there is only mutation frequency data for the (AG)₄ hotspot but it would be interesting to look at the mutation spectrum to see what types of mutations CPT induces. Preliminary results suggest that CPT-induced mutagenesis is ribo-independent, as there is no change in mutagenesis in the presence or absence of CPT in an *rnh201Δ* background. Expressing Top1-T722A (CPT mimetic) in the (AG)₄ reporter led to an increase in mutation frequency (unpublished data, JE Cho and S Jinks-Robertson), further suggesting ribo-independence.

In summary, we find that CPT is mutagenic in a DSB-independent manner. The decrease in cell viability in the presence of CPT is due to toxic DSB formation and replication dependent; however, the 2-bp deletions arise from a single strand nick (Figure 9) and are replication-independent. Additionally a novel CPT-dependent hotspot appears in the (TC)₃ reporter which in future studies will allow us to elucidate the genetic consequences of stabilized Top1cc. Mutagenesis associated with CPT treatment could be a direct cause for secondary tumor formation and could play a significant role in the acquisition of chemotherapeutic drug resistance.

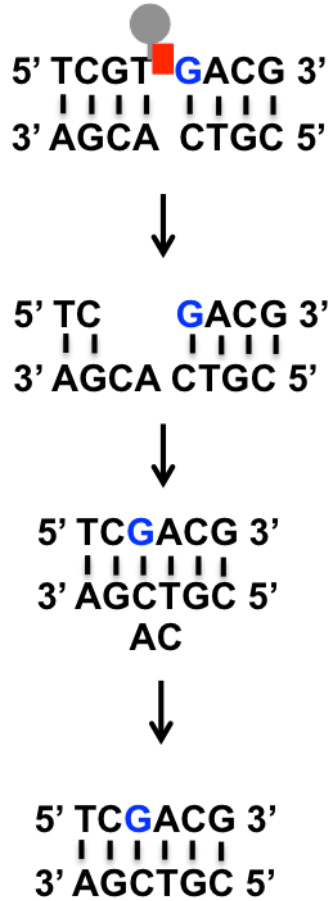


Figure 32. Proposed model for the CPT-dependent GT deletions.
 Top1 (gray circle) cleaves a single-strand of double-strand DNA. CPT (red square) stabilizes the Top1cc preventing the guanine (G, blue) from religating the DNA releasing Top1. Enzymatic processing of the CPT-stabilized Top1cc generates a 2-nt gap. The guanine of the scissile strand base pairs with the cytosine of the un-nicked strand to facilitate realignment. Ligation and replication of the top strand generates a 2-bp deletion.

4. Topoisomerase I overexpression: Can too much of a good thing be bad?

4.1 Introduction

Topoisomerases help maintain genome stability by relieving torsional stress generated by cellular processes such as replication, transcription and chromosome segregation. There are two main classes of topoisomerases: Type I, which encompasses Type IA and Type IB enzymes that nick one strand of duplex DNA, and Type II, which includes Type IIA and Type IIB enzymes that cut both strands of DNA. Type IA topoisomerases (*Saccharomyces cerevisiae* Top3, mammalian Top3 α and Top3 β , *Drosophila melanogaster* Top3 α and Top3 β , bacterial Top1 and Top3) relax negatively supercoiled DNA and catalyze the breakage and rejoining in a single-stranded region. Type IB topoisomerases (eukaryotic Top1, mammalian mitochondria Top1, Pox virus topoisomerase) relax both positive and negative supercoils and the single-stranded nick is generated within duplex DNA. Type II topoisomerases (Top2) decatenate chromosomes, remove intertwinings between newly synthesized DNA duplexes and relax supercoils (Nitiss 1998; Wang 2002).

Top1 transiently cleaves one strand of a DNA duplex through a tyrosine-mediated transesterification reaction, generating a covalent 3'-phosphotyrosine linkage (referred to as the Top1 cleavage complex [Top1cc]) and a 5'OH. The nicked strand then rotates around the intact strand to remove supercoiling and reduce torsional stress. Re-ligation of

the nicked DNA and release of Top1 occurs through a second transesterification reaction mediated by the 5'OH (Wang 2002). Increased *TOP1* gene copy numbers have been detected in metastatic colorectal, breast, bile duct and pancreatic cancers (Romer *et al.* 2013; Grunnet *et al.* 2015; Kumler *et al.* 2015). Elevated levels of Top1 in tumor cells make Top1 an attractive drug target and numerous studies have shown that the cytotoxic activity of topoisomerase inhibitors correlates with Top1 activity and cellular levels (Pommier 2013). Consequently, tumor cells with elevated Top1 protein levels have increased sensitivity towards Top1 inhibitors (Romer *et al.* 2012; Pommier 2013). Champoux and colleagues investigated the effects of human Top1 overexpression in baby hamster kidney cells and reported no affect on cell growth and cell morphology, suggesting that higher levels of Top1 are not cytotoxic (Madden and Champoux 1992).

In yeast, elevated levels of Top1 sensitize cells to alkylating agents, UV light, ionizing radiation and camptothecin (CPT) (Bjornsti *et al.* 1989; Nitiss *et al.* 2001). In the current study, we examine the mutagenic and recombinogenic effects of Top1 overexpression. Increased Top1 levels significantly elevated mutagenesis at three previously characterized Top1-dependent deletion hotspots. Recombination at the rDNA locus also was stimulated by Top1 overexpression, but instability at the *CUP1* locus was not.

4.2 Experimental methods

4.2.a. Strain and plasmids.

Haploid yeast strains used in the *lys2* reversion assays were derived from YPH45 (*MATa ura3-52 ade2-101oc trp1Δ1*) (Sikorski and Hieter 1989). The (AT)₂ WT and *top1Δ*, (TC)₃ WT and *top1Δ*, and (AG)₄ WT, *top1Δ*, *rnh201Δ*, *rnh201Δ top1Δ* and *rnh201Δ pol2-M644LΔ* strains were previously described (Lippert *et al.* 2011; Cho *et al.* 2013). All WT strains are Top1- and Rnh201-proficient. The *TOP1* gene was deleted via one-step gene disruption (Rothstein 1983) to generate the (AG)₄ *rnh201Δ pol2-M644L top1Δ* triple mutant. The diploid yeast strains used in the recombination studies were previously described (Andersen *et al.* 2015), and were derived by crossing derivatives of W303-1A (Thomas and Rothstein 1989) and YJM789 (Wei *et al.* 2007). For a complete list of all strains used and their genotypes see **Table 6**.

The *pCUP-TOPI* plasmid (pWJ1491) used to regulate *TOPI* gene expression was previously described (Reid *et al.* 2011; Cho *et al.* 2013; Andersen *et al.* 2015). A *pCUP-top1-Y727F* plasmid was constructed by excising an *MluI/EagI* fragment containing the *top1-Y727F* mutant allele from the YCpSCtop1-Y727F (Lynn *et al.* 1989). This fragment was then used to replace the corresponding *MluI/EagI* fragment in the *pCUP-TOPI* plasmid. A complete list of plasmids used can be found in **Table 7**.

4.2.b. Copper-induced mutation frequency assay and mutation spectra generation.

To examine the effects of Top1 overexpression, *CEN-URA3* plasmids carrying *TOPI* under the control of the *CUP1* promoter (*pCUP-TOPI*) were introduced into *top1Δ*

Table 6. Strains used in Top1 overexpression studies.

Name	Strain	Genotype	Reference
(AT) ₂	SJR3076	<i>MATa ura3-52 ade2-101_{oc} trp1Δ1 lys2Δ::hyg leu2-K:TetR'-Ssn6:LEU2 [pSR857] his4Δ::kan-pTET-lys2FΔA746,NR, (AT)2</i>	(Lippert <i>et al.</i> 2011; Cho <i>et al.</i> 2013)
(AT) ₂ <i>top1Δ</i>	SJR3095	<i>MATa ura3-52 ade2-101_{oc} trp1Δ1 lys2Δ::hyg leu2-K:TetR'-Ssn6:LEU2 [pSR857] his4Δ::kan-pTET-lys2FΔA746,NR, (AT)2 top1Δ::loxP-TRP1-loxP</i>	(Lippert <i>et al.</i> 2011; Cho <i>et al.</i> 2013)
(TC) ₃	SJR3077	<i>MATa ura3-52 ade2-101_{oc} trp1Δ1 lys2Δ::hyg leu2-K:TetR'-Ssn6:LEU2 [pSR857] his4Δ::kan-pTET-lys2FΔA746,NR, (TC)3</i>	(Lippert <i>et al.</i> 2011; Cho <i>et al.</i> 2013)
(TC) ₃ <i>top1Δ</i>	SJR3096	<i>MATa ura3-52 ade2-101_{oc} trp1Δ1 lys2Δ::hyg leu2-K:TetR'-Ssn6:LEU2 [pSR857] his4Δ::kan-pTET-lys2FΔA746,NR, (TC)3 top1Δ::loxP-TRP1-loxP</i>	(Lippert <i>et al.</i> 2011; Cho <i>et al.</i> 2013)
(AG) ₄	SJR3215	<i>MATa ura3-52 ade2-101_{oc} trp1Δ1 lys2Δ::hyg leu2-K:TetR'-Ssn6:LEU2 [pSR857] his4Δ::kan-pTET-lys2FΔA746,NR, (AG)4</i>	(Lippert <i>et al.</i> 2011; Cho <i>et al.</i> 2013)
(AG) ₄ <i>top1Δ</i>	SJR3639	<i>MATa ura3-52 ade2-101_{oc} trp1Δ1 lys2Δ::hyg leu2-K:TetR'-Ssn6:LEU2 [pSR857] his4Δ::kan-pTET-lys2FΔA746,NR, (AG)4 top1Δ::NATmx4</i>	(Lippert <i>et al.</i> 2011; Cho <i>et al.</i> 2013)
(AG) ₄ <i>rnh201Δ</i>	SJR3226	<i>MATa ura3-52 ade2-101_{oc} trp1Δ1 lys2Δ::hyg leu2-K:TetR'-Ssn6:LEU2[pSR857] his4Δ::pTET-lys2FΔA746,NR,(AG)4 rnh201Δ::NAT</i>	(Cho <i>et al.</i> 2013)
(AG) ₄ <i>rnh201Δ top1Δ</i>	SJR3242	<i>MATa ura3-52 ade2-101_{oc} trp1Δ1 lys2Δ::hyg leu2-K:TetR'-Ssn6:LEU2[pSR857] his4Δ::pTET-lys2FΔA746,NR,(AG)4 rnh201Δ::NAT top1Δ::loxP-TRP1-loxP</i>	(Cho <i>et al.</i> 2013)
(AG) ₄ <i>rnh201Δ pol2-M644L</i>	SJR3544	<i>MATa ura3-52 ade2-101_{oc} trp1Δ1 lys2Δ::hyg leu2-K:TetR'-Ssn6:LEU2[pSR857] his4Δ::pTET-lys2FΔA746,NR,(AG)4 rnh201Δ::NAT pol2-M644L</i>	(Cho <i>et al.</i> 2013)
(AG) ₄ <i>rnh201Δ pol2-m644L top1Δ</i>	SJR4638	<i>MATa ura3-52 ade2-101_{oc} trp1Δ1 lys2Δ::hyg leu2-K:TetR'-Ssn6:LEU2[pSR857] his4Δ::pTET-lys2FΔA746,NR,(AG)4 rnh201Δ::NAT pol2-M644L top1Δ::loxP-TRP1-loxP</i>	This paper
JSC25	SJR3981 (JSC25)	<i>MATa/MATα::hyg leu2-3,112/LEU2 his3-11,15/HIS3 trp1-1/TRP1 ura3-1/ura3 GAL2/gal2 ade2-1/ade2-1 RAD5/RAD5 can1-100Δ:NAT/can1-100Δ::NAT IV1510386::kanMX-can1-100/IV1510386::SUP4-o</i>	(Andersen <i>et al.</i> 2015)
JSC25 <i>top1Δ</i>	SJR4058 (SLA46.D)	<i>MATa/MATα::hyg leu2-3,112/LEU2 his3-11,15/HIS3 trp1-1/TRP1 ura3-1/ura3 GAL2/gal2 ade2-1/ade2-1</i>	(Andersen <i>et al.</i> 2015)

4) *RAD5/RAD5 can1-100/can1-100 IV1510386::kanMX-
can1-100/IV1510386::SUP4-o top1Δ::NAT
/top1Δ::NAT +TOP1-URA plasmid (pSR1013)*

cells by lithium acetate transformation and transformants were selected on synthetic complete dextrose medium lacking uracil (SD-Ura). As a control, WT and *top1Δ* cells were transformed with the parent *CEN-URA3* control plasmid (Vector). Independent cultures were directly started from transformants with no prior purification and grown selectively in SD-Ura liquid medium for three days at 30°C. Stimulation of the *CUP1* promoter was achieved by supplementing SD-Ura liquid medium with cupric sulfate (CuSO₄) to the final concentration of 100μM. Following the three-day incubation, cells were plated on SD-Ura to determine the total number of cells that maintained plasmid and on SD-Ura-Lys to determine the number of Lys⁺ revertants in each culture. The Lys⁺ revertant frequency was calculated by dividing the number of Lys⁺ revertants by the number of cells that maintained plasmid. After calculating the median Lys⁺ mutation frequency, 95% confidence intervals were determined (Altman 1991). All synthetic media were made using yeast nitrogen base lacking cupric sulfate (Sunrise Science Products).

To generate mutation spectra, an 800-bp fragment of the *LYS2* reversion window was amplified with primers LYSWINF (5'-GCCTCATGATAGTTTTTCTAACAATAACG-3') AND LYSWINR (5'-CCCATCACACATACCATCAAATCCAC-3'). The PCR-generated products were sequenced by Eton Bioscience with primer MO18 (5'-GTAACCGGTGACGATGAT-3').

Table 7. Plasmids.

Name	Plasmid	Plasmid Description	Reference
Vector	pRS416	<i>CEN</i> - and <i>URA3</i> -containing control plasmid	(Sikorski and Hieter 1989)
<i>pCUP-TOP1</i>	pWJ1491	pRS416 containing the <i>pCUP1-TOP1</i> gene	(Reid <i>et al.</i> 2011; Andersen <i>et al.</i> 2015)
<i>top1-T727F</i>	pSR1014 (pRS416-top1-Y727F)	pRS416 containing mutant <i>top1-Y727F</i> gene under control of the WT <i>TOP1</i> promoter	(Lynn <i>et al.</i> 1989)
<i>pCUP-top1-T727F</i>	pSR1135	pRS416 containing mutant <i>top1-Y727F</i> gene under control of the <i>CUP1</i> promoter	This paper

The frequency of a specific mutation class was calculated by multiplying the proportion of the class in the spectrum by the median Lys⁺ mutation frequency. 95% confidence intervals were calculated for specific mutation classes by multiplying the proportion of the class in the spectrum by the upper and lower limits.

4.2.c. Quantitative real time RT-PCR (qRT-PCR).

Total RNA was extracted from 5mL of exponentially growing yeast cells cultured in SD-Ura with or without 100μM CuSO₄. RNA extraction was performed as previously described (Kim *et al.* 2007). Real time RT-PCR was performed using the Quantitect One Step SYBR Green RT-PCR kit (Qiagen) and the amount of DNA amplified during each cycle was measured using a StepOne Plus Real-Time PCR System (Applied Biosystems). To control for the starting amount of RNA, qRT-PCR was done in parallel for *RFC1*

transcripts. *TOP1*-specific primers were TOP1F1 (5'-TCGTCGTCATTACCATCGCC-3') and TOP1R1 (5'-TCCTCCTTCGCTTTCTTGTC-3') and *RFC1*-specific primers were RFC2134F (5'-CGCTTCTGATGTTCGCTC-3') and RFC2295R(5'-CCTCCGCTCATAACCATCAAC-3'). The $2^{-\Delta\Delta C_T}$ method was used to determine the relative transcript levels (Livak and Schmittgen 2001).

4.2.d. Sub-culturing of diploids

JSC25 and JSC25 *top1* Δ were transformed with *CEN-URA* plasmids as described above. Independent colonies were streaked on SD-Ura and SD-Ura plates containing 100 μ M CuSO₄. Plates were incubated at 30°C for two days and a single colony was then streaked again onto the same plates. This was repeated 10 times and is equivalent to ~250 generations.

4.2.e. Detection of crossovers initiating at the rDNA locus using a SpeI polymorphism.

A region 21 kb downstream of rDNA locus on Chromosome XII was amplified from the genomic DNA of sub-cultured diploids, as described previously (Andersen *et al.* 2015). A 750-bp PCR product containing a *SpeI* polymorphism specific to the YJM789 allele was generated using primers ChrXIIF490730 (5'-CTGATGAGTTCTGCATCTGTCC-3') and ChrXIIR491473 (5'-TCCGTTACCATTGCATACAGAA-3'). *SpeI* digestion of the PCR product resulted in three fragments (750, 500 and 250 bp) if both W303-1A and YJM789 alleles were

present, two fragments (500 and 250 bp) if only the YJM789 allele was present and one fragment (750 bp) if only the W303-1A was present. *SpeI* digests were analyzed on 1% agarose gels to determine whether the diploid strain remained heterozygous or became homozygous for the relevant SNP during sub-culturing. To ensure that the crossover occurred within the rDNA locus, a region 60 kb upstream of the rDNA locus was checked for maintenance of heterozygosity. A 780 bp PCR product containing a *PspXI* polymorphism specific for YJM789 was amplified with the following primers: ChrXIIuprDNA391662F (5'-GACGCAGAGGAAGAAACAAATC-3') and ChrXIIuprDNA392432R (5'-TCCCACAGCCAGTTCAATATC-3'). If both W303-1A and YJM789 alleles were present after *PspXI*-digestion there were 3 bands (780, 490, and 290 bp), indicating that heterozygosity was maintained.

4.2.f. Analysis of the CUP1 tandem array by Southern blots.

Southern analysis of sub-cultured clones was performed using a previously described digoxigenin-UTP (DIG)-labeling protocol (Zhao *et al.* 2014; Andersen *et al.* 2015). Sub-cultured clones were grown to saturation in 5mL YPD (1% yeast extract, 2% Bacto-peptone, 2% dextrose) and genomic DNA was isolated using a modified standard genomic DNA isolation procedure (http://jinks-robertsonlab.duhs.duke.edu/protocols/yeast_prep.html). DNAs were digested with *EcoRI* overnight and fragments separated by electrophoresis on a 1% agarose gel using the BioRad CHEF Mapper XA System. The switching interval was optimized for DNA

molecules in the size range of 10-60 kb. Separated DNA fragments were transferred to a positively charged nitrocellulose membrane before hybridizing a DIG-label *CUPI* probe at 42°C for at least 16 hours. To generate the probe, a 1-kb segment of the *CUPI* repeat that contained the entire *CUPI* gene was amplified from the genomic DNA of an isogenic derivative of YPH45 (Sikorski and Hieter 1989) using the primers CUP1-amp3 (5'-CTCCTTGTCTTGTATCAATTGCAT-3') and CUP1-amp5-2 (5'-CGAGATGAAATGAATAGCAACGG-3') (Zhao *et al.* 2014). The PCR product was labeled with DIG using Roche DIG-High Prime DNA Labeling and Detection Starter Kit II (Roche). Hybridization of the probe to the membrane was detected with CSPD [disodium 3-(4-methoxyspiro {1,2-dioxetane-3,2'-(5'-chloro)tricyclo[3.3.1.1^{3,7}]decan}4-yl)phenyl phosphate] chemiluminescent alkaline phosphatase substrate. Alterations in the number of *CUPI* repeats per array were determined as described previously (Andersen *et al.* 2015) by comparing the sizes of the *CUPI*-hybridizing fragments to those in the starting strain.

4.3 Results

We previously identified three Top1-dependent, 2-bp deletion hotspots in a highly transcribed *CANI* gene: (AT)₂, (TC)₃ and (AG)₄. In each case, the size of deletion equaled the size of the tandem repeat unit. To study each hotspot in isolation, ~20 bp of surrounding DNA were transplanted into a *lys2*-based frameshift-reversion reporter that detects 2-bp deletions (Kim *et al.* 2011; Lippert *et al.* 2011; Cho *et al.* 2013). Fusion of

the reporter to *pTET* confirmed that deletions at each hotspot are elevated under high-transcription conditions and confirmed that each depends on Top1 (Lippert *et al.* 2011). These hotspots can be further classified as either ribo-independent or ribo-dependent based on their mutagenic behavior in the presence/absence of RNase H2 (*rnh201Δ* mutant), which initiates removal of rNMPs from DNA. (AT)₂ is a ribo-independent hotspot while (AG)₄ and (TC)₃ are ribo-dependent hotspots (Kim *et al.* 2011; Cho *et al.* 2013). Additional support that (AT)₂ is a ribo-independent hotspot was provided by expression of the *pol2-M644L* mutant version of Pol2, which incorporates fewer rNMPs in DNA than wild-type Pol2 (Nick McElhinny *et al.* 2010). Expressing this mutant in (AT)₂ reporter strains resulted in no significant reduction in 2-bp deletion frequency at the hotspot (Cho *et al.* 2013). The opposite was found for both (TC)₃ and (AG)₄ reporters, where a decrease in 2-bp deletion frequency at the hotspot occurred when Pol2-M644L was expressed (Cho *et al.* 2013). Additionally, experiments expressing the Top1-T722A mutant protein, which has been reported to have reduced re-ligation activity (Megonigal *et al.* 1997), increased 2-bp deletions at the (AT)₂ hotspot 11-fold in an Rnh201-defective background. This increase in deletion frequency provided strong genetic evidence that deletions are generated at this hotspot by the irreversible trapping of the Top1-cleavage complex (Top1cc) (Cho *et al.* 2013). In the experiments below, we investigate the role of increased levels of Top1 on the activity of each hotspot.

4.3.a. Overexpression of Top1 is mutagenic and leads to an increase in 2-bp deletions.

To elevate the levels of Top1, plasmids containing the *TOP1* gene under the control of a copper-inducible promoter (*pCUP1-TOP1*) were transformed into *top1Δ* strains containing a *pTET-lys2ΔA746,NR::hotspot*. The allele contains a 1-bp deletion and reversion to lysine prototrophy occurs via a net 1-bp insertion. As a control, we transformed an empty vector plasmid into both wild-type and *top1Δ* strain backgrounds. The increase in *TOP1* transcript levels was assessed by real time PCR. Relative to an endogenous *TOP1* allele under its native promoter, we found that addition of the *pCUP-TOP1* plasmid in the absence of exogenously added copper resulted in a 5-fold increase in transcript level (**Table 8**). In the presence of 100μM copper, the relative transcript level was elevated over 200-fold (**Table 8**), indicating that Top1 protein levels are likely highly elevated.

Table 8. Steady-state *TOP1* transcript levels in WT and *pCUP-TOP1* strains.

Genotype	CuSO ₄ concentration [μM]	Relative transcript level (±SD)
WT + Vector	0	1.0
<i>top1Δ</i> + <i>pCUP-TOP1</i>	0	4.7 (± 0.82)
<i>top1Δ</i> + <i>pCUP-TOP1</i>	100	228 (± 57.4)

The steady-state levels of the *TOP1* transcript were measured by quantitative real time-PCR. The amount of *TOP1* transcript in each strain was normalized to the amount of corresponding *RFC1* transcript. *TOP1* transcript levels are relative to the WT + vector and arbitrarily set at 1.0. Steady-state RNA levels in each strain are based on at least two independent RNA isolations, with 6 threshold cycle number determinations for each independent RNA preparation (Kim *et al.* 2007).

In the absence of Top1 (*top1Δ* + vector), the frequency of Lys⁺ revertants in a strain containing an (AT)₂ reporter was 7.7 x 10⁻⁸, and there were no 2-bp deletions at the hotspot. With endogenous *TOP1* expression, there was a 31-fold increase in median Lys⁺ frequency and all events were 2-bp deletions at the (AT)₂ hotspot (**Appendices 3A and 3B**). This translates into an ~400 fold increase in 2-bp deletions and demonstrates their complete dependence on Top1. Relative to endogenous Top1 expression, we found that presence of the *pCUP-TOP1* plasmid elevated the median frequency of 2-bp deletions at the (AT)₂-containing hotspot 4-fold. Addition of copper resulted in a 15-fold elevation in 2-bp deletion frequency (**Figure 33 and Appendices 3A and 3B**).

4.3.b. Top1 overexpression elevates deletions in the (TC)₃ hotspot and reveals novel hotspots.

Next we analyzed the (TC)₃ reporter for the effects of Top1 overexpression. The Lys⁺ frequency increased 2-fold and 17-fold with the addition of the *pCUP-TOP1* plasmid in the absence and presence of copper, respectively (**Appendix 3A**). Sequence analysis of Lys⁺ revertants revealed the expected 2-bp deletions at the (TC)₃ hotspot, but we also saw 2-bp deletions occurring at imperfect repeats throughout the *lys2* reversion window (**Figure 34, Appendix 3C**). The frequency of 2-bp deletions at the (TC)₃ hotspot increased 2-fold and 10-fold with the addition of the *pCUP-TOP1* plasmid in the absence and presence of copper, respectively (**Figure 35 gray bars and Appendix 3A**). In the presence of the *pCUP-TOP1* plasmid, the frequency of 2-bp deletions that occurred outside of the (TC)₃ hotspot increased 4- and 125-fold in the absence and presence of

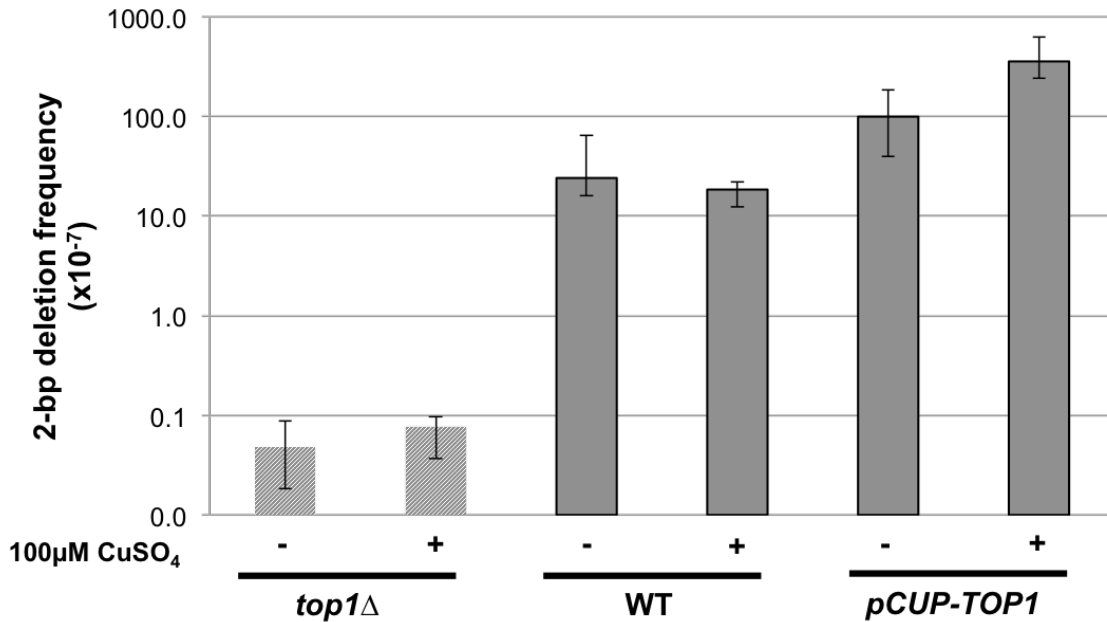


Figure 33. Top1 overexpression increases 2-bp deletions at the (AT)₂ hotspot. The frequencies of 2-bp deletions are shown as gray bars with 95% confidence intervals (C.I.) indicated. No deletion events were detected at the hotspot in the *top1Δ* strain so the frequency was calculated assuming one event (diagonal bars). *top1Δ* (*top1Δ* + vector); WT (WT *TOP1* + vector); *pCUP-TOP1* (*top1Δ* + *pCUP1-TOP1* plasmid).

copper, respectively (**Figure 35** white bars and **Appendix 3A**). Most of these were at two additional hotspots: deletion of GT near the (TC)₃ hotspot within the transplanted DNA fragment and a GA deletion within sequence that was present in all reporters. The GT deletion was identical to that observed in the presence of CPT (**Chapter 3**). Events at the GA deletion hotspot in the (AT)₂ reporter were likely obscured by the very high level of deletions at the (AT)₂ hotspot (**Appendix 3B**). The GT and GA deletions likely occur due to the ability of Top1 to cause deletions at imperfect repeats *in vitro* (Henningfeld and

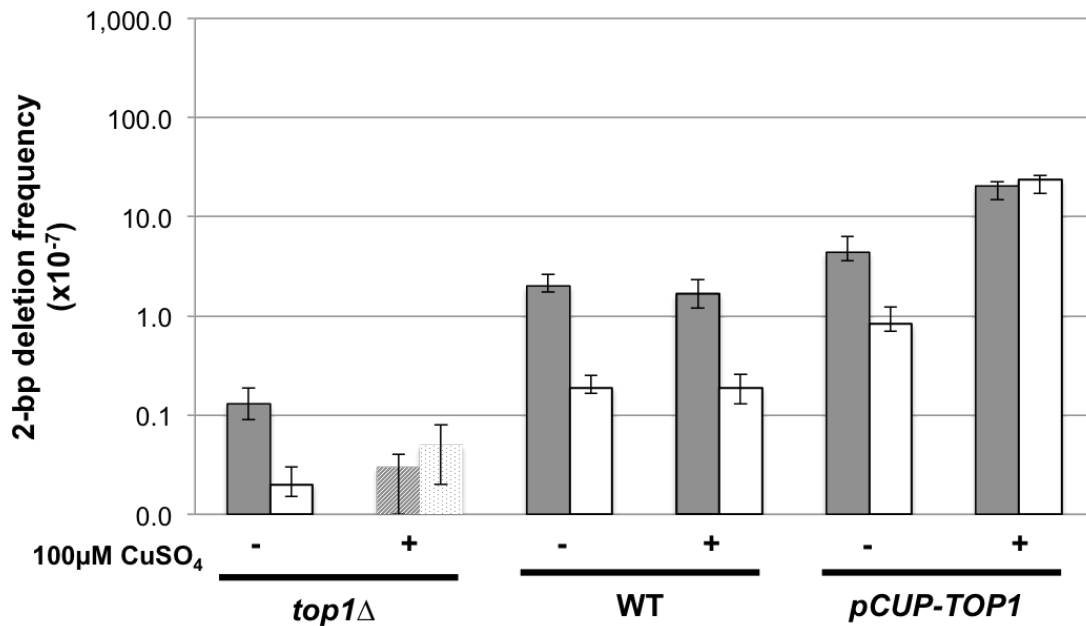


Figure 35. Top1 overexpression increases 2-bp deletions at the (TC)₃ hotspot. The frequency of 2-bp deletions within (gray bars) and outside (white bars) the hotspot are shown with 95% C.I. No 2-bp deletion events were detected in the *top1Δ* strain in the presence of CuSO₄ within or outside of the hotspot, so the frequencies were calculated assuming one event (diagonal and dotted, respectively). *top1Δ* (*top1Δ* + vector); WT (WT *TOP1* + vector); *pCUP-TOP1* (*top1Δ* + *pCUP1-TOP1* plasmid).

the presence of RNase H2, the frequency of 2-bp deletions at the (AG)₄ hotspot increased 19-fold when Top1 was overexpressed in the presence of copper, but was not elevated in the absence of exogenous copper (**Figure 36**; **Appendices 3D** and **3E**). As previously indicated, loss of *RNH201*, the catalytic subunit of RNase H2, highly elevates 2-bp deletions at the (AG)₄ hotspot (Kim *et al.* 2011; Cho *et al.* 2013). While the frequency of 2-bp deletions at the hotspot in a *rnh201Δ* background increased 430-fold relative to WT,

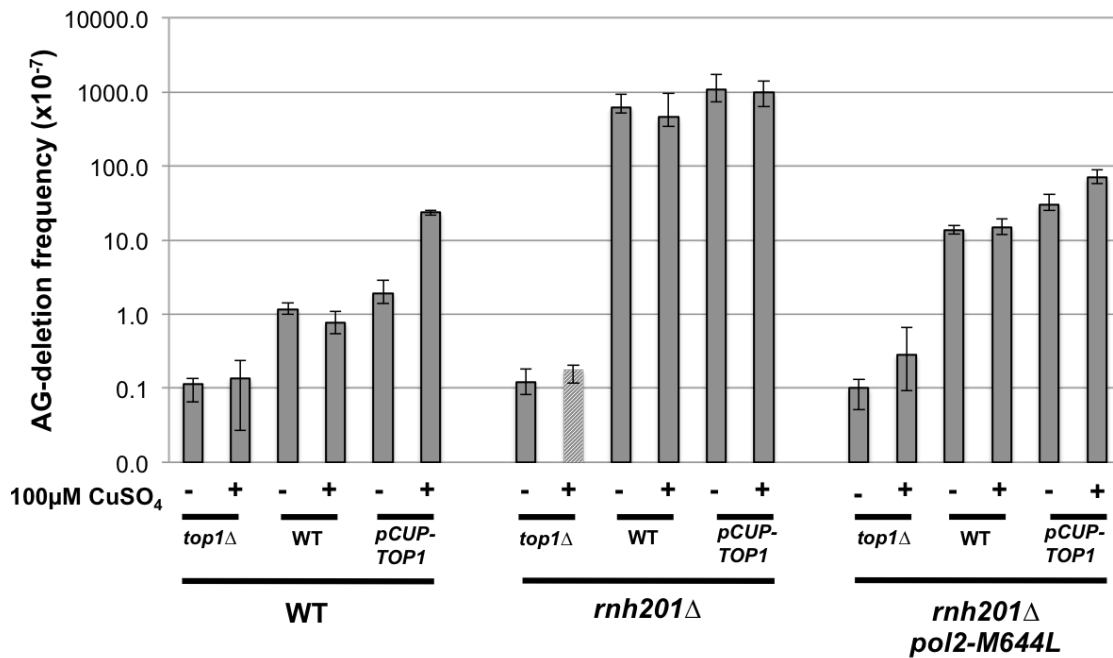


Figure 36. Top1 overexpression increases 2-bp deletions at the (AG)₄ hotspot. No deletion events were detected at the hotspot in the *rnh201*Δ *top1*Δ strain so the frequency was calculated assuming one event (diagonal bars). *top1*Δ (*top1*Δ + vector); WT (WT *TOP1* + vector); *pCUP-TOP1* (*top1*Δ + *pCUP-TOP1* plasmid).

we only detected a 2- and 3-fold increase in mutagenesis at the hotspot with the addition of the *pCUP-TOP1* plasmid in the absence and presence of copper (**Figure 36; Appendices 3D and 3F**). Although not as pronounced as in the Rnh201-proficient background, the increase is significant by Mann-Whitney ($p=0.0015$ and $p<0.0001$, respectively).

To confirm ribonucleotide dependence of deletions at the (AG)₄ hotspot in the *rnh201*Δ background, we used an *rnh201*Δ *pol2-M644L* double mutant, which contains a

mutant version of replicative polymerase Polε that reduces the number of ribonucleotides incorporated into DNA (Nick McElhinny *et al.* 2010). If Top1 overexpression causes an increase in mutagenesis that is dependent on ribonucleotide incorporation we would expect a decrease in mutagenesis when we overexpress Top1 in the *rnh201Δ pol2-m644L* double mutant. The 2-bp deletion frequency at the (AG)₄ hotspot in the *rnh201Δ pol2-M644L* double mutant decreased 42-fold compared to *rnh201Δ* single mutant (**Figure 36, Appendices 4D and 4G**), confirming ribo-dependence. Based on the sequential-cleavage model previously proposed by our lab for Top1- and ribo-dependent deletions (Cho *et al.* 2013), the data presented here suggest that higher levels of Top1 further promote this mechanism of mutagenesis.

4.3.d. Crossovers (COs) at the rDNA locus increase with increasing levels of Top1.

The increase in mutagenesis caused by Top1 overexpression led us to explore whether higher levels of Top1 also stimulate recombination. We examined two naturally existing tandem-repeat loci in yeast: the ribosomal DNA cluster (rDNA) and the *CUP1* locus. The decision to investigate these two loci was based on known effects of Top1 loss and the Top1cc on each (Christman *et al.* 1988; Andersen *et al.* 2015). For these studies, we used diploid strains constructed by mating two sequence-diverged haploids (W303-1a and YJM789) that differ by ~55,000 SNPs (Wei *et al.* 2007).

The rDNA gene cluster is a 1-2 Mb region located on Chromosome XII and is comprised of 100-200 tandem copies of a 9.1 kb repeat; this repeat cluster represents 10% of the yeast genome (Petes and Botstein 1977). Previous studies investigating Top1

behavior in relation to rDNA have shown that both the accumulation of Top1-cleavage complexes and the loss of Top1 greatly enhance instability at the rDNA locus (Christman *et al.* 1988; Andersen *et al.* 2015). Using a previously described technique that allows us to measure crossovers that are initiated within the rDNA locus by monitoring a centromere-distal restriction site polymorphism (Andersen *et al.* 2015), we were able to determine the effect that increased levels of Top1 have on the rDNA stability. We sub-cultured WT (JSC25 with transformed vector plasmid), *pCUP-TOP1/pCUP-TOP1* (JSC25 *top1* Δ with transformed *pCUP-TOP1* plasmid) and *top1* Δ /*top1* Δ (JSC25 *top1* Δ with transformed vector plasmid) diploids 10 times, which is equivalent to ~250 generations before examining them for loss of heterozygosity (LOH) distal to the rDNA locus. We monitored a *SpeI* site (specific for the YJM789 chromosome) located 21-kb centromere-distal of the rDNA locus. If clones maintain heterozygosity then three DNA fragments of 750, 500 and 250 bp are produced. If clones are homozygous for YJM789 allele only the 500 and 250-bp DNA fragments are produced; if clones are homozygous for the W303-1a allele, only a 750-bp fragment is detected.

Among the 24 WT isolates examined, no LOH events were detected (**Figure 37 and Appendix 3H**), a result previously reported (Andersen *et al.* 2015). Sub-culturing 23 WT isolates in the presence of 100 μ M CuSO₄ similarly revealed no LOH events (**Figure 37 and Appendix 3H**), suggesting that copper alone in the presence of Top1 causes no instability at the rDNA locus. *pCUP-TOP1/pCUP-TOP1* sub-cultured isolates had significant levels of instability at the rDNA locus, with 67% and 74% of clones exhibiting LOH in the absence and presence of copper, respectively (**Figure 37 and**

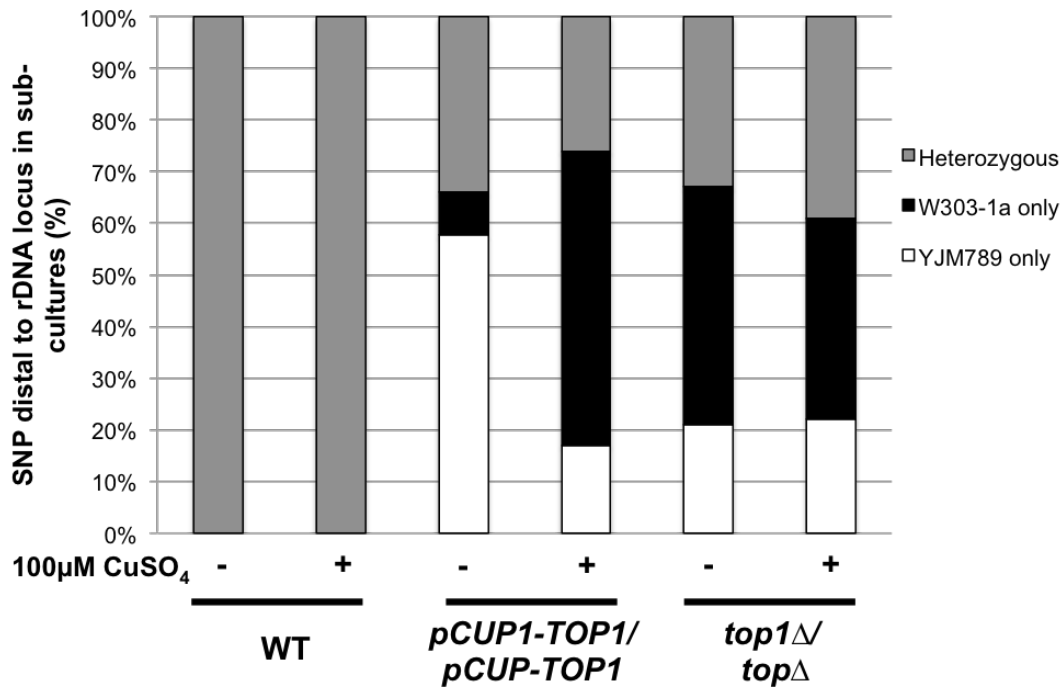


Figure 37. Top1 overexpression results in increased LOH distal to rDNA locus. An rDNA-distal PCR product from sub-culture 10 clones was digested with *SpeI* and analyzed by gel electrophoresis. Dotted, heterozygous; black, homozygous for W303-1A; white, homozygous for YJM789.

Appendix 3H). Interestingly, there was a strong bias to lose the W303-1A allele in sub-cultured isolates containing *pCUP-TOP1* in the absence of copper but a bias to lose the YJM789 allele in the presence of copper. The *top1Δ/top1Δ* isolates in the absence and presence of copper had similarly elevated levels of LOH, 67% and 61% respectively.

Although elevated instability at the rDNA locus in *top1Δ* background has been previously reported (Christman *et al.* 1988; Andersen *et al.* 2015), a similar effect of Top1 overexpression has not been demonstrated.

The *CUPI* locus, encoding metallothionein, is a tandem repeat locus located on Chromosome VIII. It has been shown that different yeast strains have variations in the total number of repeats as well as in the size of the repeat unit (Fogel *et al.* 1983; Karin *et al.* 1984; Zhao *et al.* 2014). The size and nature of the *CUPI* locus make it a suitable region to measure copy-number variation. The diploid contains the W303-1A allele with 14 copies of a 2-kb repeat and the YJM789 allele with seven copies of a 1.2-kb repeat (Zhao *et al.* 2014). Previous studies using camptothecin or a *top1-T722A* mutant allele in this strain background found a significant increase in instability at the *CUPI* locus after 10 sub-cultures, most of which was loss of *CUPI* repeats (Andersen *et al.* 2015). Since stabilization of Top1-cleavage complexes results in instability, we wanted to see if increasing levels of Top1 also resulted in instability at *CUPI*. Based on the small number of sub-cultured clones analyzed, our results indicate that Top1 overexpression does not cause a significant amount of instability at *CUPI* (**Figure 38** and **Appendix 3I**). However, we do detect instability in the *top1Δ* clones ($p=0.05$) that has not been reported.

4.4 Discussion

In this chapter we investigated the potential for higher levels of Top1 to cause instability and found that elevated levels of Top1 are mutagenic in a 2-bp deletion reporter assay and recombinogenic at the rDNA locus. Top1 overexpression in all three reporters [(AT)₂, (TC)₃ and (AG)₄] led to an increase in 2-bp deletions in a Top1-dependent manner. Expression of the catalytic dead protein, Top1-Y727F, resulted in a

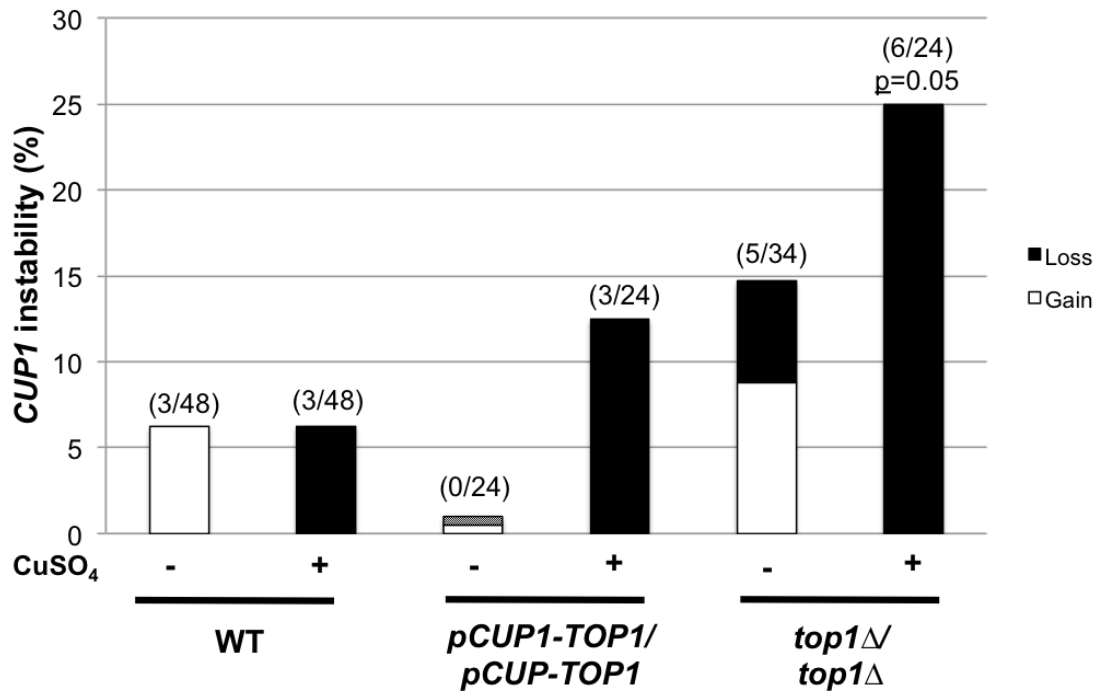


Figure 38. Copy number variation (CNV) at *CUP1* locus is not significantly elevated with Top1 overexpression. Top1 overexpression does not lead to a significant increase in CNV after 10 sub-cultures. Also shown is the percentage of alleles that lose (black bars) compared to alleles that gained *CUP1* repeats (white bars). No CNV events were detected in the *pCUP1/pCUP1* no copper so assumed 1 event (dotted). Fisher's exact probability test was used to determine significance. Proportions (number of alleles with changes/total number of alleles analyzed) are shown above each bar.

Lys⁺ frequency similar to that in *top1Δ* cells, further confirming previous reports that 2-bp deletions in our reporters require the catalytic activity of Top1 (Lippert *et al.* 2011). There was a significant increase in 2-bp deletions that occurred within as well as outside of the (TC)₃ hotspot, with a majority of the novel deletion events resulting in a GT (within the transplanted fragment) and a GA (outside of transplanted fragment) deletion (Figure 34). We predict the mechanism for deletion formation is similar to that presented

in **Chapter 3**, which focused on CPT-induced mutagenesis, where deletion formation is initiated by the processing of the Top1cc into a gap and requires realignment facilitated by 1-bp homology at the cleavage site (see model presented in **Chapter 3, Figure 32**). The GT deletion in the (TC)₃ reporter was additionally elevated in the presence of CPT, suggesting that increased levels of Top1 result in increased levels of stabilized Top1cc. We likely did not detect GA deletions in the (AT)₂ reporter due to the high level of deletions at the hotspot; however, we did detect one GA deletion (out of 27 sequenced revertants) in the (AG)₄ reporter. The GA deletion was not detected in the presence of CPT, but this could be due to the previously reported CPT-sequence specificity (Jaxel *et al.* 1991).

Top1 overexpression in the (AG)₄ reporter strain revealed a ribo-dependent signature. Increased levels of Top1 resulted in an increase in 2-bp deletions at the hotspot and loss of *rmh201Δ* in combination with elevated Top1 resulted in an increase in 2-bp deletion frequency as well. Expression of Pol2-M644L mutant polymerase, which incorporates 70% less ribonucleotides, resulted in a 42-fold decrease in 2-bp deletion frequency. Overall we have provided genetic evidence that high levels of Top1 are mutagenic at all hotspots, regardless of ribo-dependence.

Top1 overexpression caused significant instability at the rDNA locus, resulting in distal LOH of a restriction site polymorphism. We previously reported that both loss of Top1 and stabilization of Top1cc by CPT increased instability at rDNA (Andersen *et al.* 2015) using the same assay. This would suggest that stability at the rDNA locus requires wild-type activity and no fluctuation in Top1 levels; if Top1 activity or abundance is

altered the likelihood of instability increases. Our *CUPI* assay measures changes within the endogenous *CUPI* locus and Top1 overexpression did not elevate instability. Loss of Top1 increased instability.

Numerous yeast studies have shown that overexpression of Top1 sensitizes cells to the Top1 inhibitor, CPT (Bjornsti *et al.* 1989; Nitiss *et al.* 2001). Elevated levels of Top1 are found in numerous forms of cancer and this has been correlated with higher sensitivity of tumor cells to Top1 inhibitors (Potmesil 1994; Romer *et al.* 2012), thus making Top1 an attractive drug target. This study is the first to report that Top1 overexpression is mutagenic and recombinogenic. An essential next step in this study is to look at the effect of increased Top1 levels in the presence of CPT in relation to mutagenesis and recombination. These data would likely provide critical information essential for understanding the effect of Top1 inhibitors as anti-cancer drugs in tumors with elevated levels of Top1.

5. Summary and future directions

5.1 Summary

This dissertation examined Top1-associated genome instability in yeast focusing on the effects of persistent Top1cc or increased Top1 levels. Top1 functions to relieve transcription- and replication-associated torsional stress in DNA (Wang 2002). Elucidating the correlation between persistent Top1cc and genome instability will answer questions about the genetic consequences of processing a trapped Top1cc and provide reliable starting points for improving the efficacy of CPT treatment for suitable combination therapies. Top1 is often elevated in tumor tissues making it an attractive target for anti-cancer treatment (Potmesil 1994; Pommier 2013) and gaining a better understanding of the potential detrimental effects of increased levels of Top1 is equally important for improving treatment regimens. Most importantly, the work presented here supports the utility of yeast as a model system and its applicability to preclinical studies that focus on genome instability.

5.1.a. Effects of persistent Top1cc

Our investigation of the effects of persistent Top1cc on genome stability revealed that stabilized Top1cc are both recombinogenic and mutagenic. Chapter 2 used two assays to illustrate the recombinogenic effects of persistent Top1cc, where Top1cc were

generated by CPT or by expression of the mutant *top1-T722A* (CPT mimetic). Experiments were done in a diploid strain constructed by mating two haploids with about 0.5% sequence divergence. First, a well-characterized sectoring assay that detects loss of heterozygosity (LOH) on either the right arm of Chromosome IV or the left arm of Chromosome V was used to measure the rate of reciprocal crossovers (RCO). We found that both CPT and expression of *top1-T722A* increased RCOs 5 to 10-fold above the spontaneous level. Further analysis suggests that most RCO initiated by a Top1cc occurred after DNA synthesis, while most spontaneous RCO occurred prior to DNA replication. In the second assay used, cells were sub-cultured for ~250 generations and LOH was examined genome-wide using SNP microarrays. Although analyses revealed no significant increase in recombination-associated LOH, copy number variation (CNV) was detected at the *CUPI* tandem-repeat locus. Subsequent, more sensitive analyses confirmed elevated CNV at the *CUPI* locus in the presence of CPT or when the *top1-T722A* allele was expressed. Most CNVs were consistent with sister chromatid exchange, suggesting that the Top1cc initiates instability during or after DNA replication (Andersen *et al.* 2015). These results are consistent with the conversion of Top1cc into DSBs during replication and their processing through the homologous recombination pathway.

Previous studies investigating CPT-induced mutagenesis have indicated that large deletions, which are also likely initiated by a DSB, result from CPT treatment (Hashimoto *et al.* 1995; Balestrieri *et al.* 2001; Myung and Kolodner 2003). Chapter 3 examined the mutagenic effects of persistent Top1cc, specifically looking at the potential for CPT to induce mutagenesis at Top1-dependent deletion hotspots. Two-bp deletion

formation in these reporters is DSB-independent because loss of Rad51, required for strand invasion in HR, does not affect these events (Lippert *et al.* 2011). Therefore, Top1-dependent deletions in these reporters reflect events initiated by a single-strand nick. In the presence of CPT we saw a 3 to 14-fold elevation in mutagenesis, confirming CPT is mutagenic (Nitiss and Wang 1988; Hashimoto *et al.* 1995; Balestrieri *et al.* 2001; Myung and Kolodner 2003). Most importantly, the identification of a novel CPT-dependent deletion (GT deletion in the (TC)₃ reporter) will be useful in elucidating the mechanism of CPT-generated or stabilized Top1cc-induced deletions (discussed below). Our recombination and mutagenesis results have important implications for understanding the effects of CPT as a chemotherapeutic agent.

5.1.b. Mutagenic consequence of increased Top1 levels

Chapter 4 investigated the mutagenic potential of elevated Top1 protein levels. Several studies suggest that increased levels of Top1 in tumor tissues make Top1 inhibitors more effective for anti-cancer treatment (Potmesil 1994; Romer *et al.* 2012; Pommier 2013; Grunnet *et al.* 2015; Kumler *et al.* 2015). Associated mutagenic and recombinogenic effects of having elevated Top1 levels, however, had not been considered. Mutagenesis studies revealed that increased Top1 levels are mutagenic in all three reporters [(AT)₂, (TC)₃, and (AG)₄] and that this increase in mutagenesis is correlated with an increase in Top1-dependent 2-bp deletions. Additionally, these studies revealed that Top1 overexpression is mutagenic regardless of ribo-dependence. All

recombination analyses focused on the rDNA and *CUPI* loci. Instability at the rDNA locus in the presence of increased Top1 levels was elevated in a similar manner to that caused by loss of Top1 or stabilization of Top1cc (Andersen *et al.* 2015). Southern analysis at the *CUPI* locus revealed Top1 overexpression does not cause a significant amount of instability, although loss of Top1 did. This is the first study to show that too much Top1 can be as problematic as loss of Top1 and suggests that elevated Top1 may contribute to genetic instability in tumors.

5.2 Future directions

Results from my studies have revealed that stabilization of Top1cc (CPT treatment) and Top1 overexpression are both mutagenic and recombinogenic. These results provide a broader understanding of the impact Top1 has on genome instability. Our results on the effect of Top1cc stabilization are not surprising, but the effect of Top1 overexpression is. Additionally, the data obtained by our studies suggest that our assays can answer other lingering questions in the field some of which are discussed below.

5.2.a. Mechanism of CPT-induced CNV

In Chapter 2 we showed that stabilization of Top1cc by CPT or expression of Top1-T722A mutant protein significantly increased CNV at the *CUPI* locus, with a

majority of events resulting from a loss of *CUPI* repeats (**Figure 22**). Unequal crossovers, break-induced replication (BIR), gene conversions, single-strand annealing (SSA) and intrachromatid “pop-out” are all possible mechanisms for CNV at *CUPI* locus (**Figure 24**), but the observed bias for deletions suggest that SSA predominates. Our analysis did not allow us to distinguish between the proposed mechanisms but with a few modifications, the mechanisms of CPT-induced CNV at *CUPI* locus could be determined. By taking advantage of the difference in *CUPI* array size that naturally exists between the W303-1A and YJM789 alleles (2 kb and 1.2 kb, respectively) we can create a *CUPI* probe that specifically hybridizes to the W303-1A allele. This would allow us to determine the composition of the *CUPI* array and whether changes that occur are between sisters or homologs. Additionally, performing the *CUPI* analysis in a Rad1 or Rad10-deficient background in the presence of CPT should result in a significant decrease in CNV if the deletion bias is SSA-dependent.

5.2.b. CPT-induced 2-bp deletion formation

CPT treatment resulted in a 3- to 14-fold increase in median Lys⁺ mutation frequency which was directly correlated with an increase in 2-bp deletion frequency; this was true for the (AT)₂ and (TC)₃ reporter, but needs to be confirmed in the (AG)₄ reporter. A novel CPT-dependent 2-bp deletion hotspot, the GT deletion, was also identified in our studies. We can determine whether the increased events seen in the (TC)₃ reporter are ribo-dependent by expressing the *pol2-M644L* mutant, which

incorporates less ribonucleotides, in the presence of CPT. This would reveal whether CPT favors attack by the 2'-OH over the 5'-OH on the other side of the nick and based on the current CPT-ternary complex model (**Figure 8**) this seems possible. An interesting feature of these results is that 2-bp deletions are DSB-independent and all previously reported CPT-mutagenesis has been large deletions and rearrangements, which are likely replication and DSB-dependent (Hashimoto *et al.* 1995; Balestrieri *et al.* 2001; Myung and Kolodner 2003). **Figure 3** illustrates a short-list of possible DNA repair proteins that repair a stabilized Top1cc, which were identified from replication-dependent studies focusing primarily on survival in the absence/presence of CPT. Focusing on the 2-bp deletion frequency of the CPT-dependent GT deletion in various mutant backgrounds (for example: MRX, Sae2, Wss1, Tdp1, Mus81, Rad1, etc.) in the presence of CPT, would elucidate the mechanism of DSB-independent CPT-induced deletion formation. We would specifically be able to identify the protein(s) involved in processing the Top1cc to generate the 2-nt gap (**Figure 32**).

5.2.c. CPT-induced mechanism of lethality

The chain of events leading from stabilization of the Top1-cleavage complex (Top1cc) to cell death has always been of interest (Nitiss and Wang 1988). What is known is that CPT binds to the Top1cc and prevents the re-ligation of DNA, resulting in an accumulation of Top1cc (Hsiang *et al.* 1989). The interaction of the advancing replication fork, or transcriptional machinery, with the stabilized Top1cc results in an

arrest of DNA replication (or transcription) leading to the formation of double-strand breaks (DSBs) (Nitiss and Wang 1988; Hsiang *et al.* 1989). In the last ten years, global supercoiling analysis revealed a CPT-induced accumulation of positive supercoils associated with the stabilization of the Top1cc. This leads to the question of whether or not toxic DSBs are a product of replication fork collision or accumulated positive supercoils, which can act as a barrier for replication fork progression. Blocked replication fork progression can lead to fork stalling/collapse or fork reversal and subsequent processing into a DSB (Koster *et al.* 2007; Ray Chaudhuri *et al.* 2012). A better understanding of the mechanism of CPT lethality is necessary because of the wide use of Top1 inhibitors in combination therapies (Pommier 2013).

John Nitiss (University of Illinois at Chicago) suggested an experiment to genetically test whether the lethal lesion induced by CPT is the result of positive supercoil accumulation rather than replication fork collision (Koster *et al.* 2007). The two proposed models can, in principle, be distinguished by assessing dominance when co-expressing CPT-sensitive and CPT-resistant *TOP1* alleles in the presence of CPT. If replication fork collision is the culprit, we would expect dominance of the CPT-sensitive allele and a decrease in viability. If positive supercoils are the culprit, then we would expect dominance of the CPT-resistant allele because of its ability to remove positive supercoils. We have begun to use the CPT-resistant mutant, *top1vac*, to test this hypothesis. I introduced *top1vac* into our (AT)₂ reporter background and confirmed CPT-resistance as well as Top1 activity. Importantly, the median Lys⁺ mutation frequency in the *top1vac* was similar to that in WT and did not change in the presence of 100μM CPT.

Initial experiments that used a heterozygous diploid strain (WT *TOP1/top1vac*) to test if *top1vac* expression rescued the CPT sensitivity of the WT Top1 were inconclusive due to similar CPT resistance displayed by the WT *TOP1/top1Δ* diploid control strain. We believe that overexpressing *top1vac* in a WT *TOP1* background and performing the reverse (overexpressing WT *TOP1* in a *top1vac* background) in the presence of CPT may give a clearer picture of whether replication fork collisions with the Top1cc or accumulated positive supercoils generate CPT-induced lethal lesions.

5.2.d. Top1 overexpression and camptothecin treatment

A correlation between elevated levels of Top1 in tumor cells and effectiveness of CPT derivatives has previously been shown (Romer *et al.* 2012; Pommier 2013). Mutagenesis studies in the (TC)₃ reporter with CPT treatment or Top1 overexpression (Chapter 3 and 4, respectively) revealed a novel 2-bp deletion, the GT deletion, that was significantly elevated under both conditions (**Figures 28, 29, 34 and 35**). This could suggest that elevated levels of Top1 can be correlated with elevated Top1cc. Looking at the combined effect of Top1 overexpression and CPT on the GT deletion or mutagenesis as a whole in the (TC)₃ reporter would be interesting.

5.2.e. Top1 and Top2 redundancy

It is widely accepted that Top1 and Top2 function redundantly, with both relaxing supercoiled DNA *in vitro* (Goto and Wang 1985; Saavedra and Huberman 1986; Brill *et al.* 1987; Giaever *et al.* 1988; Wallis *et al.* 1989). *top1Δ top2^{ts}* double mutants excise single rDNA repeat units as extrachromosomal rings and expression of either *TOP1* or *TOP2* is associated with reintegration of the rings into the chromosomal rDNA locus (Kim and Wang 1989). While yeast grows fine in the absence of Top1, loss of Top2 is lethal due to the inability of *top2Δ* cells to decatenate chromosomes (Wang 2002; Pendleton *et al.* 2014).

Top1/Top2 redundancy can be tested in the diploid strains (used in Chapter 2 and Chapter 4 studies) and in the Top1-dependent deletion hotspot strains (used Chapter 3 and Chapter 4 studies). The main question that can be addressed is whether or not overexpression of Top1 rescues loss or inhibition of Top2 mediated religation. The diploid strains can assess recombination-associated repair tracts, rDNA and *CUP1* stability. The Top1-dependent deletion hotspot strains allow us to analyze Top1-dependent mutagenesis at the *lys2*-reversion window and see how loss of or inhibition of Top2 mediated religation affects the mutation signature at hotspots. We can additionally investigate novel mutation signatures at the *CAN1* locus by performing an unbiased forward mutation assay. By getting a genome instability profile from the above assays for *top1Δ*, elevated Top1, temperature sensitive *top2-1*, constitutively expressed Top2, and stabilization of Top2 generated DSB intermediate by Etoposide (Top2 inhibitor), we can

assess redundancy. If Top1 and Top2 are functionally redundant, we would expect a rescue of any phenotypes associated with loss of or stabilization of Top2 when we overexpress Top1. Alternatively, we can test whether or not constitutively expressed Top2 is able to rescue any Top1, stabilized Top1cc or *top1*Δ associated phenotypes.

Appendix 1: Genome-wide effects of persistent Top1cc Supplemental Tables.

Appendix 1A. SGD coordinates for heterozygous and homozygous transitions on chromosome IV in CPT treated red/white sectors

Sector	Event Class ¹	Transition Label ²	Markers flanking transitions ³	
			Left	Right
1RW	D6	a	863830	865277
		b	866935	867665
		c	868904	890618
		d	890618	892648
2RW	B2	a	841060	841976
		b	845945	846463
3RW	A	a	1017595	1036052
4RW	A	a	1190182	1216161
5RW	B1	a	1261075	1262375
		b	1264869	1267763
10RW	B1	a	1252616	1254293
		b	1275176	1276330
11RW	B2	a	1368605	1370985
		b	1370985	1374486
12RW	N36	a	830740	831863
		b	831863	832341
		c	832341	832583
		d	832830	833159
		e	839752	840535
		f	848693	849541
13RW	N37	g	852302	855308
		a	1157254	1161545
		b	1188862	1189112
		c	1189112	1189481
14RW	A	a	1089446	1111969
15RW	N38	a	1366726	1367557
		b	1367557	1368003
		c	1372403	1374198
		d	1374246	1374333
16RW	B2	a	1328086	1330102
		b	1330538	1330866
17RW	A	a	1089446	1111969
18RW	A	a	509817	512801
19RW	B1	a	687816	688339
		b	701164	701224
20RW	B2	a	1040924	1044556
		b	1047033	1051325
21RW	B2	a	579229	579742
		b	587100	587919
22RW	N20	a	1264435	1264855

		b	1264937	1265186
		c	1265332	1266551
23RW	B1	a	1039370	1040924
		b	1040924	1044556
24RW	N39	a	1485798	1486091
		b	1486159	1486789
		c	1488015	1488287
		d	1489226	1490813
		e	1491125	1491302
		f	1491920	1492290

¹ Event Class: Classes of events are defined in Table 2.

² Transition Label: These lower case letters reflect the transition from heterozygous to homozygous regions as shown in Table 2.

³ Markers flanking transition: SGD coordinates of SNPs located on each side of the transition.

Appendix 1B. SGD coordinates for heterozygous and homozygous transitions on chromosome IV in top1-T722A red/white sectors

Sector	Event Class ¹	Transition Label ²	Markers flanking transitions ³	
			Left	Right
1RW	B1	a	774716	775504
		b	785867	787240
2RW	B2	a	839006	839752
		b	842052	842312
4RW	B1	a	1171413	1173657
		b	1181603	1182080
5RW	D5	a	546605	551730
		b	553854	554380
		c	555575	556844
		d	557100	558167
7RW	A	a	729738	730597
8RW	N40	a	599224	601671
		b	608319	609891
		c	616610	617827
		d	620573	623017
9RW	B2	a	1156998	1157254
		b	1173657	1171413
10RW	A	a	485657	495183
11RW	B1	a	598460	598715
		b	608376	608572
		c	609138	611611
12RW	A	a	1394070	1397989
13RW	B1	a	764803	764830
		b	1190182	1225482
14RW	B1	a	1453193	1455114
		b	1459821	1460352
15RW	B2	a	1171413	1173640
		b	1174594	1174705
16RW	B2	a	1221462	1225482
		b	1333878	1336486
17RW	A	a	1235569	1240156
18RW	B1	a	1283911	1284092
		b	1287823	1289866
19RW	D6	a	701908	702466
		b	723149	724557
		c	725231	726748
		d	730720	731914

21RW	B1	a	970231	971058
		b	978358	978621
23RW	A	a	1171413	1173657
24RW	B1	a	1240303	1241971
		b	1249203	1251733

¹ Event Class: Classes of events are defined in Table 3.

² Transition Label: These lower case letters reflect the transition from heterozygous to homozygous regions as shown in Table 3.

³ Markers flanking transition: SGD coordinates of SNPs located on each side of the transition

Appendix 1C. SGD coordinates for events detected in sub-cultured clones.

Strain	Genotype	Condition	Clone No.	Chr	Event Class*	Markers flanking transitions**			
						Left	Right		
JSC25	WT	YPD + DMSO	29.1	13	a1	681653	684380		
						684380	685125		
						685125	687473		
			30.1	10	b1	149069	153061		
						157586	157675		
						157675	157805		
		157805				157905			
		157905				159185			
		161580				163352			
		YPD + CPT	20.1	2	a2	102421	116691		
						3	a3	260184	269360
								8	b2
			11	b2	225165	225901			
					176121	177475			
					205590	206366			
21.1	12		a1	962667	963376				
				d1	447834	490725			
22.1	7		b2	138007	142576				
		146589		159699					
SLA46.D4	<i>top1Δ</i>	+ <i>top1-T722A</i> plasmid	1.1	8	c1	277513	281875		
						211711	215271		
						215902	216553		
			2.1	8	c1	211711	215271		
						215902	216553		
						12	b3	447537	490725
								493683	493832
						12	d1	606117	607697
								608083	611242
			3.1	12	d1	665333	665741		
						665742	678184		
						1394070	1398890		
						1411220	1414657		
						7	b3	122369	123323
								130707	131363
4.1	8	c1	211711	215271					
			216113	216553					
			12	b3	545557	548317			
					552864	554927			
			12	a1	1048627	1051101			
					211711	215271			
11	b2	216113	216553						
		83483	83729						
			84426	84604					

* Event class: Classes of events are defined in Table 4.

** Markers flanking transitions: SGD coordinates of SNPs located on each side of the transition.

Appendix 1D. CUP1 Southern data for sub-cultured clones.

Strain	Geno- type	Cond.	Clone No.	Subculture 1			Subculture 10			
				Copy No. Status*		Insta- bility	Copy No. Status*		Insta- bility	
				W303	YJM 789	(Y/N)	W303	YJM 789	(Y/N)	
JSC25	WT	YPD + DMSO	1	-5	NC	N	-5	NC	N	
			2	NC	NC	N	NC	NC	N	
			3	NC	NC	N	NC	NC	N	
			4	NC	NC	N	NC	NC	N	
			5	NC	NC	N	NC	NC	N	
			6	NC	NC	N	NC	NC	N	
			8				NC	NC	N	
			9				NC	NC	N	
			11				NC	NC	N	
			12				NC	-1	N	
			13	NC	NC	N				
			14	NC	NC	N				
			15	NC	NC	N				
			29.1	NC	NC	N		-2	NC	N
			30.1					NC	NC	N
	YPD	1					NC	NC	N	
		2					NC	NC	N	
		3					NC	NC	N	
		4					NC	NC	N	
		5					NC	NC	N	
		6					NC	NC	N	
		8					-3	NC	N	
		9					NC	NC	N	
		10					NC	NC	N	
		11					NC	NC	N	
		12					NC	NC	N	
		33.1					NC	NC	N	
		34.1					NC	NC	N	
		YPD + CPT	1	NC	+1	Y	+5	NC	N	
			2	NC	NC	Y	+5	NC	N	
			3	NC	NC	Y	-2	-2	N	
			4	NC	NC	Y	-2	-2	N	
			5	NC	NC	Y	+5	-4	N	
			6	NC	NC	Y	-3	-4	N	
7					-6	NC	N			
8					-6	NC	N			
12					-7	-2	N			
13	NC		NC	Y						
14	NC		NC	Y						
15	NC		NC	Y						
19.1	NC		NC	Y		-3	-5	Y		
20.1						-6	-1	Y		
21.1					-1	-2	Y			
22.1					-1	NC	N			
PG311	WT	YPD + DMSO	1	NC	NC	N	NC	NC	N	
			2	NC	NC	N	NC	NC	N	
			3	NC	NC	N	NC	NC	N	
			4	NC	NC	N	NC	NC	N	

	5	NC	NC	N	NC	NC	N
	6				NC	NC	N
	7				NC	+4	N
	8				NC	NC	N
	9				NC	NC	N
	10				NC	+3	N
	11				NC	NC	N
	12				NC	NC	N
	13	+2	NC				
	14	NC	NC				
	15	NC	NC				
	19				NC	NC	N
	20				NC	NC	N
	21				NC	NC	N
	22				+2	NC	N
	23				NC	NC	N
	24				NC	NC	N
	27.1				NC	NC	N
	28.1				-5	NC	N
YPD	1				+2	NC	N
	2				-6	NC	N
	3				NC	-3	N
	4				NC	NC	N
	5				NC	NC	N
	6				NC	NC	N
	7				NC	NC	N
	8				NC	NC	N
	9				NC	NC	N
	10				NC	NC	N
	11				NC	NC	N
	12				NC	NC	N
	19				NC	NC	N
	20				NC	NC	N
	21				NC	NC	N
	22				-1	NC	N
	23				NC	+1	N
	24				NC	NC	N
YPD + CPT	1	-2	NC	Y			
	2	NC	NC	Y			
	3	NC	NC	Y			
	4	NC	NC	Y	-2	NC	N
	5	NC	NC	Y			
	6				NC	-2	N
	7				-3	+1	N
	8				-3	-5	N
	9				-4	+4	N
	10				-2	+3	N
	11				-2	NC	N
	13	NC	NC	Y			
	14	NC	NC	Y			
	15	NC	NC	N			
	19				NC	NC	
	20				-6	NC	Y
	21				-2	NC	N
	22				-2	-3	N
	23				-4	NC	N
	23.1				-2	NC	Y
	24				-6	NC	N

			24.1	NC	NC	Y	-1	-1	Y	
			25.1	NC	NC	Y	+5	+1	Y	
SLA46. D4	<i>top1Δ</i>	+ Vector plasmid	1	NC	NC	N	NC	NC	N	
			2	NC	NC	N	NC	NC	N	
			3	NC	NC	N	NC	NC	N	
			4	NC	NC	N	-5	NC	N	
			5	NC	NC	N	-5	NC	N	
			6	NC	NC	N	NC	NC	N	
			7	NC	NC	N	NC	NC	N	
			8	NC	NC	N	NC	NC	N	
			9	NC	NC	N	+2	NC	N	
			10	NC	NC	N	NC	NC	N	
			11	NC	NC	N	NC	NC	N	
			12	NC	NC	N	NC	NC	N	
			13	NC	NC	N				
			13.1					NC	NC	N
			14	NC	NC	N				
			14.1					NC	+2	N
15	NC	NC	N							
16	NC	NC	N							
17.1					NC	NC	N			
39.1					NC	NC	N			
45.1					NC	NC	N			
46.1					NC	NC	N			
		+ WT TOPI plasmid	1	NC	NC					
			7	NC	NC					
			7.1				NC	NC	N	
			8	NC	NC					
			8.1				NC	NC	N	
			9	NC	NC					
			9.1				NC	NC	N	
			10	NC	NC					
			10.1				NC	NC	N	
			11.1				NC	NC	N	
			12	NC	NC					
			37.1				NC	NC	N	
			38.1				NC	NC	N	
			43.1				NC	NC	N	
			44.1				NC	NC	N	
			51.1				NC	NC	N	
		52.1				NC	NC	N		
		53.1				NC	NC	N		
		54.1				NC	NC	N		
		+ <i>top1-T722A</i> plasmid	1	+2	NC	N				
			1.1				NC	NC	N	
			2.1				+1	NC	Y	
			3.1				-8	NC	N	
			4.1				NC	NC	Y	
			5	-5	-2	Y				
			5.1				-1	-1	Y	
			6	-2	NC	N				
			6.1				-1	NC	Y	
			7	NC	NC	Y				
			8	-4	NC	Y				
		9	NC	NC	Y					
		10	+1	NC	Y					
		11	+1	NC	Y					

12	NC	NC	Y			
14	NC	NC	Y			
16	NC	NC	N			
35.1				-1	NC	Y
36.1				-5	-6	Y
41.1				-4	NC	Y
42.1				-2	+2	Y
47.1				+2	-2	Y
48.1				NC	NC	Y
49.1				+1	-4	Y
50.1				+6	-3	N

* Copy Number Status: The estimated number of *CUPI* repeats lost (blue) or gained (red)

Appendix 1E. Reciprocal crossovers at the rDNA locus after 10 sub-cultures.

Strain	Geno- type	Conditions	SNP Distal to rDNA locus			Total Clones Analyzed
			Both	W303-1A only	YJM789 only	
JSC25	WT	YPD	40	0	0	40
		YPD + DMSO	21	0	0	21
		YPD + CPT	23	15	5	43
SLA46.D4	<i>top1</i> Δ	+ Vector plasmid	24	14	6	44
		+ WT <i>TOPI</i> plasmid	30	7	7	44
		+ <i>top1-T722A</i> plasmid	10	22	12	44

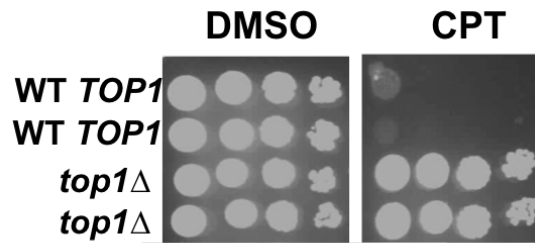
Appendix 2: CPT-induced mutagenesis supplemental material

Appendix 2A. CPT-induced mutation frequency data for all three reporters.

<i>lys2ΔA746</i> allele	Genotype	CPT conc [μM]	Lys ⁺ reversion frequency (x10 ⁻⁶)			Total Frequency
			2bpΔ at hotspot	GT 2-bpΔ hotspot	Other mutations	
(AT) ₂	WT	0	14.6 [45/48]	<0.33 [0/48]	0.98 [3/48]	15.6
		100	40.4 [46/48]	<0.88 [0/48]	1.76 [2/48]	42.2
	<i>top1Δ</i>	0		No spectra		0.77
		100		No spectra		2.16
(TC) ₃	WT	0	2.35 [31/48]	0.15 [2/48]	1.14 [15/48]	3.64
		100	9.72 [21/48]	5.56 [12/48]	6.92 [15/48]	22.2
(AG) ₄	WT	0	0.42 [8/11]	<0.06 [0/11]	0.18 [3/11]	0.65
		100	1.27 [13/14]	<0.1 [0/14]	0.1 [1/14]	1.37
	<i>rnh201Δ</i>	0		No spectra		2450
		100		No spectra		2950

Appendix 2B. CPT treatment causes a significant decrease in cell viability.

10-fold serial dilutions were spotted on YPD plates containing DMSO with or without 100μM CPT. Plates were incubated at 30°C for four days.



Appendix 3. Top1 overexpression supplemental tables and figures

Appendix 3A. Effect of Top1 overexpression on mutations in the (AT)₂ and (TC)₃ reporters.

<i>lys2</i> ΔA746 allele	Genotype + Plasmid	CuSO ₄ [μM]	Lys ⁺ reversion frequency (x10 ⁻⁷)				
			2-bpΔ at hotspot ^[1]	2-bpΔ outside hotspot ^[2]	Other mutations ^[3]	Total Frequency (95% CI)	
(AT) ₂	<i>top1</i> Δ + Vector	0	<0.06	0.06	0.72	0.77	
		(N=30)	[0/14]	[1/14]	[13/14]	(0.38-1.52)	
		100	<0.08	<0.08	1.23	1.23	
	WT+ Vector	(N=6)	[0/16]	[0/16]	[16/16]	(0.6-1.6)	
		0	24.2	<0.86	<0.86	24.2	
		(N=42)	[28/28]	[0/28]	[0/28]	(16.0-64.5)	
	<i>top1</i> Δ + <i>pCUP-TOP1</i>	100	18.5	<0.69	<0.69	18.5	
		(N=18)	[27/27]	[0/27]	[0/27]	(11.8-22.2)	
		0	99.5	<4.52	4.52	104	
	(TC) ₃	<i>top1</i> Δ + Vector	(N=42)	[22/23]	[0/23]	[1/23]	(41.7-193)
			100	358	<13.3	<13.3	358
			(N=42)	[27/27]	[0/27]	[0/27]	(243-627)
WT+ Vector		0	0.13	0.02	0.50	0.65	
		(N=24)	[6/30]	[1/30]	[23/30]	(0.47-0.97)	
		100	<0.03	<0.05	0.8	0.8	
<i>top1</i> Δ + <i>pCUP-TOP1</i>		(N=6)	[0/16]	[0/16]	[16/16]	(0.33-1.22)	
		0	1.99	0.19	0.45	2.64	
		(N=36)	[31/41]	[3/41]	[7/41]	(2.31-3.47)	
<i>top1</i> Δ + <i>pCUP-TOP1</i>		100	1.68	0.19	0.61	2.42	
		(N=24)	[18/26]	[2/26]	[6/26]	(1.72-3.38)	
		0	4.36	0.84	0.42	6.2	
<i>top1</i> Δ + <i>pCUP-top1Y727F</i>	(N=36)	[31/44]	[6/44]	[7/44]	(5.11-9.0)		
	100	20.32	23.71	1.69	45.7		
	(N=36)	[36/81]	[42/81]	[3/81]	(33.3-50.9)		
<i>top1</i> Δ + <i>pCUP-top1Y727F</i>	0	0			0.46		
	(N=24)		No Spectra		(0.34-0.77)		
<i>top1</i> Δ + <i>pCUP-top1Y727F</i>	100				0.73		
	(N=24)		No Spectra		(0.4-1.05)		

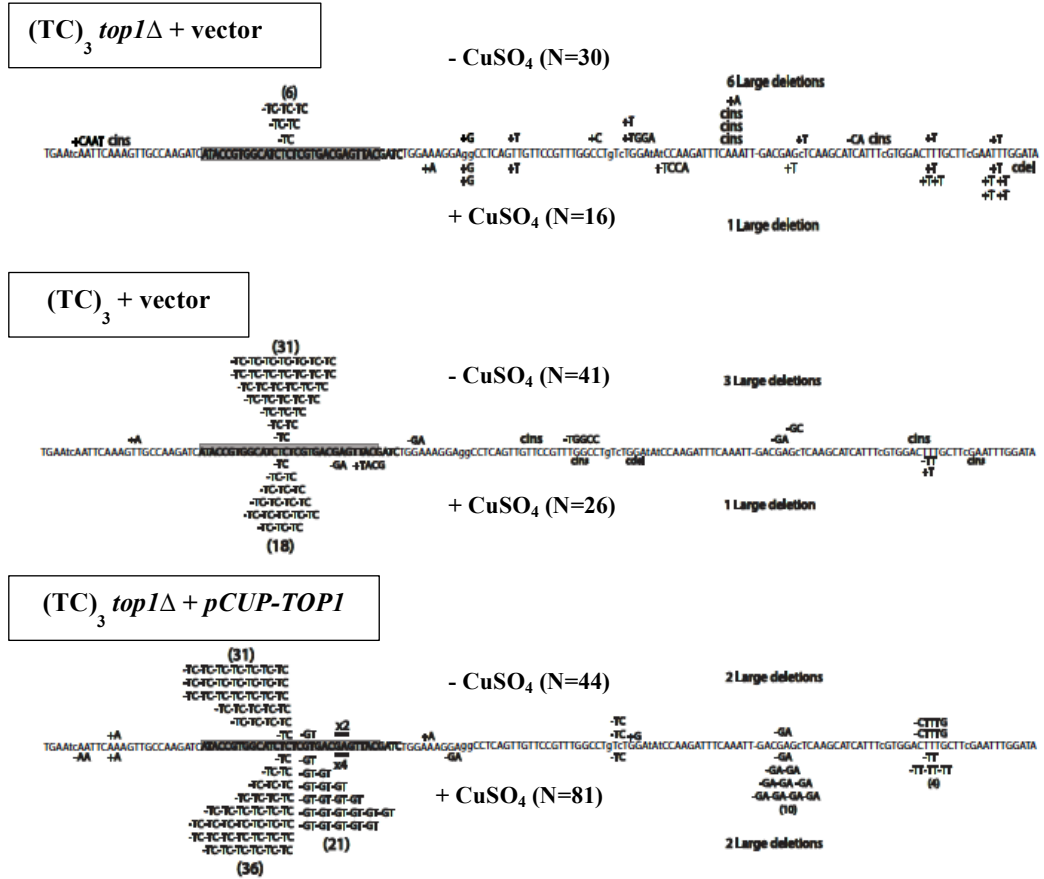
N= number of cultures used to determine the total Lys⁺ frequency.

^[1] In brackets is the number of Lys⁺ revertants with 2-bp deletions at the hotspot (yellow shaded region in Appendices 4B and 4C) out of the total number sequenced.

^[2] In brackets is the number of Lys⁺ revertants with 2-bp deletions outside of the hotspot (yellow shaded region in Appendices 4B and 4C) out of the total number sequenced.

^[3] In brackets is the number of Lys⁺ revertants with mutations other than 2-bp deletions out of the total number sequenced. These mutations include insertions, large deletions (greater than 5-bp), and complex insertion/deletion events.

Appendix 3C. (TC)₃ reporter spectra.



Appendix 3D. Effect of Top1 overexpression on mutations in the (AG)₄ reporter.

<i>lys2ΔA746</i> allele	Genotype + Plasmid	CuSO ₄ [μM]	Lys ⁺ reversion frequency (x10 ⁻⁷)				
			2bpΔ at hotspot ^[1]	2bpΔ outside hotspot ^[2]	Other mutations ^[3]	Total Frequency (95% CI)	
(AG) ₄	<i>top1Δ</i> + Vector	0	0.12	0.04	0.47	0.62	
		(N=30)	[3/16]	[1/16]	[12/16]	(0.44-0.91)	
		100	0.14	<0.05	0.5	0.64	
		(N=6)	[3/14]	[0/14]	[11/14]	(0.15-1.11)	
		WT+ Vector	0	1.16	0.17	0.23	1.56
			(N=42)	[20/27]	[3/27]	[4/27]	(1.34-1.9)
	<i>top1Δ</i> + <i>pCUP-TOP1</i>	0	1.93	0.44	0.44	2.87	
		(N=42)	[18/26]	[4/26]	[4/26]	(2.03-4.1)	
		100	23.82	6.28	3.77	33.9	
		(N=42)	[19/27]	[5/27]	[3/27]	(30.7-36.1)	
		<i>top1Δ</i> + <i>pCUP-TOP1</i>	0	1074	<43	<43	1074
			(N=36)	[25/25]	[0/25]	[0/25]	(726-1739)

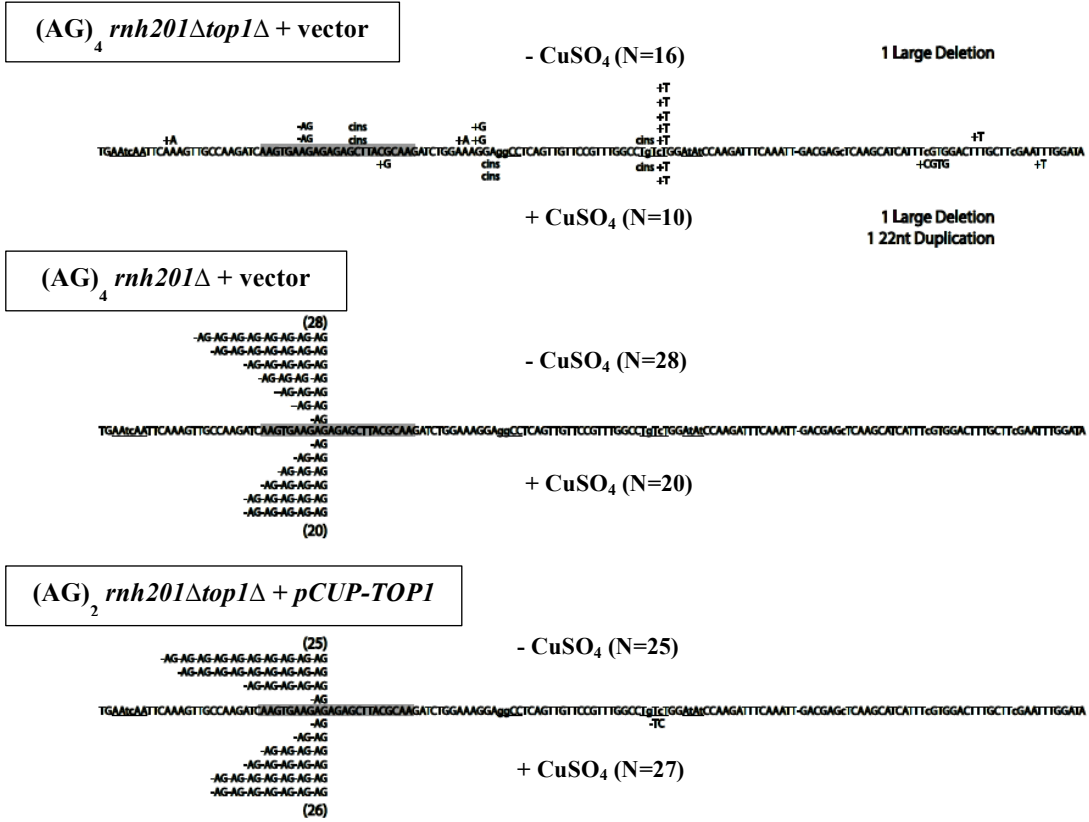
N= number of cultures used to determine the total Lys⁺ frequency.

^[1] In brackets is the number of Lys⁺ revertants with 2-bp deletions at the hotspot (yellow shaded region in Appendices 4E, 4F and 4G) out of the total number sequenced.

^[2] In brackets is the number of Lys⁺ revertants with 2-bp deletions outside of the hotspot (yellow shaded region in Appendices 4E, 4F and 4G) out of the total number sequenced.

^[3] In brackets is the number of Lys⁺ revertants with mutations other than 2-bp deletions out of the total number sequenced. These mutations include insertions, large deletions (greater than 5-bp), and complex insertion/deletion events

Appendix 3F. (AG)₄ *rnh201*Δ spectra.



Appendix 3H. Crossovers initiated within the rDNA locus in sub-culture 10 clones.

Genotype	Strain + Plasmid	CuSO ₄ conc [μM]	SNP status distal to rDNA locus			Total Analyzed
			Heterozygous	W303-1a only	YJM789 only	
WT	JSC25 + Vector	0	24 (100%)	0 (0%)	0 (0%)	24
		100	23 (100%)	0 (0%)	0 (0%)	23
<i>top1Δ/top1Δ</i> + <i>pCUP-TOPI</i>	JSC25 <i>top1Δ</i> + <i>pCUP1-TOPI</i>	0	8 (33%)	2 (8%)	14 (59%)	24
		100	6 (26%)	13 (57%)	4 (17%)	23
<i>top1Δ/top1Δ</i>	JSC25 <i>top1Δ</i> + Vector	0	8 (33%)	11 (46%)	5 (21%)	24
		100	9 (39%)	9 (39%)	5 (22%)	23

Appendix 3I. CUP1 Southern hybridization data for sub-culture 10 clones.

Genotype	Strain + Plasmid	CuSO ₄ conc [μM]	Behavior at <i>CUP1</i> locus				Total Alleles Analyzed	
			Alleles with changes to W303-1a		Alleles with changes to YJM789			Alleles with No Changes
			Gain	Loss	Gain	Loss		
WT	JSC25 + Vector	0	3	-	-	-	45	48
		100	-	2	-	1	-	45
<i>top1Δ/top1Δ</i> + <i>pCUP-TOPI</i>	JSC25 <i>top1Δ</i> + <i>pCUP-TOPI</i>	0	-	-	-	-	24	24
		100	-	3	-	-	21	24
<i>top1Δ/top1Δ</i>	JSC25 <i>top1Δ</i> + Vector	0	2	-	1	2	29	34
		100	-	5	-	1	18	24

References

Altman, D.G. (1991). *Practical Statistics for Medical Research*

Andersen, S.L., Sloan, R.S., Petes, T.D., and Jinks-Robertson, S. (2015). Genome-destabilizing effects associated with top1 loss or accumulation of top1 cleavage complexes in yeast. *PLoS Genet* *11*, e1005098.

Balestrieri, E., Zanier, R., and Degrassi, F. (2001). Molecular characterisation of camptothecin-induced mutations at the hprt locus in Chinese hamster cells. *Mutation research* *476*, 63-69.

Been, M.D., Burgess, R.R., and Champoux, J.J. (1984). Nucleotide sequence preference at rat liver and wheat germ type 1 DNA topoisomerase breakage sites in duplex SV40 DNA. *Nucleic Acids Res* *12*, 3097-3114.

Bjornsti, M.A., Benedetti, P., Viglianti, G.A., and Wang, J.C. (1989). Expression of human DNA topoisomerase I in yeast cells lacking yeast DNA topoisomerase I: restoration of sensitivity of the cells to the antitumor drug camptothecin. *Cancer Res* *49*, 6318-6323.

Brill, S.J., DiNardo, S., Voelkel-Meiman, K., and Sternglanz, R. (1987). DNA topoisomerase activity is required as a swivel for DNA replication and for ribosomal RNA transcription. *NCI Monogr*, 11-15.

Champoux, J.J. (1988). Topoisomerase I is preferentially associated with isolated replicating simian virus 40 molecules after treatment of infected cells with camptothecin. *J Virol* *62*, 3675-3683.

Cho, J.E., Kim, N., Li, Y.C., and Jinks-Robertson, S. (2013). Two distinct mechanisms of Topoisomerase 1-dependent mutagenesis in yeast. *DNA Repair (Amst)* *12*, 205-211.

Christiansen, K., Svejstrup, A.B., Andersen, A.H., and Westergaard, O. (1993). Eukaryotic topoisomerase I-mediated cleavage requires bipartite DNA interaction. Cleavage of DNA substrates containing strand interruptions implicates a role for topoisomerase I in illegitimate recombination. *J Biol Chem* *268*, 9690-9701.

Christiansen, K., and Westergaard, O. (1999). Mapping of eukaryotic DNA topoisomerase I catalyzed cleavage without concomitant religation in the vicinity of DNA structural anomalies. *Biochim Biophys Acta* 1489, 249-262.

Christman, M.F., Dietrich, F.S., and Fink, G.R. (1988). Mitotic recombination in the rDNA of *S. cerevisiae* is suppressed by the combined action of DNA topoisomerases I and II. *Cell* 55, 413-425.

Covey, J.M., Jaxel, C., Kohn, K.W., and Pommier, Y. (1989). Protein-linked DNA strand breaks induced in mammalian cells by camptothecin, an inhibitor of topoisomerase I. *Cancer Res* 49, 5016-5022.

D'Arpa, P., Machlin, P.S., Ratrie, H., 3rd, Rothfield, N.F., Cleveland, D.W., and Earnshaw, W.C. (1988). cDNA cloning of human DNA topoisomerase I: catalytic activity of a 67.7-kDa carboxyl-terminal fragment. *Proc Natl Acad Sci U S A* 85, 2543-2547.

Dancey, J., and Eisenhauer, E.A. (1996). Current perspectives on camptothecins in cancer treatment. *British journal of cancer* 74, 327-338.

Datta, A., and Jinks-Robertson, S. (1995). Association of increased spontaneous mutation rates with high levels of transcription in yeast. *Science* 268, 1616-1619.

Deng, C., Brown, J.A., You, D., and Brown, J.M. (2005). Multiple endonucleases function to repair covalent topoisomerase I complexes in *Saccharomyces cerevisiae*. *Genetics* 170, 591-600.

Drolet, M., Wu, H.Y., and Liu, L.F. (1994). Roles of DNA topoisomerases in transcription. *Adv Pharmacol* 29A, 135-146.

El Hage, A., French, S.L., Beyer, A.L., and Tollervy, D. (2010). Loss of Topoisomerase I leads to R-loop-mediated transcriptional blocks during ribosomal RNA synthesis. *Genes Dev* 24, 1546-1558.

Eng, W.K., Pandit, S.D., and Sternglanz, R. (1989). Mapping of the active site tyrosine of eukaryotic DNA topoisomerase I. *J Biol Chem* 264, 13373-13376.

Engel, C., and Fischer, C. (2015). Breast cancer risks and risk prediction models. *Breast Care (Basel)* 10, 7-12.

- Fasullo, M., Zeng, L., and Giallanza, P. (2004). Enhanced stimulation of chromosomal translocations by radiomimetic DNA damaging agents and camptothecin in *Saccharomyces cerevisiae* rad9 checkpoint mutants. *Mutat Res* 547, 123-132.
- Fiorani, P., and Bjornsti, M.A. (2000). Mechanisms of DNA topoisomerase I-induced cell killing in the yeast *Saccharomyces cerevisiae*. *Ann N Y Acad Sci* 922, 65-75.
- Fogel, S., Welch, J.W., Cathala, G., and Karin, M. (1983). Gene amplification in yeast: CUP1 copy number regulates copper resistance. *Curr Genet* 7, 347-355.
- Fricke, W.M., and Brill, S.J. (2003). Slx1-Slx4 is a second structure-specific endonuclease functionally redundant with Sgs1-Top3. *Genes Dev* 17, 1768-1778.
- Giaever, G.N., Snyder, L., and Wang, J.C. (1988). DNA supercoiling in vivo. *Biophys Chem* 29, 7-15.
- Giovanella, B.C., Stehlin, J.S., Wall, M.E., Wani, M.C., Nicholas, A.W., Liu, L.F., Silber, R., and Potmesil, M. (1989). DNA topoisomerase I--targeted chemotherapy of human colon cancer in xenografts. *Science* 246, 1046-1048.
- Goldstein, A.L., and McCusker, J.H. (1999). Three new dominant drug resistance cassettes for gene disruption in *Saccharomyces cerevisiae*. *Yeast* 15, 1541-1553.
- Goto, T., and Wang, J.C. (1985). Cloning of yeast TOP1, the gene encoding DNA topoisomerase I, and construction of mutants defective in both DNA topoisomerase I and DNA topoisomerase II. *Proc Natl Acad Sci U S A* 82, 7178-7182.
- Gresham, D., Curry, B., Ward, A., Gordon, D.B., Brizuela, L., Kruglyak, L., and Botstein, D. (2010). Optimized detection of sequence variation in heterozygous genomes using DNA microarrays with isothermal-melting probes. *Proc Natl Acad Sci U S A* 107, 1482-1487.
- Grunnet, M., Calatayud, D., Schultz, N.A., Hasselby, J.P., Mau-Sorensen, M., Brunner, N., and Stenvang, J. (2015). TOP1 gene copy numbers are increased in cancers of the bile duct and pancreas. *Scand J Gastroenterol* 50, 485-494.

Gueldener, U., Heinisch, J., Koehler, G.J., Voss, D., and Hegemann, J.H. (2002). A second set of loxP marker cassettes for Cre-mediated multiple gene knockouts in budding yeast. *Nucleic Acids Res* 30, e23.

Guldener, U., Heck, S., Fielder, T., Beinhauer, J., and Hegemann, J.H. (1996). A new efficient gene disruption cassette for repeated use in budding yeast. *Nucleic Acids Res* 24, 2519-2524.

Guthrie C, F.G. (1991). *Guide to yeast genetics and molecular biology*. (San Diego: Academic Press.).

Harfe, B.D., and Jinks-Robertson, S. (1999). Removal of frameshift intermediates by mismatch repair proteins in *Saccharomyces cerevisiae*. *Molecular and cellular biology* 19, 4766-4773.

Hartsuiker, E., Neale, M.J., and Carr, A.M. (2009). Distinct requirements for the Rad32(Mre11) nuclease and Ctp1(CtIP) in the removal of covalently bound topoisomerase I and II from DNA. *Mol Cell* 33, 117-123.

Hashimoto, H., Chatterjee, S., and Berger, N.A. (1995). Mutagenic activity of topoisomerase I inhibitors. *Clinical cancer research : an official journal of the American Association for Cancer Research* 1, 369-376.

Heck, M.M., Hittelman, W.N., and Earnshaw, W.C. (1988). Differential expression of DNA topoisomerases I and II during the eukaryotic cell cycle. *Proc Natl Acad Sci U S A* 85, 1086-1090.

Henningfeld, K.A., and Hecht, S.M. (1995). A model for topoisomerase I-mediated insertions and deletions with duplex DNA substrates containing branches, nicks, and gaps. *Biochemistry* 34, 6120-6129.

Heyer, W.D., Ehmsen, K.T., and Liu, J. (2010). Regulation of homologous recombination in eukaryotes. *Annu Rev Genet* 44, 113-139.

Hsiang, Y.H., Lihou, M.G., and Liu, L.F. (1989). Arrest of replication forks by drug-stabilized topoisomerase I-DNA cleavable complexes as a mechanism of cell killing by camptothecin. *Cancer research* 49, 5077-5082.

Huang, S.Y., Ghosh, S., and Pommier, Y. (2015). Topoisomerase I alone is sufficient to produce short DNA deletions and can also reverse nicks at ribonucleotide sites. *J Biol Chem* 290, 14068-14076.

Iossifov, I., Ronemus, M., Levy, D., Wang, Z., Hakker, I., Rosenbaum, J., Yamrom, B., Lee, Y.H., Narzisi, G., Leotta, A., *et al.* (2012). De novo gene disruptions in children on the autistic spectrum. *Neuron* 74, 285-299.

Iyama, T., and Wilson, D.M., 3rd (2013). DNA repair mechanisms in dividing and non-dividing cells. *DNA Repair (Amst)* 12, 620-636.

Jasin, M., and Rothstein, R. (2013). Repair of strand breaks by homologous recombination. *Cold Spring Harb Perspect Biol* 5, a012740.

Jaxel, C., Capranico, G., Kerrigan, D., Kohn, K.W., and Pommier, Y. (1991). Effect of local DNA sequence on topoisomerase I cleavage in the presence or absence of camptothecin. *J Biol Chem* 266, 20418-20423.

Jaxel, C., Kohn, K.W., and Pommier, Y. (1988). Topoisomerase I interaction with SV40 DNA in the presence and absence of camptothecin. *Nucleic Acids Res* 16, 11157-11170.

Kadyk, L.C., and Hartwell, L.H. (1992). Sister chromatids are preferred over homologs as substrates for recombinational repair in *Saccharomyces cerevisiae*. *Genetics* 132, 387-402.

Karin, M., Najarian, R., Haslinger, A., Valenzuela, P., Welch, J., and Fogel, S. (1984). Primary structure and transcription of an amplified genetic locus: the CUP1 locus of yeast. *Proc Natl Acad Sci U S A* 81, 337-341.

Kawanishi, M. (1993). Topoisomerase I and II activities are required for Epstein-Barr virus replication. *J Gen Virol* 74 (Pt 10), 2263-2268.

Kim, N., Abdulovic, A.L., Gealy, R., Lippert, M.J., and Jinks-Robertson, S. (2007). Transcription-associated mutagenesis in yeast is directly proportional to the level of gene expression and influenced by the direction of DNA replication. *DNA repair* 6, 1285-1296.

Kim, N., Huang, S.N., Williams, J.S., Li, Y.C., Clark, A.B., Cho, J.E., Kunkel, T.A., Pommier, Y., and Jinks-Robertson, S. (2011). Mutagenic processing of ribonucleotides in DNA by yeast topoisomerase I. *Science* 332, 1561-1564.

Kim, R.A., and Wang, J.C. (1989). A subthreshold level of DNA topoisomerases leads to the excision of yeast rDNA as extrachromosomal rings. *Cell* 57, 975-985.

King, I.F., Yandava, C.N., Mabb, A.M., Hsiao, J.S., Huang, H.S., Pearson, B.L., Calabrese, J.M., Starmer, J., Parker, J.S., Magnuson, T., *et al.* (2013). Topoisomerases facilitate transcription of long genes linked to autism. *Nature* 501, 58-62.

Knab, A.M., Fertala, J., and Bjornsti, M.A. (1993). Mechanisms of camptothecin resistance in yeast DNA topoisomerase I mutants. *J Biol Chem* 268, 22322-22330.

Koster, D.A., Palle, K., Bot, E.S., Bjornsti, M.A., and Dekker, N.H. (2007). Antitumour drugs impede DNA uncoiling by topoisomerase I. *Nature* 448, 213-217.

Krogh, B.O., and Shuman, S. (2000). Catalytic mechanism of DNA topoisomerase IB. *Mol Cell* 5, 1035-1041.

Kumler, I., Balslev, E., Poulsen, T.S., Nielsen, S.L., Nygard, S.B., Romer, M.U., Christensen, I.J., Hogdall, E., Moreira, J., Nielsen, D.L., *et al.* (2015). Topoisomerase-1 gene copy aberrations are frequent in patients with breast cancer. *Int J Cancer* 137, 2000-2006.

Lee, M.P., Brown, S.D., Chen, A., and Hsieh, T.S. (1993). DNA topoisomerase I is essential in *Drosophila melanogaster*. *Proc Natl Acad Sci U S A* 90, 6656-6660.

Lee, P.S., Greenwell, P.W., Dominska, M., Gawel, M., Hamilton, M., and Petes, T.D. (2009). A fine-structure map of spontaneous mitotic crossovers in the yeast *Saccharomyces cerevisiae*. *PLoS Genet* 5, e1000410.

Lee, P.S., and Petes, T.D. (2010). From the Cover: mitotic gene conversion events induced in G1-synchronized yeast cells by gamma rays are similar to spontaneous conversion events. *Proc Natl Acad Sci U S A* 107, 7383-7388.

Legarza, K., and Yang, L.X. (2006). New molecular mechanisms of action of camptothecin-type drugs. *Anticancer research* 26, 3301-3305.

- Levin, N.A., Bjornsti, M.A., and Fink, G.R. (1993). A novel mutation in DNA topoisomerase I of yeast causes DNA damage and RAD9-dependent cell cycle arrest. *Genetics* *133*, 799-814.
- Li, C.J., Zhang, L.J., Dezube, B.J., Crumpacker, C.S., and Pardee, A.B. (1993). Three inhibitors of type 1 human immunodeficiency virus long terminal repeat-directed gene expression and virus replication. *Proc Natl Acad Sci U S A* *90*, 1839-1842.
- Lin, C.Y., Loven, J., Rahl, P.B., Paranal, R.M., Burge, C.B., Bradner, J.E., Lee, T.I., and Young, R.A. (2012). Transcriptional amplification in tumor cells with elevated c-Myc. *Cell* *151*, 56-67.
- Lippert, M.J., Kim, N., Cho, J.E., Larson, R.P., Schoenly, N.E., O'Shea, S.H., and Jinks-Robertson, S. (2011). Role for topoisomerase 1 in transcription-associated mutagenesis in yeast. *Proc Natl Acad Sci U S A* *108*, 698-703.
- Liu, C., Pouliot, J.J., and Nash, H.A. (2004). The role of TDP1 from budding yeast in the repair of DNA damage. *DNA repair* *3*, 593-601.
- Livak, K.J., and Schmittgen, T.D. (2001). Analysis of relative gene expression data using real-time quantitative PCR and the 2(-Delta Delta C(T)) Method. *Methods* *25*, 402-408.
- Lobachev, K.S., Gordenin, D.A., and Resnick, M.A. (2002). The Mre11 complex is required for repair of hairpin-capped double-strand breaks and prevention of chromosome rearrangements. *Cell* *108*, 183-193.
- Lynn, R.M., Bjornsti, M.A., Caron, P.R., and Wang, J.C. (1989). Peptide sequencing and site-directed mutagenesis identify tyrosine-727 as the active site tyrosine of *Saccharomyces cerevisiae* DNA topoisomerase I. *Proc Natl Acad Sci U S A* *86*, 3559-3563.
- Madden, K.R., and Champoux, J.J. (1992). Overexpression of human topoisomerase I in baby hamster kidney cells: hypersensitivity of clonal isolates to camptothecin. *Cancer Res* *52*, 525-532.
- Malik, M., and Nitiss, J.L. (2004). DNA repair functions that control sensitivity to topoisomerase-targeting drugs. *Eukaryot Cell* *3*, 82-90.

- Megonigal, M.D., Fertala, J., and Bjornsti, M.A. (1997). Alterations in the catalytic activity of yeast DNA topoisomerase I result in cell cycle arrest and cell death. *J Biol Chem* 272, 12801-12808.
- Merino, A., Madden, K.R., Lane, W.S., Champoux, J.J., and Reinberg, D. (1993). DNA topoisomerase I is involved in both repression and activation of transcription. *Nature* 365, 227-232.
- Miao, Z.H., Player, A., Shankavaram, U., Wang, Y.H., Zimonjic, D.B., Lorenzi, P.L., Liao, Z.Y., Liu, H., Shimura, T., Zhang, H.L., *et al.* (2007). Nonclassic functions of human topoisomerase I: genome-wide and pharmacologic analyses. *Cancer Res* 67, 8752-8761.
- Mimitou, E.P., and Symington, L.S. (2009). DNA end resection: many nucleases make light work. *DNA Repair (Amst)* 8, 983-995.
- Morham, S.G., Kluckman, K.D., Voulomanos, N., and Smithies, O. (1996). Targeted disruption of the mouse topoisomerase I gene by camptothecin selection. *Mol Cell Biol* 16, 6804-6809.
- Myung, K., and Kolodner, R.D. (2003). Induction of genome instability by DNA damage in *Saccharomyces cerevisiae*. *DNA Repair (Amst)* 2, 243-258.
- Neale, B.M., Kou, Y., Liu, L., Ma'ayan, A., Samocha, K.E., Sabo, A., Lin, C.F., Stevens, C., Wang, L.S., Makarov, V., *et al.* (2012). Patterns and rates of exonic de novo mutations in autism spectrum disorders. *Nature* 485, 242-245.
- Newcombe, R.G. (1998). Two-sided confidence intervals for the single proportion: comparison of seven methods. *Stat Med* 17, 857-872.
- Nick McElhinny, S.A., Kumar, D., Clark, A.B., Watt, D.L., Watts, B.E., Lundstrom, E.B., Johansson, E., Chabes, A., and Kunkel, T.A. (2010). Genome instability due to ribonucleotide incorporation into DNA. *Nature chemical biology* 6, 774-781.
- Nitiss, J., and Wang, J.C. (1988). DNA topoisomerase-targeting antitumor drugs can be studied in yeast. *Proceedings of the National Academy of Sciences of the United States of America* 85, 7501-7505.

- Nitiss, J.L. (1998). Investigating the biological functions of DNA topoisomerases in eukaryotic cells. *Biochim Biophys Acta* *1400*, 63-81.
- Nitiss, J.L., Nitiss, K.C., Rose, A., and Waltman, J.L. (2001). Overexpression of type I topoisomerases sensitizes yeast cells to DNA damage. *J Biol Chem* *276*, 26708-26714.
- Oberlies, N.H., and Kroll, D.J. (2004). Camptothecin and taxol: historic achievements in natural products research. *Journal of natural products* *67*, 129-135.
- Padgett, K., Carr, R., Pearson, A.D., Tilby, M.J., and Austin, C.A. (2000). Camptothecin-stabilised topoisomerase I-DNA complexes in leukaemia cells visualised and quantified in situ by the TARDIS assay (trapped in agarose DNA immunostaining). *Biochem Pharmacol* *59*, 629-638.
- Paques, F., and Haber, J.E. (1999). Multiple pathways of recombination induced by double-strand breaks in *Saccharomyces cerevisiae*. *Microbiol Mol Biol Rev* *63*, 349-404.
- Pendleton, M., Lindsey, R.H., Jr., Felix, C.A., Grimwade, D., and Osheroff, N. (2014). Topoisomerase II and leukemia. *Ann N Y Acad Sci* *1310*, 98-110.
- Petes, T.D., and Botstein, D. (1977). Simple Mendelian inheritance of the reiterated ribosomal DNA of yeast. *Proc Natl Acad Sci U S A* *74*, 5091-5095.
- Petes, T.D., Malone, R.E., and Symington, L.S. (1991). Recombination in yeast. In *The Molecular and Cellular Biology of the Yeast Saccharomyces* (Cold Spring Harbor Laboratory Press), pp. pp. 407-421.
- Pommier, Y. (2006). Topoisomerase I inhibitors: camptothecins and beyond. *Nature reviews Cancer* *6*, 789-802.
- Pommier, Y. (2013). Drugging topoisomerases: lessons and challenges. *ACS Chem Biol* *8*, 82-95.
- Pommier, Y., Leo, E., Zhang, H., and Marchand, C. (2010). DNA topoisomerases and their poisoning by anticancer and antibacterial drugs. *Chemistry & biology* *17*, 421-433.

Pommier, Y., Leo, E., Zhang, H., and Marchand, C. (2010). DNA topoisomerases and their poisoning by anticancer and antibacterial drugs. *Chem Biol* *17*, 421-433.

Pommier, Y., and Marchand, C. (2012). Interfacial inhibitors: targeting macromolecular complexes. *Nat Rev Drug Discov* *11*, 25-36.

Pommier, Y., Pourquier, P., Fan, Y., and Strumberg, D. (1998). Mechanism of action of eukaryotic DNA topoisomerase I and drugs targeted to the enzyme. *Biochim Biophys Acta* *1400*, 83-105.

Pommier, Y., Pourquier, P., Urasaki, Y., Wu, J., and Laco, G.S. (1999). Topoisomerase I inhibitors: selectivity and cellular resistance. *Drug resistance updates : reviews and commentaries in antimicrobial and anticancer chemotherapy* *2*, 307-318.

Pommier, Y., Redon, C., Rao, V.A., Seiler, J.A., Sordet, O., Takemura, H., Antony, S., Meng, L., Liao, Z., Kohlhagen, G., *et al.* (2003). Repair of and checkpoint response to topoisomerase I-mediated DNA damage. *Mutat Res* *532*, 173-203.

Porter, S.E., and Champoux, J.J. (1989). Mapping in vivo topoisomerase I sites on simian virus 40 DNA: asymmetric distribution of sites on replicating molecules. *Mol Cell Biol* *9*, 541-550.

Potenski, C.J., and Klein, H.L. (2014). How the misincorporation of ribonucleotides into genomic DNA can be both harmful and helpful to cells. *Nucleic Acids Res* *42*, 10226-10234.

Potmesil, M. (1994). Camptothecins: from bench research to hospital wards. *Cancer Res* *54*, 1431-1439.

Pouliot, J.J., Robertson, C.A., and Nash, H.A. (2001). Pathways for repair of topoisomerase I covalent complexes in *Saccharomyces cerevisiae*. *Genes to cells : devoted to molecular & cellular mechanisms* *6*, 677-687.

Pouliot, J.J., Yao, K.C., Robertson, C.A., and Nash, H.A. (1999). Yeast gene for a Tyr-DNA phosphodiesterase that repairs topoisomerase I complexes. *Science* *286*, 552-555.

- Pourquier, P., and Pommier, Y. (2001). Topoisomerase I-mediated DNA damage. *Adv Cancer Res* 80, 189-216.
- Prakash, S., and Prakash, L. (2000). Nucleotide excision repair in yeast. *Mutat Res* 451, 13-24.
- Ray Chaudhuri, A., Hashimoto, Y., Herrador, R., Neelsen, K.J., Fachinetti, D., Bermejo, R., Cocito, A., Costanzo, V., and Lopes, M. (2012). Topoisomerase I poisoning results in PARP-mediated replication fork reversal. *Nat Struct Mol Biol* 19, 417-423.
- Redinbo, M.R., Stewart, L., Kuhn, P., Champoux, J.J., and Hol, W.G. (1998). Crystal structures of human topoisomerase I in covalent and noncovalent complexes with DNA. *Science* 279, 1504-1513.
- Reid, R.J., Benedetti, P., and Bjornsti, M.A. (1998). Yeast as a model organism for studying the actions of DNA topoisomerase-targeted drugs. *Biochim Biophys Acta* 1400, 289-300.
- Reid, R.J., Gonzalez-Barrera, S., Sunjevaric, I., Alvaro, D., Ciccone, S., Wagner, M., and Rothstein, R. (2011). Selective ploidy ablation, a high-throughput plasmid transfer protocol, identifies new genes affecting topoisomerase I-induced DNA damage. *Genome Res* 21, 477-486.
- Romer, M.U., Jensen, N.F., Nielsen, S.L., Muller, S., Nielsen, K.V., Nielsen, H.J., and Brunner, N. (2012). TOP1 gene copy numbers in colorectal cancer samples and cell lines and their association to in vitro drug sensitivity. *Scand J Gastroenterol* 47, 68-79.
- Romer, M.U., Nygard, S.B., Christensen, I.J., Nielsen, S.L., Nielsen, K.V., Muller, S., Smith, D.H., Vainer, B., Nielsen, H.J., and Brunner, N. (2013). Topoisomerase 1(TOP1) gene copy number in stage III colorectal cancer patients and its relation to prognosis. *Mol Oncol* 7, 101-111.
- Romig, H., and Richter, A. (1990). Expression of the type I DNA topoisomerase gene in adenovirus-5 infected human cells. *Nucleic Acids Res* 18, 801-808.
- Rothstein, R.J. (1983). One-step gene disruption in yeast. *Methods Enzymol* 101, 202-211.

Saavedra, R.A., and Huberman, J.A. (1986). Both DNA topoisomerases I and II relax 2 micron plasmid DNA in living yeast cells. *Cell* 45, 65-70.

Sekiguchi, J., and Shuman, S. (1997). Site-specific ribonuclease activity of eukaryotic DNA topoisomerase I. *Mol Cell* 1, 89-97.

Shao, R.G., Cao, C.X., Zhang, H., Kohn, K.W., Wold, M.S., and Pommier, Y. (1999). Replication-mediated DNA damage by camptothecin induces phosphorylation of RPA by DNA-dependent protein kinase and dissociates RPA:DNA-PK complexes. *EMBO J* 18, 1397-1406.

Sikorski, R.S., and Hieter, P. (1989). A system of shuttle vectors and yeast host strains designed for efficient manipulation of DNA in *Saccharomyces cerevisiae*. *Genetics* 122, 19-27.

Sobczak, J., Tournier, M.F., Lotti, A.M., and Duguet, M. (1989). Gene expression in regenerating liver in relation to cell proliferation and stress. *Eur J Biochem* 180, 49-53.

Song, W., Dominska, M., Greenwell, P.W., and Petes, T.D. (2014). Genome-wide high-resolution mapping of chromosome fragile sites in *Saccharomyces cerevisiae*. *Proc Natl Acad Sci U S A* 111, E2210-2218.

Sparks, J.L., and Burgers, P.M. (2015). Error-free and mutagenic processing of topoisomerase 1-provoked damage at genomic ribonucleotides. *EMBO J* 34, 1259-1269.

Sparks, J.L., Chon, H., Cerritelli, S.M., Kunkel, T.A., Johansson, E., Crouch, R.J., and Burgers, P.M. (2012). RNase H2-initiated ribonucleotide excision repair. *Mol Cell* 47, 980-986.

St. Charles, J., Hazkani-Covo, E., Yin, Y., Andersen, S.L., Dietrich, F.S., Greenwell, P.W., Malc, E., Mieczkowski, P., and Petes, T.D. (2012). High-resolution genome-wide analysis of irradiated (UV and gamma-rays) diploid yeast cells reveals a high frequency of genomic loss of heterozygosity (LOH) events. *Genetics* 190, 1267-1284.

St. Charles, J., and Petes, T.D. (2013). High-resolution mapping of spontaneous mitotic recombination hotspots on the 1.1 Mb arm of yeast chromosome IV. *PLoS Genet* 9, e1003434.

Stewart, L., Redinbo, M.R., Qiu, X., Hol, W.G., and Champoux, J.J. (1998). A model for the mechanism of human topoisomerase I. *Science* 279, 1534-1541.

Stingele, J., Schwarz, M.S., Bloemeke, N., Wolf, P.G., and Jentsch, S. (2014). A DNA-dependent protease involved in DNA-protein crosslink repair. *Cell* 158, 327-338.

Stivers, J.T., Harris, T.K., and Mildvan, A.S. (1997). Vaccinia DNA topoisomerase I: evidence supporting a free rotation mechanism for DNA supercoil relaxation. *Biochemistry* 36, 5212-5222.

Subramanian, D., Kraut, E., Staubus, A., Young, D.C., and Muller, M.T. (1995). Analysis of topoisomerase I/DNA complexes in patients administered topotecan. *Cancer Res* 55, 2097-2103.

Symington, L.S., Rothstein, R., and Lisby, M. (2014). Mechanisms and regulation of mitotic recombination in *Saccharomyces cerevisiae*. *Genetics* 198, 795-835.

Takahashi, H., Matsuda, M., Kojima, A., Sata, T., Andoh, T., Kurata, T., Nagashima, K., and Hall, W.W. (1995). Human immunodeficiency virus type 1 reverse transcriptase: enhancement of activity by interaction with cellular topoisomerase I. *Proc Natl Acad Sci U S A* 92, 5694-5698.

Takahashi, T., Burguiere-Slezak, G., Van der Kemp, P.A., and Boiteux, S. (2011). Topoisomerase 1 provokes the formation of short deletions in repeated sequences upon high transcription in *Saccharomyces cerevisiae*. *Proc Natl Acad Sci U S A* 108, 692-697.

Tanizawa, A., Kohn, K.W., and Pommier, Y. (1993). Induction of cleavage in topoisomerase I c-DNA by topoisomerase I enzymes from calf thymus and wheat germ in the presence and absence of camptothecin. *Nucleic Acids Res* 21, 5157-5166.

Thomas, B.J., and Rothstein, R. (1989). Elevated recombination rates in transcriptionally active DNA. *Cell* 56, 619-630.

Thomsen, B., Mollerup, S., Bonven, B.J., Frank, R., Blocker, H., Nielsen, O.F., and Westergaard, O. (1987). Sequence specificity of DNA topoisomerase I in the presence and absence of camptothecin. *EMBO J* 6, 1817-1823.

Trigueros, S., and Roca, J. (2002). Failure to relax negative supercoiling of DNA is a primary cause of mitotic hyper-recombination in topoisomerase-deficient yeast cells. *J Biol Chem* 277, 37207-37211.

Ulukan, H., and Swaan, P.W. (2002). Camptothecins: a review of their chemotherapeutic potential. *Drugs* 62, 2039-2057.

Vance, J.R., and Wilson, T.E. (2001). Repair of DNA strand breaks by the overlapping functions of lesion-specific and non-lesion-specific DNA 3' phosphatases. *Mol Cell Biol* 21, 7191-7198.

Vance, J.R., and Wilson, T.E. (2002). Yeast Tdp1 and Rad1-Rad10 function as redundant pathways for repairing Top1 replicative damage. *Proc Natl Acad Sci U S A* 99, 13669-13674.

Vekhoff, P., Duca, M., Guianvarc'h, D., Benhida, R., and Arimondo, P.B. (2012). Sequence-specific base pair mimics are efficient topoisomerase IB inhibitors. *Biochemistry* 51, 43-51.

Wach, A., Brachat, A., Pohlmann, R., and Philippsen, P. (1994). New heterologous modules for classical or PCR-based gene disruptions in *Saccharomyces cerevisiae*. *Yeast* 10, 1793-1808.

Wallis, J.W., Chrebet, G., Brodsky, G., Rolfe, M., and Rothstein, R. (1989). A hyper-recombination mutation in *S. cerevisiae* identifies a novel eukaryotic topoisomerase. *Cell* 58, 409-419.

Wang, J.C. (2002). Cellular roles of DNA topoisomerases: a molecular perspective. *Nature reviews Molecular cell biology* 3, 430-440.

Wang, J.C., and Lynch, A.S. (1993). Transcription and DNA supercoiling. *Curr Opin Genet Dev* 3, 764-768.

Warren, K., Warrilow, D., Meredith, L., and Harrich, D. (2009). Reverse Transcriptase and Cellular Factors: Regulators of HIV-1 Reverse Transcription. *Viruses* 1, 873-894.

Wei, W., McCusker, J.H., Hyman, R.W., Jones, T., Ning, Y., Cao, Z., Gu, Z., Bruno, D., Miranda, M., Nguyen, M., *et al.* (2007). Genome sequencing and comparative

analysis of *Saccharomyces cerevisiae* strain YJM789. *Proc Natl Acad Sci U S A* *104*, 12825-12830.

Woo, M.H., Losasso, C., Guo, H., Pattarello, L., Benedetti, P., and Bjornsti, M.A. (2003). Locking the DNA topoisomerase I protein clamp inhibits DNA rotation and induces cell lethality. *Proc Natl Acad Sci U S A* *100*, 13767-13772.

Yamada, Y., Yamamoto, N., Maeno, K., and Nishiyama, Y. (1990). Role of DNA topoisomerase I in the replication of herpes simplex virus type 2. *Arch Virol* *110*, 121-127.

Yim, E., O'Connell, K.E., St Charles, J., and Petes, T.D. (2014). High-Resolution Mapping of Two Types of Spontaneous Mitotic Gene Conversion Events in *Saccharomyces cerevisiae*. *Genetics* *198*, 181-192.

Yin, Y., and Petes, T.D. (2013). Genome-wide high-resolution mapping of UV-induced mitotic recombination events in *Saccharomyces cerevisiae*. *PLoS Genet* *9*, e1003894.

Zhang, H., Wang, J.C., and Liu, L.F. (1988). Involvement of DNA topoisomerase I in transcription of human ribosomal RNA genes. *Proc Natl Acad Sci U S A* *85*, 1060-1064.

Zhao, X., Muller, E.G., and Rothstein, R. (1998). A suppressor of two essential checkpoint genes identifies a novel protein that negatively affects dNTP pools. *Mol Cell* *2*, 329-340.

Zhao, Y., Strobe, P.K., Kozmin, S.G., McCusker, J.H., Dietrich, F.S., Kokoska, R.J., and Petes, T.D. (2014). Structures of Naturally-Evolved CUP1 Tandem Arrays in Yeast Indicate that These Arrays Are Generated by Unequal Non-Homologous Recombination. *G3 (Bethesda)*.

Biography

Roketa Sloan was born in Midwest City, Oklahoma and is from Sumter, SC. She completed her undergraduate work at Saint Augustine's University (B.S. 2005) and obtained her M.S. Degree in Biology from North Carolina Central University (M.S. 2010). Sloan is completing her dissertation research in the laboratory of Sue Jinks-Robertson where her research utilizes budding yeast to investigate genomic instability induced by the chemotherapeutic drug, camptothecin, or increased levels of the enzyme, topoisomerase I. During her time at Duke, Sloan served as the President for both the Bouchet Society and the Black Graduate & Professional Student Association. She helped coordinate outreach programs at local colleges and universities, promoting the option of a Ph.D. in the sciences to minority undergraduates and served as a student coordinator for the Duke Summer Research Opportunity Program. Sloan was involved in the creation of the Ida Stephens Owens Black Tie Dinner in honor of Duke Graduate School's first black female Ph.D., designed to highlight the significant achievements of African Americans with a STEM Ph.D from Duke. More recently, Sloan was involved in the Duke Black Lives Matter Initiative, an effort to increase awareness that students of color are equally a part of the Duke community. Sloan was awarded a 2014 Samuel DuBois Cook Award and was one of the 2015 Duke University Graduate Young Trustee Finalists. Following graduation from Duke, Sloan will conduct post-doctoral research at St. Jude Children's Research Hospital in Memphis, TN in the laboratory of Dr. Peter McKinnon.

Publications:

1. Andersen, S.L., Sloan, R.S., Petes, T.D., and Jinks-Robertson, S. (2015). Genome-destabilizing effects associated with top1 loss or accumulation of top1 cleavage complexes in yeast. *PLoS Genet* *11*, e1005098.
2. Sloan, R.S., Swanson, C.I., Gavilano, L., Smith, K.N., Malek, P.Y., Snow-Smith, M., Duronio, R.J., and Key, S.C. (2012). Characterization of null and hypomorphic alleles of the *Drosophila* l(2)dtl/cdt2 gene: Larval lethality and male fertility. *Fly (Austin)* *6*, 173-183.